

AD-A173 015

A STUDY OF EXPLOSIVE WAVE PROPAGATION IN GRANULAR
MATERIALS WITH MICROSTR (U) RHODE ISLAND UNIV KINGSTON
DEPT OF MECHANICAL ENGINEERING AND M H SADD ET AL

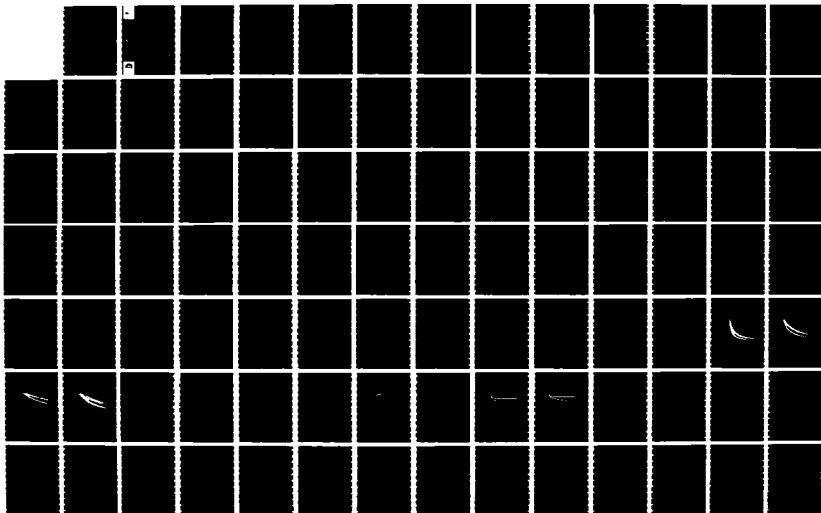
1/2

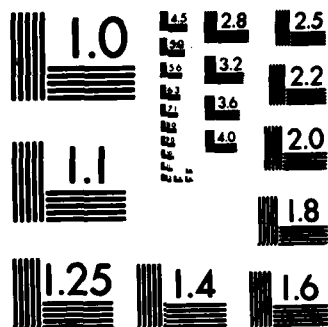
UNCLASSIFIED

SEP 86 WES/TR/SL-86-35 DACA39-85-C-0023

F/G 19/4

NL





MICROCOPY RESOLUTION TEST CHART
NATIONAL BUREAU OF STANDARDS-1963-A

2

TECHNICAL REPORT SL-86-35



US Army Corps
of Engineers

AD-A173 015



A STUDY OF EXPLOSIVE WAVE PROPAGATION IN GRANULAR MATERIALS WITH MICROSTRUCTURE

by

Martin H. Sadd, Mohammad Hossain

Department of Mechanical Engineering
and Applied Mechanics
University of Rhode Island
Kingston, Rhode Island 02881

and

Behzad Rohani

DEPARTMENT OF THE ARMY
Waterways Experiment Station, Corps of Engineers
PO Box 631, Vicksburg, Mississippi 39180-0631



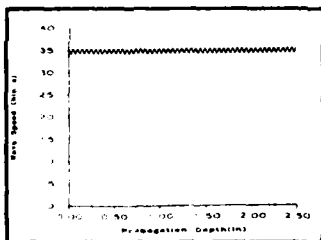
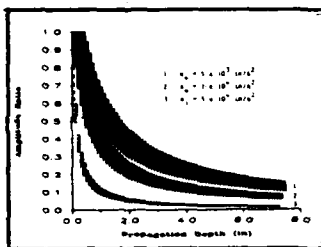
September 1986
Final Report

Approved For Public Release; Distribution Unlimited

DTIC
ELECTE
OCT 16 1986
S B

Prepared for DEPARTMENT OF THE ARMY
Assistant Secretary of the Army (R&D)
Washington, DC 20310-1000
Under Project No. 4A161101A91D

86 10 16 132



FILE COPY



Destroy this report when no longer needed. Do not return
it to the originator.

The findings in this report are not to be construed as an official
Department of the Army position unless so designated
by other authorized documents.

This program is furnished by the Government and is accepted and used
by the recipient with the express understanding that the United States
Government makes no warranties, expressed or implied, concerning the
accuracy, completeness, reliability, usability, or suitability for any
particular purpose of the information and data contained in this pro-
gram or furnished in connection therewith, and the United States shall
be under no liability whatsoever to any person by reason of any use
made thereof. The program belongs to the Government. Therefore, the
recipient further agrees not to assert any proprietary rights therein or to
represent this program to anyone as other than a Government program.

The contents of this report are not to be used for
advertising, publication, or promotional purposes.
Citation of trade names does not constitute an
official endorsement or approval of the use of
such commercial products.

Unclassified

SECURITY CLASSIFICATION OF THIS PAGE

REPORT DOCUMENTATION PAGE				Form Approved OMB No 0704-0188 Exp Date Jun 30, 1986	
1a REPORT SECURITY CLASSIFICATION Unclassified			1b RESERVATION MARKINGS A173 015		
2a SECURITY CLASSIFICATION AUTHORITY			3 DISTRIBUTION/AVAILABILITY OF REPORT Approved for public release; distribution unlimited.		
2b DECLASSIFICATION/DOWNGRADING SCHEDULE					
4 PERFORMING ORGANIZATION REPORT NUMBER(S) Technical Report SL-86-35			5 MONITORING ORGANIZATION REPORT NUMBER(S)		
6a NAME OF PERFORMING ORGANIZATION See reverse		6b OFFICE SYMBOL (If applicable)	7a NAME OF MONITORING ORGANIZATION		
6c ADDRESS (City, State, and ZIP Code)			7b ADDRESS (City, State, and ZIP Code)		
8a NAME OF FUNDING/SPONSORING ORGANIZATION Assistant Secretary of the Army (R&D)		8b OFFICE SYMBOL (If applicable)	9. PROCUREMENT INSTRUMENT IDENTIFICATION NUMBER		
8c ADDRESS (City, State, and ZIP Code) Washington, DC 20310-1000			10. SOURCE OF FUNDING NUMBERS		
PROGRAM ELEMENT NO.		PROJECT NO.	TASK NO.	WORK UNIT ACCESSION NO.	
11 TITLE (Include Security Classification) A Study of Explosive Wave Propagation in Granular Materials with Microstructure					
12 PERSONAL AUTHOR(S) See reverse.					
13a TYPE OF REPORT Final report		13b TIME COVERED FROM TO		14 DATE OF REPORT (Year, Month, Day) September 1986	15. PAGE COUNT 134
16 SUPPLEMENTARY NOTATION Available from National Technical Information Service, 5285 Port Royal Road, Springfield, VA 22161.					
17 COSATI CODES			18. SUBJECT TERMS (Continue on reverse if necessary and identify by block number)		
FIELD	GROUP	SUB-GROUP	Airblast loading, Probabilistic analyses, Constitutive relationship, Microstructural model, Granular material, Wave propagation		
19 ABSTRACT (Continue on reverse if necessary and identify by block number) This report describes an investigation into one-dimensional stress wave propagation in granular materials with microstructure. The study employs the distributed body concept advanced by Goodman and Cowin and the associated wave propagation studies conducted by Nunziato, Walsh, et al. A one-dimensional computer program, referred to as MICAD, has been developed for studying wave propagation in granular materials due to airblast loading. The computer program allows for: (1) arbitrary surface airblast loading, (2) depth-dependent volume distribution function simulating gravity effects in a granular mass, and (3) treatment of grain size and local porosity as random variables. Three forms of depth-dependent volume distribution functions, are incorporated in the program, i.e., a periodic form, an exponential form, and a combined periodic-exponential formulation. The user can select any of these forms for the particular application at hand. The probabilistic treatment of grain size and local porosity is accomplished by using a moment-generating procedure due (Continued)					
20 DISTRIBUTION/AVAILABILITY OF ABSTRACT <input type="checkbox"/> UNCLASSIFIED/UNLIMITED <input checked="" type="checkbox"/> SAME AS RPT <input type="checkbox"/> DTIC USERS			21 ABSTRACT SECURITY CLASSIFICATION Unclassified		
22a NAME OF RESPONSIBLE INDIVIDUAL			22b TELEPHONE (Include Area Code)		22c OFFICE SYMBOL

DD FORM 1473, 84 MAR

83 APR edition may be used until exhausted
All other editions are obsoleteSECURITY CLASSIFICATION OF THIS PAGE
Unclassified

6a and c. NAME OF PERFORMING ORGANIZATION/ADDRESS (Continued).

Department of Mechanical Engineering and Applied Mechanics, University of Rhode Island, Kingston, RI 02881; and Structures Laboratory, US Army Engineer Waterways Experiment Station, PO Box 631, Vicksburg, MS 39180-0631.

10. SOURCE OF FUNDING NUMBERS (Continued).

Department of the Army Project No. 4A161101A91D, In-House Laboratory Independent Research Program.

12. PERSONAL AUTHOR(S) (Continued).

Martin H. Sadd, Mohammad Hossain (University of Rhode Island), and Behzad Rohani (US Army Engineer Waterways Experiment Station).

19. ABSTRACT (Continued).

to Rosenblueth. The computer program calculates the expected value and the variance of the output quantities, such as stress and particle motion, due to the randomness in these variables.

Application of the computer program is demonstrated by presenting the results of a series of parametric calculations dealing with propagation of acceleration waves in granular media. -A documentation of MIC1D is provided in Appendix A.

13

PREFACE

This investigation was conducted by the US Army Engineer Waterways Experiment Station (WES) under Department of the Army Project 4A161101A91D, In-House Laboratory Independent Research (ILIR) Program. It was carried out as a cooperative study with the University of Rhode Island (URI) under contract DACA39-85-C-0023 during the period June 1985 to September 1986. The principal investigator at URI was Dr. Martin H. Sadd. The principal investigator at WES was Dr. Behzad Rohani. This report was typed by Mrs. P. A. Sullivan. This work was performed under the direct supervision of Dr. J. G. Jackson, Jr., Chief, Geomechanics Division, Structures Laboratory (SL), and under the general supervision of Mr. Bryant Mather, Chief, SL.

COL Allen F. Grum, USA, was the previous Director of WES. COL Dwayne G. Lee, CE, is the present Commander and Director. Dr. Robert W. Whalin is Technical Director.



Accession For	
NTIS GFA&I	<input checked="" type="checkbox"/>
DTIC TAB	<input type="checkbox"/>
Unannounced	<input type="checkbox"/>
Justification	
By	
Distribution/	
Availability Codes	
Dist	Avail and/or Special
A-1	

CONTENTS

	<u>Page</u>
PREFACE	i
LIST OF ILLUSTRATIONS	iii
CONVERSION FACTORS, NON-SI TO SI (METRIC) UNITS OF MEASUREMENT	vi
CHAPTER 1 INTRODUCTION	1
1.1 BACKGROUND	1
1.2 SCOPE	2
CHAPTER 2 REVIEW OF PREVIOUS WORK	3
2.1 GENERAL BACKGROUND	3
2.2 DISTRIBUTED BODY THEORY	5
2.3 WAVE PROPAGATION WITHIN A DISTRIBUTED BODY	7
CHAPTER 3 DEVELOPMENT OF WAVE PROPAGATION THEORY	13
3.1 GENERAL	13
3.2 VOLUME DISTRIBUTION FUNCTIONS	13
3.3 WAVE PROPAGATION ANALYSIS	15
3.4 WAVE PROFILE ANALYSIS	19
3.5 PROBABILISTIC CONSIDERATIONS	23
CHAPTER 4 PARAMETRIC STUDIES	51
4.1 GENERAL	51
4.2 DEPTH DEPENDENT BEHAVIOR	51
4.2.1 Periodic Volume Distribution Case	51
4.2.2 Exponential Volume Distribution Case	52
4.2.3 Periodic-Exponential Volume Distribution Case	52
4.3 WAVE PROFILES	53
4.3.1 Uncoupled Results	53
4.3.2 Coupled Results	53
4.4 PROBABILISTIC PROFILES	54
CHAPTER 5 SUMMARY AND RECOMMENDATIONS	81
5.1 SUMMARY	81
5.2 RECOMMENDATIONS	81
REFERENCES	83
APPENDIX A WAVE PROPAGATION COMPUTER CODE	

LIST OF ILLUSTRATIONS

Figure		Page
2.1	Schematic of a propagating singular surface	11
2.2	Average wave speed versus distance; Reference 61 Data	12
2.3	Amplitude behavior versus distance; Reference 61 Data	12
3.1	Periodic volume distribution function ($v_a = 0.8$, $l = 0.05$ in)	27
3.2	Typical two-dimensional Voronoi cells	28
3.3	Exponential volume distribution function $v_0 = 0.6$, $B = 5 \text{ in}^2/\text{lb}$, $\gamma = 7.2 \times 10^{-2} \text{ lb/in}^3$)	29
3.4	Periodic-exponential volume distribution function $v_a = 0.99$, $v_b = 0.6$, $B = 5 \text{ in}^2/\text{lb}$, $\gamma = 7.2 \times 10^{-2} \text{ lb/in}^3$, $l = 0.10$ in)	30
3.5	Typical stress-strain behavior of granular materials under uniaxial strain conditions	31
3.6	Actual wave speed versus distance for periodic volume distribution	32
3.7	Average wave speed versus distance for periodic volume distribution	33
3.8	Amplitude attenuation versus distance for periodic volume distribution	34
3.9	Actual wave speed versus distance for exponential volume distribution	35
3.10	Average wave speed versus distance for exponential volume distribution	36
3.11	Amplitude attenuation versus distance for exponential volume distribution	37
3.12	Actual wave speed versus distance for combined periodic- exponential volume distribution	38
3.13	Average wave speed versus distance for combined periodic- exponential volume distribution	39
3.14	Amplitude attenuation versus distance for combined periodic-exponential volume distribution	40
3.15	Wave profile construction	41
3.16	Four wave profile example	42
3.17	Postulated variation of material parameter v_a as a function of stress	43
3.18	Particle acceleration profile for a periodic volume distribution (Material P1) at $X = 0.125$ in	44
3.19	Stress profile for a periodic volume distribution (Material P1) at $X = 0.125$ in	45

<u>Figure</u>		<u>Page</u>
3.20	Particle velocity profile for a periodic volume distribution (Material P1) at $X = 0.125$ in	46
3.21	Particle displacement profile for a periodic volume distribution (Material P1) at $X = 0.125$ in	47
3.22	Probabilistic results for the particle acceleration profile at $X = 0.125$ in ; mean response with its one-standard-deviation bounds. Input variables: $\bar{l} = 0.059$ in , $\sigma_l = 0.02$ in , $\bar{v}_a = 0.85$, and $\sigma_{v_a} = 0.1$	48
3.23	Probabilistic results for the stress profile at $X = 0.125$ in ; mean response with its one-standard-deviation bounds. Input variables: $\bar{l} = 0.059$ in , $\sigma_l = 0.02$ in , $\bar{v}_a = 0.85$, and $\sigma_{v_a} = 0.1$	49
3.24	Probabilistic results for the velocity profile at $X = 0.125$ in ; mean response with its one-standard-deviation bounds. Input variables: $\bar{l} = 0.059$ in , $\sigma_l = 0.02$ in , $\bar{v}_a = 0.85$, and $\sigma_{v_a} = 0.1$	50
4.1	The effect of v_a on the average wave speed versus depth for a periodic volume distribution (Material P1 with $l = 0.1$ in)	55
4.2	The effect of l on the average wave speed versus depth for a periodic volume distribution (Material P1 with $v_a = 0.8$)	56
4.3	Amplitude ratio versus depth for a periodic volume distribution (Material P1 with $l = 0.1$ in and $v_a = 0.7$)	57
4.4	Amplitude ratio versus depth for a periodic volume distribution (Material P1 with $l = 0.1$ in and $v_a = 0.8$)	58
4.5	Amplitude ratio versus depth for a periodic volume distribution (Material P1 with $l = 0.1$ in and $v_a = 0.9$)	59
4.6	Amplitude ratio versus depth for a periodic volume distribution (Material P1 with $l = 0.2$ in and $v_a = 0.8$)	60
4.7	Exponential volume distribution function with $B = 10 \text{ in}^2/\text{lb}$	61
4.8	Average wave speed versus depth for an exponential volume distribution (Material E1 with $B = 10 \text{ in}^2/\text{lb}$)	62
4.9	Amplitude ratio versus depth for an exponential volume distribution (Material E1 with $B = 10 \text{ in}^2/\text{lb}$ and $v_b = 0.65$)	63
4.10	Amplitude ratio versus depth for an exponential volume distribution (Material E1 with $B = 10 \text{ in}^2/\text{lb}$ and $v_b = 0.75$)	64

<u>Figure</u>		<u>Page</u>
4.11	Combined periodic-exponential volume distribution function with $v_a = 0.992$, $B = 30 \text{ in}^2/\text{lb}$, and $\ell = 0.10 \text{ in}$	65
4.12	Average wave speed versus depth for a periodic-exponential volume distribution (Material PE1 with $\ell = 0.1 \text{ in}$)	66
4.13	Amplitude ratio versus depth for a periodic-exponential volume distribution (Material PE1 with $\ell = 0.1 \text{ in}$ and $v_b = 0.65$)	67
4.14	Amplitude ratio versus depth for a periodic-exponential volume distribution (Material PE1 with $\ell = 0.1 \text{ in}$ and $v_b = 0.75$)	68
4.15	Uncoupled particle acceleration profiles at various depths (Material P1 with $v_a = 0.85$ and $\ell = 0.1 \text{ in}$)	69
4.16	Uncoupled particle velocity profiles at various depths (Material P1 with $v_a = 0.85$ and $\ell = 0.1 \text{ in}$)	70
4.17	Uncoupled particle displacement profiles at various depths (Material P1 with $v_a = 0.85$ and $\ell = 0.1 \text{ in}$)	71
4.18	Uncoupled stress profiles at various depths (Material P1 with $v_a = 0.85$ and $\ell = 0.1 \text{ in}$)	72
4.19	Coupled particle acceleration profiles at various depths (Material P1 with $v_{a_o} = 0.85$, $\ell = 0.1 \text{ in}$, and $M = 0.04 \text{ in}^2/\text{lb}$)	73
4.20	Coupled particle velocity profiles at various depths (Material P1 with $v_{a_o} = 0.85$, $\ell = 0.1 \text{ in}$, and $M = 0.04 \text{ in}^2/\text{lb}$)	74
4.21	Coupled particle displacement profiles at various depths (Material P1 with $v_{a_o} = 0.85$, $\ell = 0.1 \text{ in}$, and $M = 0.04 \text{ in}^2/\text{lb}$)	75
4.22	Coupled stress profiles at various depths (Material P1 with $v_{a_o} = 0.85$, $\ell = 0.1 \text{ in}$, and $M = 0.04 \text{ in}^2/\text{lb}$)	76
4.23	Probabilistic acceleration profiles at various depths; mean response with its one-standard-deviation bounds for $\bar{\ell} = 0.1 \text{ in}$ and $\sigma_{\ell} = 0.03 \text{ in}$	77
4.24	Probabilistic velocity profiles at various depths; mean response with its one-standard-deviation bounds for $\bar{\ell} = 0.1 \text{ in}$ and $\sigma_{\ell} = 0.03 \text{ in}$	78
4.25	Probabilistic displacement profiles at various depths; mean response with its one-standard-deviation bounds for $\bar{\ell} = 0.1 \text{ in}$ and $\sigma_{\ell} = 0.03 \text{ in}$	79
4.26	Probabilistic stress profiles at various depths; mean response with its one-standard-deviation bounds for $\bar{\ell} = 0.1 \text{ in}$ and $\sigma_{\ell} = 0.03 \text{ in}$	80

CONVERSION FACTORS, NON-SI TO SI (METRIC)
UNITS OF MEASUREMENT

Non-SI units of measurement used in this report can be converted to SI (metric) units as follows:

<u>Multiply</u>	<u>By</u>	<u>To Obtain</u>
inches	25.4	millimeters
kips (force) per square inch	6.894757	megapascals
pounds (force) per square inch	6.894757	kilopascals
pounds (mass)	0.4535924	kilograms
pounds (mass) per cubic foot	16.01846	kilograms per cubic meter
square inches	6.4516	square centimeters
feet per second	0.3048	meters per second
inches per second	0.0254	meters per second
pounds (force)- seconds squared per inches fourth	10686893.0	kilograms per cubic meter

A STUDY OF EXPLOSIVE WAVE PROPAGATION IN
GRANULAR MATERIALS WITH MICROSTRUCTURE

CHAPTER 1

INTRODUCTION

1.1 BACKGROUND

Traditionally, in engineering practice, all stress analyses are conducted within the framework of various branches of continuum mechanics. In doing so, it is tacitly assumed that the microstructural details of the material can be neglected. The material is then "replaced" by an equivalent continuum with gross, or "overall," properties. The continuum approach has indeed been very successful and has led to the development of many useful theories of material characterization. On the other hand, since these theories disregard the microstructural details of the materials under study, they cannot be used to determine how local structure influences the gross behavior of the material. This is a real shortcoming of the continuum theories, especially when they are applied for characterization of geological materials such as sand, clay and/or rock. These types of materials are commonly classified as materials with microstructure since, at the micro level, the density, along with other important variables, are not continuous. Modeling of these materials using classical continuum mechanics (e.g., elasticity, plasticity, viscoelasticity, etc.) has progressed to a point where any fundamentally new information will probably have to come from a theory incorporating properties such as grain size, local porosity, packing, etc. Some advances have been made recently in developing analytical tools and models, which account for some of the structural details of particulate materials such as sand. Two examples of such work are: (1) the so-called "distributed body" concept advanced by Goodman and Cowin (Reference 31) and (2) "discrete element" modeling pioneered by Cundall (Reference 20). The central theme of the distributed body concept is the introduction of the "volume distribution function" (a new kinematic variable) which accounts for local porosity and its spatial gradient. The discrete element concept is basically a numerical procedure requiring large computer simulations of grain-to-grain interaction.

The objective of this investigation was to develop a theoretical framework, and the associated computer software, based on the distributed body concept for studying plane wave propagation in granular materials due to airblast loading. This theory will allow specific relationships to be developed between microstructure and wave propagation variables. Wave propagation studies based on the distributed body concept were originally conducted by Nunziato, Walsh, et al. (References 57-63). The present investigation will extend their pioneering work to incorporate (1) a more realistic depth-dependent volume distribution function simulating gravity effects in granular soil, (2) arbitrary surface input including finite times for loading and unloading waves, and (3) probabilistic considerations for treating non-uniform grain size and random distribution of local porosity.

1.2 SCOPE

Chapter 2 contains a literature study of previous work in micromechanics and a summary of the Nunziato, Walsh, et al., distributed body wave propagation studies. Extension of this theory to include items 1 through 3 in the above paragraph is documented in Chapter 3. Parametric results from the extended theory are presented in Chapter 4. A summary and recommendations are given in Chapter 5. Finally, a user's guide for the microstructural wave propagation code MIC1D is given in Appendix A.

CHAPTER 2

REVIEW OF PREVIOUS WORK

2.1 GENERAL BACKGROUND

Studies of geological materials with microstructure started many years ago with research on granular materials modeled as aggregate assemblies of discs or spheres. An excellent review article by Deresiewicz (Reference 22) presents both static and dynamic studies prior to 1958. Another more recent review article by Krizek (Reference 48) appeared in 1971, and presented basically the dynamic response of cohesionless granular soils. Three recent symposia on this subject (References 16, 45, and 83) have indicated renewed research interest.

The concept of modeling granular media as an array of elastic particles (spheres or discs) lead to the initial attempts at predicting wave propagation through such media. Early work by Iida (References 41 and 42), Takahashi and Sato (Reference 79), Hughes and Cross (Reference 39), Hughes and Kelly (Reference 40), Gassman (Reference 33) and Brandt (Reference 4) employed a normal granular contact force concept. This initial work investigated the propagation velocity as a function of confining pressure, particle size and aggregate geometry.

It was discovered, however, that the classical theory of contact due only to normal forces does not, in general, accurately model real materials. With this in mind, Duffy and Mindlin (Reference 26) proposed a theory for granular media which included both normal and tangential contact forces. This theory produced a nonlinear and inelastic stress-strain relation. Hendron (Reference 34) has also done work in this area.

More recent theories of granular media have included statistical-stochastic approaches, e.g., Hudson (Reference 38), Fletcher (Reference 29), Fu (Reference 30), Chambre (Reference 9), Varadan, et al., (Reference 81) and Endley and Peyrot (Reference 28). Quite recently, Mroz (Reference 53) and Kuo (Reference 49) employed continuum plasticity concepts and general contact theory in an attempt to unify the treatment of granular materials at both the particulate and continuum levels. Cundall, et al., (References 20 and 21) proposed a numerical method called the discrete element technique for granular and rock assemblies, and Brown, et al., (Reference 5) have used this approach for rubble screens. Morland (Reference 52) considered a rock/granular media

as a regularly jointed media and used an anisotropic elasticity approach. Particulate media has also been studied by Hill and Harr (Reference 36) based upon a diffusion equation derived from probabilistic models, while Soo (Reference 78) has considered the dynamic interactions of granules. Rohani, et al., (References 43, 71, and 72) have been doing wave propagation research in this area for granular sands and layered soils using continuum models. Endochronic theories have also been applied to granular soils, e.g., Read and Valanis (Reference 70), Lin and Wu (Reference 50), and Bazant, et al., (Reference 2). Studies have been made of the propagation of waves through elastic materials containing spherical inclusions, e.g., Mal and Bose (Reference 51). Bleich, et al., (Reference 3) employed an elastic-plastic constitutive law to model a specific geomechanics boundary value problem. Fluid saturated granular media have been studied by Garg, et al. (Reference 32), Hsieh and Yew (Reference 37), Vardoulakis and Beskos (Reference 82) and Zienkiewicz and Shiomi (Reference 84). Nachlinger and Nunziato (Reference 55) used an internal state variable approach to wave propagation problems. Modern mixture theories (References 25, 64-66, 68, and 69) also show some promise of modeling porous and/or granular media.

With regard to experimental work, the method of photoelasticity has been used. This particular method is quite well suited for studying the detailed load transfer between individual granules as whole field data are obtained during the experiment. Photoelasticity has been used for granular media by Drescher and de Josselin de Jong (Reference 23), Drescher (Reference 24), and Durelli and Wu (Reference 27). This work was, however, only for static behavior. The only dynamic analysis of granular media employing photoelasticity was performed by Rossmannith and Shukla (Reference 75). Their technique employed the use of high speed photography to record wave propagation through an assembly of birefringent discs.

Of the previous work, three new constitutive theories which show special promise in modeling granular and porous media are: the so-called "pore-collapse" models (References 6-8, 33, 46, and 47); the microstructural models based upon "fabric tensors" (References 11, 44, 45, 56, and 67); and the Goodman-Cowin distributed body approach (References 1, 12-18, 31, and 80). The pore-collapse model, originally developed by Carrol and Holt, is based upon the collapse of a single pore within the media. Researchers at the Sandia National Laboratories have used this approach with some success to

model the dynamic response of porous and granular media. This theory, however, cannot relate the effects of neighboring pores on one another, and, hence, the effect of pore distribution cannot be accounted for. With regard to the Goodman-Cowin distributed body theory, the medium is assumed to be distributed in space by an independent kinematical function called the volume distribution function. Nunziato, Walsh, et al., (References 57-63) have applied this theory to several wave propagation studies and found success in modeling particular situations. Consequently, this particular theory looks quite fruitful. The fabric tensor models proposed by Oda, Nemat-Nasser, et al., (Reference 67) also look promising; however, their application to specific boundary value problems appears to be several years away. At present, they are looking at the details of the microstructural fabric, and they eventually may give insight as to the nature of the volume distribution function for a Goodman-Cowin body.

2.2 DISTRIBUTED BODY THEORY

The distributed body theory originally developed by Cowin and Goodman was constructed to allow a continuum theory to be applied to materials with noncontinuous fields of mass density, stress, body force, etc. Thus, the model could be used to describe the behavior of a wide variety of materials having granular and/or porous structures. Fundamental to the theory is the assumption that, at any point in the material, the overall mass density ρ may be written as

$$\rho = v\gamma \quad (2.1)$$

where γ is the density of the granules (or matrix material) and $v = v(X,t)$ is referred to as the volume distribution function. This function describes the way the medium is distributed in space allowing for voids or other particular granular structures. Thus, the theory uncouples the mass density of the granules from the mass density of the entire material, and allows compressibility due to both granule compressibility and void compaction. In general, $0 < v \leq 1$, and v is related to the porosity n and void ratio e by the expression

$$v = 1 - n = \frac{1}{1+e} \quad (2.2)$$

Within a one-dimensional framework, the classical balance law of conservation of linear momentum reads

$$\rho_o \ddot{x} = \frac{\partial T}{\partial X} + \rho_o b \quad (2.3)$$

where T is the stress, b is the body force, x is the particle position, \ddot{x} is the particle acceleration, X is the reference position coordinate, and subscript o denotes values in reference state. In addition to this classical balance law, the distributed body theory also requires an independent balance equation governing the volume distribution. In one dimension, this second equation governing void change is given by

$$\rho_o k \ddot{v} = \frac{\partial h}{\partial X} + \rho_o g \quad (2.4)$$

where k is called the equilibrated inertia, h the equilibrated stress and g the intrinsic body force. Physical interpretation of the microstructural variables k , h and g is somewhat difficult to make. In general, these variables are related to the local contact mechanics at the granular level and can be related to particular self-equilibrated singular stress states from classical elasticity (e.g., double force systems, centers of dilatation). It has been proposed (Reference 63) that k is related to the void mean surface area and to the number of voids present, h is a result of the interaction forces between neighboring voids and will vanish when the voids are sufficiently separated, and g is related to the coupling between the total deformation of the medium and the changes in void volume.

For granular geological materials, we assume that the media is composed of compressible granules at relatively high confining pressures so as to prevent material flow. For this case, an appropriate constitutive formulation would read

$$T = T(v_o, v, \frac{\partial v}{\partial X}, \epsilon) \quad (2.5)$$

and, hence, the stress depends upon the reference and current volume distributions, the gradient of the volume distribution, and the strain ϵ . An explicit form of Equation 2.5 which has been proposed (References 31 and 61) uses an even quadratic form in the gradient of v ,

$$T = v [\Lambda(v_0, v, \epsilon) + \frac{1}{2} \alpha(v_0, v, \epsilon) \left(\frac{\partial v}{\partial X}\right)^2] \quad (2.6)$$

where Λ and α are two material functions of the indicated variables. First and second order moduli defined by

$$\begin{aligned} E &= \frac{\partial T}{\partial \epsilon} = v [\Lambda_{\epsilon} + \frac{1}{2} \alpha_{\epsilon} \left(\frac{\partial v}{\partial X}\right)^2] \\ \bar{E} &= \frac{\partial^2 T}{\partial \epsilon^2} = v [\Lambda_{\epsilon\epsilon} + \frac{1}{2} \alpha_{\epsilon\epsilon} \left(\frac{\partial v}{\partial X}\right)^2] \end{aligned} \quad (2.7)$$

will be needed for subsequent wave analyses. Normally $E > 0$, but the second order modulus \bar{E} may be positive or negative.

2.3 WAVE PROPAGATION WITHIN A DISTRIBUTED BODY

As previously mentioned, the wave propagation theories set forth by Nunziato, Walsh and coworkers for Goodman-Cowin distributed bodies appear to have excellent promise for application to granular geological materials. This section will briefly review some basic details and previous results about these theories.

The basic premise of this particular wave theory lies in modeling the wave as a propagating singular surface across which there exists a jump discontinuity in a particular variable. Commonly dynamic loadings will produce second-order acceleration waves, having a jump discontinuity in the particle acceleration at the wave front. In some cases, however, the loading could produce a first-order shock wave, having a jump in the particle velocity at the wave front. Most modeling in these materials has been done for acceleration waves, and this case will now be described.

As mentioned, a wave is modeled as a propagating singular surface of zero thickness with speed U , see Figure 2.1. The jump of a quantity ϕ across this surface is defined by

$$[\phi] = \phi^- - \phi^+ \quad (2.8)$$

where ϕ^+ and ϕ^- are the limiting values of ϕ immediately ahead of and behind the wave. An acceleration wave is therefore defined as a wave across

which the particle velocity, strain, and volume distribution are continuous but their spatial and temporal derivatives are not. Thus, this type of motion carries propagating discontinuities in the particle acceleration and various other gradients of the strain and volume distribution. The jump in the particle acceleration $[\ddot{x}]$ is called the wave amplitude, and will be denoted by $a(t)$. Note that for compressive waves, $a(t) > 0$, while for expansive waves, $a(t) < 0$.

Following singular surface analysis procedures which have now become somewhat standardized (Reference 10), Nunziato, et al., developed the following expressions for two different types of waves

$$\begin{aligned} U_F^2 &= \frac{1}{2} \left[C_1^2 + C_2^2 + \sqrt{(C_1^2 - C_2^2)^2 + 4\beta} \right] \\ U_S^2 &= \frac{1}{2} \left[C_1^2 + C_2^2 - \sqrt{(C_1^2 - C_2^2)^2 + 4\beta} \right] \end{aligned} \quad (2.9)$$

where

$$C_1^2 = \frac{(vT_\epsilon)^+}{\rho_0 v_0}, \quad C_2^2 = \frac{(h_{vX})^+}{\rho_0 k}, \quad \beta = \left(\frac{v}{v_0}\right)^+ \frac{(h_F)^+(T_{vX})^+}{\rho_0 k} \quad (2.10)$$

with subscripts ϵ , v , and X meaning partial differentiation with respect to the indicated variable, and $(\cdot)^+$ meaning immediately ahead of the wave. The speed U_F denotes the "fast" wave speed which is associated predominantly with the elasticity of the granules. The quantity U_S is the "slow" wave speed and is connected to the compressibility of the material due to consolidation.

The wave amplitude a , which is equal to the jump discontinuity in the acceleration across the wave front, has also been studied. Nunziato, et al., have found that the amplitude for one-dimensional wave propagation satisfies the following nonlinear Bernoulli equation

$$\frac{da}{dX} = \kappa(X)a^2 - \mu(X)a \quad (2.11)$$

where $\mu(X)$ and $\kappa(X)$ are material coefficients given in general by rather lengthy expressions. The coefficient $\mu(X)$ is related to dispersive effects,

while $\kappa(X)$ reflects both the elastic response of the granules and dispersive effects. Depending on the nature of κ and μ , the theory can predict growth or decay of wave amplitude.

Nunziato, et al., (Reference 61) presented an application of these general theoretical results to a specific granular medium, PBX-9404 (an explosive powder). They chose a volume distribution to be periodic in nature, i.e.,

$$v_o(X) = v_a + (1 - v_a) \cos \frac{2\pi X}{l} \quad (2.12)$$

where v_a is a material constant, and l is a characteristic length presumably related to the grain size. For PBX-9404, $v_a = 0.984$ and $l = 1.5$ mm were chosen. The specific constitutive form for this application was selected as that given in Equation 2.6.

Using the previous specific forms and assuming that the wave starts at $X = 0$ in a granule, the fast wave speed becomes

$$U_F^2 = U_g^2 [1 - M^2 \sin^2 \frac{2\pi X}{l}] \quad (2.13)$$

where U_g is the wave speed in a granule and

$$M^2 = - \frac{2(1 - v_a)^2 \pi^2}{\gamma_o U_g^2 l^2} (\alpha_\epsilon)_o \quad (2.14)$$

In attempting to compare with experimental data, Nunziato, et al., (Reference 61) point out that what is actually measured is the transit time of the wave τ . This quantity is a function of the propagation distance X , and is related to the average wave velocity \bar{U} by the expression

$$\bar{U}(X) = \frac{X}{\tau(X)} \quad (2.15)$$

Applying this to the fast wave, one can write

$$\tau(X) = \int_0^X \frac{d\xi}{U_F(\xi)} = \frac{1}{U_g} \int_0^X \frac{d\xi}{\left[1 - M^2 \sin^2 \frac{2\pi \xi}{l}\right]^{1/2}} \quad (2.16)$$

which can be expressed in terms of an elliptic integral of the first kind F , i.e.,

$$\tau(X) = \frac{l}{2\pi U_g} F(2\pi X/l, M) \quad (2.17)$$

Using the boundary condition $\tau(l) = \tau_g$, with known values of U_g , τ_g , and l yields an equation whose root gives the value of M . For PBX-9404, with $U_g = 3.71$ km/s and $\tau_g = 0.4934$ μ s, Equation 2.17 yields $M = 0.7525$.

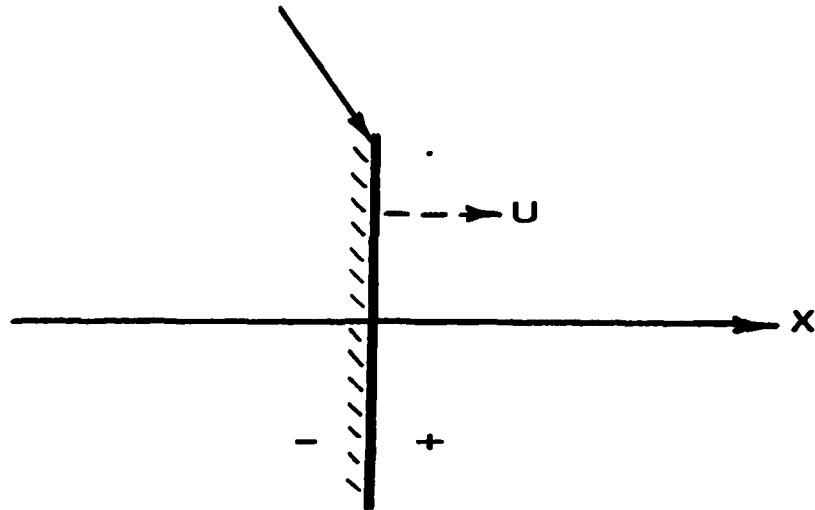
The amplitude behavior is governed by Equation 2.11 and, for this specific case, the coefficients κ and μ become

$$\begin{aligned} \kappa(X) &= -\frac{1}{2\gamma_o U_F} \left[(\Lambda_{\epsilon\epsilon})_o + \frac{1}{2} (\alpha_{\epsilon\epsilon})_o \left(\frac{\partial v}{\partial X} \right)_o^2 \right] \\ \mu(X) &= \frac{1}{2U_F^2} \left[\frac{U_F^2}{v_o} + \frac{(\alpha_{\epsilon})_o}{2\gamma_o} \left(\frac{\partial^2 v}{\partial X^2} \right)_o \right] \left(\frac{\partial v}{\partial X} \right)_o \end{aligned} \quad (2.18)$$

Again, for the specific material PBX-9404, Nunziato, et al., using low-amplitude shock wave experiments, found that $(\Lambda_{\epsilon\epsilon})_o = -58$ GPa and $(\alpha_{\epsilon\epsilon})_o = 7.31 \times 10^5$ GPa - mm².

Further developments of this theory, along with a general purpose computer program, have been developed by Sadd (Reference 76), to evaluate the average wave speed and amplitude behavior. Typical results for the specific material values for PBX-9404 are shown in Figures 2.2 and 2.3. Figure 2.2 illustrates the behavior of the average wave speed with propagation distance. It is evident that the microstructural effects predominate at initial distances producing a large variation in wave speed. Gradually, as the wave moves further into the medium, the speed has less variation and approaches a constant value. The amplitude behavior with propagation distance is shown in Figure 2.3 for the case of an initial amplitude of 2.7 Gm/s². For this case, the amplitude decays with a superimposed periodic oscillation. Nunziato, et al., (Reference 61) also presented actual speed and amplitude experimental data for this material and found fairly good agreement with the theory.

SINGULAR SURFACE WAVE



Propagating Discontinuity: $[\phi] = \phi^- - \phi^+$

Wave Amplitude: $a = [\ddot{x}]$

Figure 2.1. Schematic of a propagating singular surface.

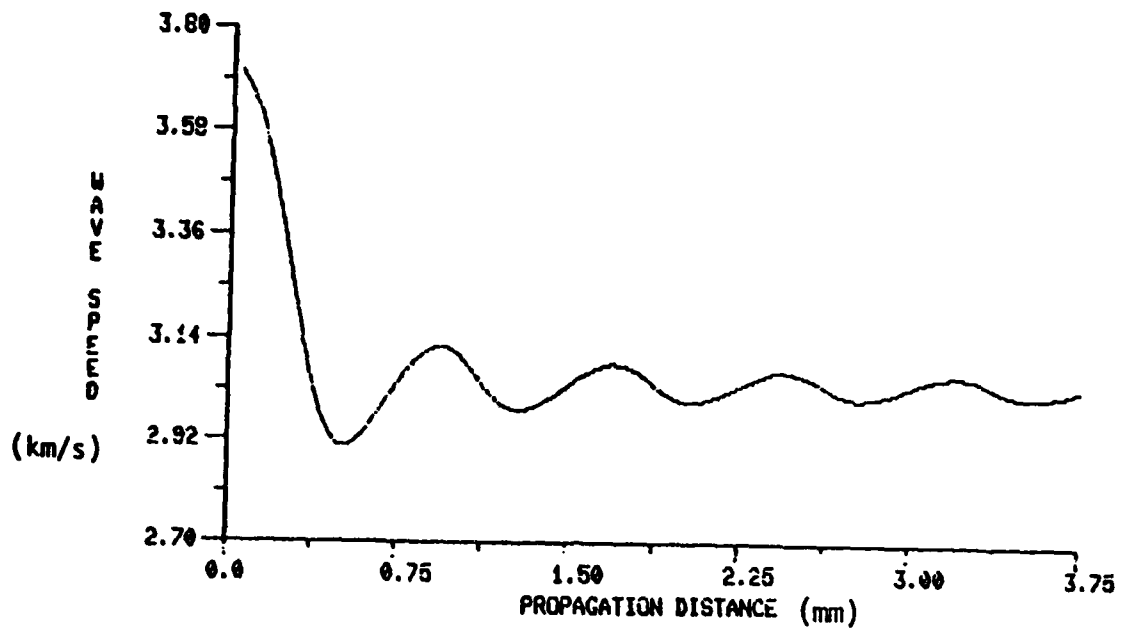


Figure 2.2. Average wave speed versus distance; Reference 61 data.

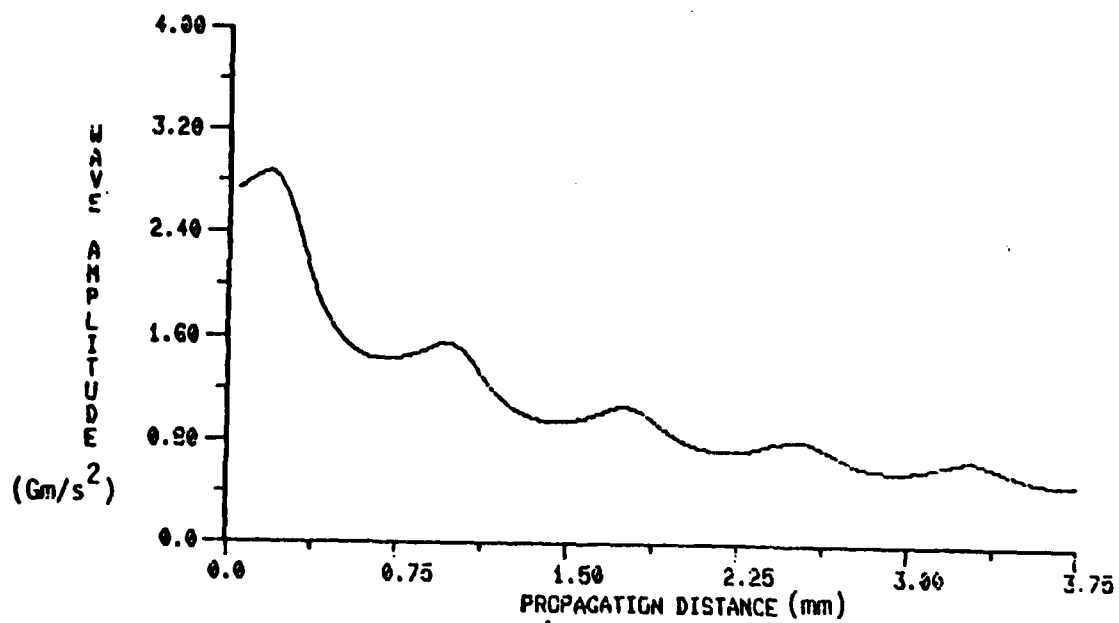


Figure 2.3. Amplitude behavior versus distance; Reference 61 data.

CHAPTER 3

DEVELOPMENT OF WAVE PROPAGATION THEORY

3.1 GENERAL

The major purpose of the research, herein reported was to develop a one-dimensional wave propagation theory and associated computer code incorporating the distributed body theory to account for material microstructure. The developed theory is general in that it can handle a variety of volume distribution functions, and, thus, it can model several types of microstructure. In addition, the theory has been extended to include the wave motion description of more than simply one singular surface as discussed previously in Section 2.3. In this regard, a wave profile constructed of several singular surface waves has been analyzed. An uncoupled theory in which each wave propagates independently has been developed. In addition, a coupled theory incorporating microstructural changes with the passage of each wave in a profile has also been constructed. The final step of the theoretical work was to construct a probabilistic analysis based upon the developed code using a moment-generating procedure due to Rosenblueth (Reference 73). The probabilistic analysis allows for the treatment of grain size and local porosity as random variables. The following sections discuss in detail each of these developments.

3.2 VOLUME DISTRIBUTION FUNCTIONS

In order to apply the distributed body theory and develop a wave propagation analysis, it is necessary to have explicit constitutive forms, see for example Equation 2.6, and the initial volume distribution $v_0(X)$ must also be specified. Any proposed volume distribution function should reflect the density variations and other microstructural features within the material. It is difficult to construct such a function which characterizes these variations precisely and yet has the smoothness requirements to be compatible with the theory. We will follow the approach that $v_0(X)$ should be a continuous function in order to perform certain required differentiations and integrations and that it yield the correct average density.

As discussed previously in Section 2.3, Nunziato, et al., (Reference 61) in constructing a wave propagation analysis, developed a specific volume distribution function. Their work was for a granular material, PBX-9404, an

explosive powder/binder system. They proposed a periodic structure of the form

$$v_o(X) = v_a + (1 - v_a) \cos \frac{2\pi X}{l} \quad (3.1)$$

where v_a and l are material constants. This function is plotted in Figure 3.1 versus the distance coordinate.

The quantity v_a would be given by the overall density of the material divided by the granule density and is thus related to the average value of the volume distribution. The second material constant l is referred to as a characteristic length associated with this periodic structure. Clearly l specifies the length of the repeating units of the microstructure. For granular materials, l would be related, but not necessarily equal, to the average grain size.

In regard to this characteristic length, the work of Shahinpoor (Reference 77) is appropriate to consider. Shahinpoor did experiments of randomly packed spherical granules on a flat surface. His work demonstrated the concept of distinct packing geometries referred to as Voronoi cells, see Figure 3.2. It is evident that for some packing geometries, if a periodic structure is assumed, the characteristic length l , being equal to the Voronoi cell size, could be several grain diameters.

Since the mechanical response of most geological materials like sand or gravel is affected by in situ conditions such as overburden, the microstructure will be nonhomogeneous, i.e., be depth dependent. With this in mind, a new volume distribution function was developed which can predict such a structure. One particular form uses an exponential factor and may be written as

$$v_o(X) = 1 - (1 - v_b)e^{-BYX} \quad (3.2)$$

where v_b , B , and Y are material constants. A plot of this distribution function is shown in Figure 3.3. Clearly for this case, the material becomes more dense with depth X into the medium. The constant v_b is the volume distribution at the free surface $X = 0$, Y is the average density of the material, and the constant B determines the rate of consolidation with depth. It should be pointed out that this exponential form does not contain

any periodic structure; hence, it should produce monotonic results for the wave propagation characteristics.

Another volume distribution function which was used involves the combination of the periodic form given by Equation 3.1 and the exponential form from Equation 3.2. The combined form involves simply the product of these two relations, i.e.,

$$v_o(X) = [v_a + (1 - v_a) \cos \frac{2\pi X}{l}] [1 - (1 - v_b) e^{-BYX}] \quad (3.3)$$

and again v_a , v_b , l , B and γ are material constants. It is evident that this form (shown in Figure 3.4) will thus produce a combined periodic-exponential depth dependent microstructure.

During the course of this investigation, other forms of the volume distribution function were developed including algebraic and additive periodic-exponential forms. However, the three forms given by Equations 3.1-3.3 appear to provide a broad enough microstructure model for the objectives of this research. Consequently, only these three forms will be included in the remaining sections of this report.

3.3 WAVE PROPAGATION ANALYSIS

The wave propagation analysis and the development of an associated computer code was done based upon the previous fundamental work of Goodman and Cowin (Reference 31) and Nunziato, et al. (Reference 61). The constitutive form given by Equation 2.6 was also used in this work. Equation 2.6 was used by Nunziato, et al., but was originally proposed by Goodman and Cowin in 1972. The constitutive dependence on the gradient of the volume distribution $\frac{\partial v}{\partial X}$ is significant and allows an equilibrium stress to depend on $\frac{\partial v}{\partial X}$. Since Equation 2.6 involves the square of $\frac{\partial v}{\partial X}$, it will be an isotropic form in that variable (required by material frame indifference) and, hence, the stress response will be independent of the sign of the gradient. Also, the presence of the gradient term allows the theory to predict a generalized Mohr-Coulomb failure criterion (Reference 31).

Obviously, the two material functions Λ and α defined in Equation 2.6 will specify the response of the medium to deformation. Equation 2.6 indicates that the material function α , specifies the effect of the gradient of the volume distribution. If α is small, then the stress will not be

significantly influenced by $\frac{\partial v}{\partial X}$. For a stress-free reference state (zero strain state),

$$\begin{aligned}\Lambda(v_0, v_0, 0) &= 0 \\ \alpha(v_0, v_0, 0) &= 0\end{aligned}\tag{3.4}$$

Considering the stress-strain behavior which could come from Equation 2.6, Figure 3.5 illustrates some typical curves for various volume distribution functions. It should be pointed out that the shape of this curve could vary considerably for various types of geological materials and is a function of rate of loading. This figure demonstrates the stress-strain behavior of the granular assembly medium accounting for the particular reference values of $v(X)$ and $\frac{\partial v}{\partial X}$, i.e.,

$$T = T(X, \epsilon) = T(v_0, v_0, \left(\frac{\partial v}{\partial X}\right)_0, \epsilon)\tag{3.5}$$

From such typical behavior as shown in Figure 3.5, it is apparent that the two moduli E and \tilde{E} given by Equation 2.7 would satisfy the relations

$$\begin{aligned}E &= \frac{\partial T}{\partial \epsilon} > 0 \\ \tilde{E} &= \frac{\partial^2 T}{\partial \epsilon^2} \geq 0\end{aligned}\tag{3.6}$$

In particular, from the theory, it can be shown that the fast wave speed given by Equation 2.9, can also be written as

$$U_F = \sqrt{E_0 / v_0 \gamma_0}\tag{3.7}$$

where γ_0 is the density of the granules, and E is to be evaluated in the reference state. Consequently, for real wave speeds $E > 0$, and from Equation 2.7, this means that

$$E = v \left[\Lambda_\epsilon + \frac{1}{2} \alpha_\epsilon \left(\frac{\partial v}{\partial X} \right)^2 \right] > 0\tag{3.8}$$

or since $0 < v < 1$,

$$\Lambda_{\epsilon} + \frac{1}{2} \alpha_{\epsilon} \left(\frac{\partial v}{\partial X} \right)^2 > 0 \quad (3.9)$$

where subscripts on Λ and α mean partial differentiation. Equation 3.9 then gives a condition that the material functions Λ and α must satisfy for a given volume distribution.

With regard to the amplitude behavior, it was shown that the amplitude obeyed the differential equation given by Equation 2.11. By combining Equations 2.7 with 2.18, it becomes apparent that the coefficient κ is related to E by

$$\kappa = - \frac{\bar{E}}{2\gamma_0 U_F^2 v} \quad (3.10)$$

and, hence, the curvature of the stress-strain curve will affect the amplitude behavior.

In order to further elaborate on the constitutive relationship of this theory, consider the following special cases:

(1) Uniform Volume Distribution:

For this case, $v = \bar{v} = \text{constant}$, and so Equation 2.6 yields

$$T = T(\epsilon) = \bar{v} \Lambda(\bar{v}, \bar{v}, \epsilon) \quad (3.11)$$

which can be interpreted as a nonlinear elastic/plastic material. Consequently, the material parameter Λ is associated with constitutive behavior of the microstructural media based upon the local volume distribution but neglecting distribution gradients. Wave propagation studies for this case reduce to the classical one-dimensional plastic wave motion analyses (see Cristescu, Reference 19).

(2) Homogeneous Elastic Case:

For the reduction to linear elasticity, the volume distribution is taken to be unity, i.e., $v = 1$. Hence, from Equation 3.11

$$T = \Lambda(1, 1, \epsilon) \quad (3.12)$$

and for the linear elastic case,

$$\Lambda(1, 1, \epsilon) = E\epsilon \quad (3.13)$$

where E is the elastic modulus and is identical to the first order modulus previously defined in Equation 2.7. Wave motion analysis for this case yields the well known results

$$U = \sqrt{E/\rho}$$

$$a = a_0 = \text{constant} \quad (3.14)$$

Based upon this wave motion analysis, a computer code* was developed to handle any of three volume distribution functions given by Equations 3.1-3.3. The constitutive form incorporates Equation 2.6, with specific values for the two material functions Λ and α to be input by the user. The code uses general techniques of numerical integration using four-point Gauss quadrature to calculate the necessary integrals for computation of the average wave speed, see Equations 2.15 and 2.16. In addition, a fourth order Runge-Kutta scheme is used to solve the nonlinear amplitude Equation 2.11. Thus, the basic features of the code were to calculate the wave speed and amplitude (particle acceleration) at various positions and times.

Typical results of the code are shown in Figures 3.6-3.14. The first set of figures (Figures 3.6-3.8), illustrates results using the periodic volume distribution function given by Equation 3.1. Recall this distribution function was shown in Figure 3.1. The specific material parameters for these results are $v_a = 0.85$, $l = 0.1$ in, $\gamma_0 = 2.4 \times 10^{-4}$ lb-sec²/in⁴, $\alpha_\epsilon = -450$ lb, $\alpha_{\epsilon\epsilon} = 1 \times 10^9$ lb, $\Lambda_\epsilon = 3 \times 10^5$ lb/in², $\Lambda_{\epsilon\epsilon} = -1 \times 10^6$ lb/in². This material will be referred to as Material P1. The actual wave speed behavior shown in Figure 3.6 varies periodically, as given by Equation 2.13. However, the average wave speed will oscillate initially and then approach a constant value, as shown in Figure 3.7. The behavior of the amplitude ratio (normalized by a_0) is shown in Figure 3.8

* The computer code is referred to as MIC1D.

and illustrates the expected effect of the initial amplitude on the attenuation rate; i.e., the higher a_0 , the larger the attenuation.

Figures 3.9-3.11 show the corresponding results for the exponential volume distribution specified in Equation 3.2 and shown in Figure 3.3.

Material parameters for this case are $v_b = 0.65$,

$$\gamma_0 = 2.4 \times 10^{-4} \text{ lb-sec}^2/\text{in}^4, \alpha_e = -8 \times 10^6 \text{ lb}, \alpha_{ee} = 4.8 \times 10^8 \text{ lb},$$

$$\Lambda_e = 3 \times 10^5 \text{ lb/in}^2, \Lambda_{ee} = -1.0 \text{ lb/in}^2, B = 10 \text{ in}^2/\text{lb},$$

$$\gamma = 7.2 \times 10^{-2} \text{ lb/in}^3. \text{ This material will be referred to as Material E1.}$$

The wave speed (shown in Figures 3.9 and 3.10) is now a monotonically increasing function with depth X since the porosity is decreasing in that direction. Furthermore, the amplitude behavior shown in Figure 3.11 illustrates a much less pronounced attenuation rate when compared with the periodic volume distribution results in Figure 3.8. The reason for this behavior is the fact that, for the exponential distribution function, the material response rapidly approaches with depth that of an elastic material.

Finally, results of using the combined periodic-exponential volume distribution function given by Equation 3.3 are shown in Figures 3.12-3.14.

Again, this particular distribution function was shown previously in

Figure 3.4. Model parameters for this case are $v_a = 0.992$, $v_b = 0.65$,

$$l = 0.06 \text{ in}, \gamma_0 = 2.4 \times 10^{-4} \text{ lb-sec}^2/\text{in}^4, \gamma = 7.2 \times 10^{-2} \text{ lb/in}^3,$$

$$B = 30 \text{ in}^2/\text{lb}, \alpha_e = -3 \times 10^5 \text{ lb}, \alpha_{ee} = 5 \times 10^8 \text{ lb}, \Lambda_e = 3 \times 10^5 \text{ lb/in}^2,$$

$$\Lambda_{ee} = -750 \text{ lb/in}^2. \text{ This material will be referred to as Material PE1.}$$

Results for wave speed and amplitude attenuation indicate combined features of each of the two previous distribution functions.

Additional features to calculate particle velocity and displacement, stress, wave profile behavior, and probabilistic effects were also added to the basic code. These developments are discussed in the next two sections.

3.4 WAVE PROFILE ANALYSIS

This section describes the efforts to extend the basic theory to predict wave profile behavior where the wave would have a definite rise time. This situation requires that consideration be given to a train of waves moving together. The previous modeling of treating a wave as a singular surface of zero thickness and duration must be modified. Figure 3.15 illustrates the

procedure of constructing a profile from a series of impulsive singular waves. The central complication in this procedure is the fact that wave analyses are required for the cases of waves traveling behind one another. What this means is that, with the exception of the leading wave, all waves will be moving into media which are undergoing non-stationary deformation. If the wave is moving into a region which is not at rest in its reference configuration, then the analysis for the wave speed and the amplitude attenuation will be greatly complicated.

A simple example of this complication may be seen from the wave speed relations given in Equation 2.9. The velocity of propagation was given by an equation containing terms

$$C_1^2 = \frac{(vT_\epsilon)^+}{\rho_0 v_0}, \quad C_2^2 = \frac{(h_{v_X})^+}{\rho_0 k}, \quad \beta = \left(\frac{v}{v_0}\right)^+ - \frac{(h_f)^+ (T_{v_X})^+}{\rho_0 k} \quad (3.15)$$

with T_ϵ^+ , $h_{v_X}^+$ and $T_{v_X}^+$ being moduli evaluated immediately in front of the given wave and where $T_\epsilon = \frac{\partial T}{\partial \epsilon}$, $h_{v_X} = \frac{\partial h}{\partial v_X}$, and $T_{v_X} = \frac{\partial T}{\partial v_X}$. Clearly, the state of the material ahead of the wave as specified by the terms T_ϵ^+ , $h_{v_X}^+$, $T_{v_X}^+$ will have a complicating effect on the calculation of the wave speed.

Note that the quantity β will vanish if the wave is moving into a region which is stress free. The state of affairs is considerably worse for the case of the wave amplitude analysis where the coefficients of Equation 2.11 become quite long and complicated functions of the deformation state in front of the wave.

It was decided that, in light of the time restrictions of the current investigation, the analysis of constructing a profile from a group of traveling waves be made under the simplifying assumption that the propagational characteristics of each wave depend solely upon the volume distribution at the wave front. This volume distribution, in turn, depends upon the current stress state at the wave front. What this means is that waves traveling behind the leading wave will feel a different material caused by the change of stress due to all previous waves.

In order to employ this modeling concept, a method to compute the stress associated with a singular surface wave must be developed. Recall that the amplitude of the wave was originally defined as the jump in the media acceleration, i.e.,

$$a = [\ddot{x}] = \ddot{x}^- - \ddot{x}^+ \quad (3.16)$$

where \ddot{x}^+ and \ddot{x}^- are the limiting values of the acceleration just ahead of and behind the singular surface wave. The equation of motion was given by

$$\rho_0 \ddot{x} = \frac{\partial T}{\partial X} + \rho_0 b \quad (3.17)$$

where T is the stress and b is the body force which is continuous everywhere.

Using the basic definition for Equation 3.16, we evaluate the jump of Equation 3.17 across a typical wave

$$\rho_0 [\ddot{x}] = \left[\frac{\partial T}{\partial X} \right] + \rho_0 [b]$$

which, if the body force is continuous, can be written as

$$\nu_0 \gamma_0 a = \left(\frac{\partial T}{\partial X} \right)^- - \left(\frac{\partial T}{\partial X} \right)^+$$

and, thus, we can write an expression for the stress gradient behind a given wave in terms of the gradient in front of the wave as

$$\left(\frac{\partial T}{\partial X} \right)^- = \nu_0 \gamma_0 a + \left(\frac{\partial T}{\partial X} \right)^+ \quad (3.18)$$

Next, by using a simple differencing scheme

$$\frac{T_{n+1} - T_n}{(\Delta X)_n} = \left(\frac{\partial T}{\partial X} \right)_n^- \quad (3.19)$$

and so,

$$T_{n+1} = \left(\frac{\partial T}{\partial X} \right)_n^- (\Delta X)_n + T_n \quad (3.20)$$

Finally, combining Equations 3.18 and 3.20 gives

$$T_{n+1} = T_n + [v_o \gamma_o a_n + (\frac{\partial T}{\partial X})_n^+](\Delta X)_n \quad (3.21)$$

Hence, if we know the stress at one wave T_n , we can compute the new value T_{n+1} at the next wave.

As an example to implement this theory, consider the 4-wave profile as shown in Figure 3.16. The stress values for this case using Equation 3.21 follow to be

$$\begin{aligned} T_1 &= T_0 = 0 \\ T_2 &= T_1 + [v_o \gamma_o a_1 + (\frac{\partial T}{\partial X})_1^+](\Delta X_1) = v_o \gamma_o a_1(\Delta X_1) \\ T_3 &= T_2 + [v_o \gamma_o a_2 + (\frac{\partial T}{\partial X})_2^+](\Delta X_2) \\ &= T_2 + [v_o \gamma_o a_2 + (\frac{\partial T}{\partial X})_1^-](\Delta X_2) \\ &= v_o \gamma_o [a_1(\Delta X_1) + (a_1 + a_2)(\Delta X_2)] \\ T_4 &= T_3 + [v_o \gamma_o a_3 + (\frac{\partial T}{\partial X})_3^+](\Delta X_3) \\ &= v_o \gamma_o [a_1(\Delta X_1) + (a_1 + a_2)(\Delta X_2) + (a_1 + a_2 + a_3)(\Delta X_3)] \end{aligned} \quad (3.22)$$

For the general case with $n > 1$, the stress is given by

$$\begin{aligned} T_n &= v_o \gamma_o [a_1(\Delta X_1) + (a_1 + a_2)(\Delta X_2) + (a_1 + a_2 + a_3)(\Delta X_3) \\ &\quad + \dots + (a_1 + a_2 + a_3 + \dots + a_{n-1})(\Delta X_{n-1})] \end{aligned} \quad (3.23)$$

Now, since it is expected that the stress will affect the microstructure, we postulate that there must be some relationship between the average volume distribution function \bar{v} and the stress T , i.e.,

$$\bar{v} = \bar{v}(T) \quad (3.24)$$

With little or no stress $\bar{v} = \bar{v}_0$ and as the stress increases (compression positive), one would assume that $\bar{v} \rightarrow 1$. Figure 3.17 illustrates such behavior for a typical sandy soil. Based upon these ideas, the quantity v_a in the periodic distribution forms was modified as a function of the stress by the relation

$$v_a = 1 - (1 - v_{a_0}) e^{-MT} \quad (3.25)$$

where v_{a_0} is its reference value and M is a material constant. This simplified approach is essentially varying porosity with stress to predict wave coupling effects. This should be regarded as an approximate technique since Equation 3.25 might not be strictly compatible with the basic constitutive form (Equation 2.6).

Equation 3.25 was then placed into the code to provide an approximate means to calculate the wave propagational characteristics of waves traveling behind each other. Of course, an uncoupled theory would be generated by specifying $M \rightarrow 0$ which gives $v_a = v_{a_0}$ and, thus, all waves will travel independent of one another. By inputting a number of waves of various initial amplitudes with equal initial time spacings Δt_0 , a wave profile (acceleration versus time) for various depths can be constructed. With Equation 3.23, the stress profile can also be constructed. Finally, from the acceleration profiles, the velocity and displacement profiles were calculated. These profile constructions are contained within the code. Figures 3.18-3.21 illustrate some typical profiles for the periodic volume distribution case using model parameters of Material P1. These results are for the uncoupled case $M = 0$.

3.5 PROBABILISTIC CONSIDERATIONS

The purpose of a probabilistic analysis is to develop a method by which the variability or uncertainties in the independent (input) parameters in a particular problem can be evaluated or estimated in terms of their effects on the dispersion of the dependent (output) variables. An extremely useful procedure for determining the moments of a dependent variable in terms of functions of the moments of its independent variables was developed by Rosenblueth (Reference 73). The Rosenblueth procedure is quite versatile and is not bound by the restrictions often imposed on other moment generating

procedures, such as the method of partial derivatives. If Y is functionally related to two random variables X_1 and X_2 , i.e.,

$$Y = Y(X_1, X_2) \quad (3.26)$$

and, if X_1 and X_2 are uncorrelated and their probability distribution functions are symmetrical, then, according to the Rosenblueth procedure, the expected value of Y , $E(Y)$, and variance of Y , $V(Y)$, can be estimated from the following expressions

$$E(Y) = (1/4) (Y^{++} + Y^{+-} + Y^{-+} + Y^{--}) \quad (3.27)$$

$$V(Y) = E(Y^2) - [E(Y)]^2 \quad (3.28)$$

where

$$E(Y^2) = (1/4) [(Y^{++})^2 + (Y^{+-})^2 + (Y^{-+})^2 + (Y^{--})^2] \quad (3.29)$$

and

$$Y^{\pm\pm} = Y(\bar{X}_1 \pm \sigma_{X_1}, \bar{X}_2 \pm \sigma_{X_2}) \quad (3.30)$$

In Equation 3.30, \bar{X}_1 and \bar{X}_2 are the expected values of the random variables X_1 and X_2 , respectively. Similarly, σ_{X_1} and σ_{X_2} are the standard deviations of the random variables X_1 and X_2 . It should be noted from Equations 3.27-3.30 that the expected value and the variance of Y can be calculated from four (2^2) "point estimates" of the function Y , as stipulated by Equation 3.30. Each of these point estimates can be viewed as a "deterministic calculation" using the dependent random variable Y . The above system of equations can readily be generalized to n random variables requiring 2^n point estimates.

A major advantage of the Rosenblueth procedure over the Monte Carlo method can now be realized when comparing the number of deterministic calculations required to determine the moments of the random variable Y . For example, in the case of three random variables, the Rosenblueth procedure requires $2^3 = 8$ calculations. The Monte Carlo method, on the other hand, may require several hundred calculations. It should also be pointed out that

the Rosenblueth procedure is capable of handling correlated input random variables (Reference 73) and nonsymmetrical probability distribution functions (Reference 74), if such parameters are known in a problem.

For the purpose of the present investigation, it will be assumed that the input random variables are uncorrelated and their probability distribution functions are symmetrical. The assumption is motivated by the fact that the exact nature of these parameters is seldom known. Therefore, in the subsequent analysis, Equations 3.27-3.30 will be used for probabilistic wave propagation analyses.

With $E(Y)$ and $V(Y)$ known, the value of the function at one standard deviation above (Y^+) and below (Y^-) its mean value can be determined from the following relation:

$$Y^{\pm} = E(Y) \pm [V(Y)]^{1/2} \quad (3.31)$$

We can now proceed to apply the Rosenblueth procedure to the wave propagation theory developed in the previous sections in order to account for the randomness in the parameters l and v_a . In this connection, we will denote \bar{l} and \bar{v}_a as the expected values of these variables and σ_l and σ_{v_a} as their standard deviations. The values of these variables at one standard deviation above (P) and below (M) their mean values then become

$$\begin{aligned} l^P &= \bar{l} + \sigma_l \\ l^M &= \bar{l} - \sigma_l \\ v_a^P &= \bar{v}_a + \sigma_{v_a} \\ v_a^M &= \bar{v}_a - \sigma_{v_a} \end{aligned} \quad (3.32)$$

Four deterministic wave propagation calculations are conducted for the four possible combinations of l^P , l^M , v_a^P and v_a^M , as stipulated by Equation 3.30. The output from these calculations is combined at successive times (at a selected depth) according to Equations 3.27-3.29 to calculate the expected value and the variance of each of the dependent variables (acceleration, velocity, stress, etc.). Equation 3.31 can then be used to construct

the time histories of the expected value and the one-standard-deviation bounds of these variables. The computer code has been developed to also allow such probabilistic calculations to be made. To process the results, the program first calculates an expected value for the arrival time of the wave at any selected depth using the arrival time data from the four individual deterministic calculations. The program then translates (shifts) all the waveforms to this common arrival time for processing. Figures 3.22-3.24 illustrate some typical probabilistic results for the acceleration, stress and velocity. Each figure shows the expected value and the one-standard-deviation bounds for each wave form.

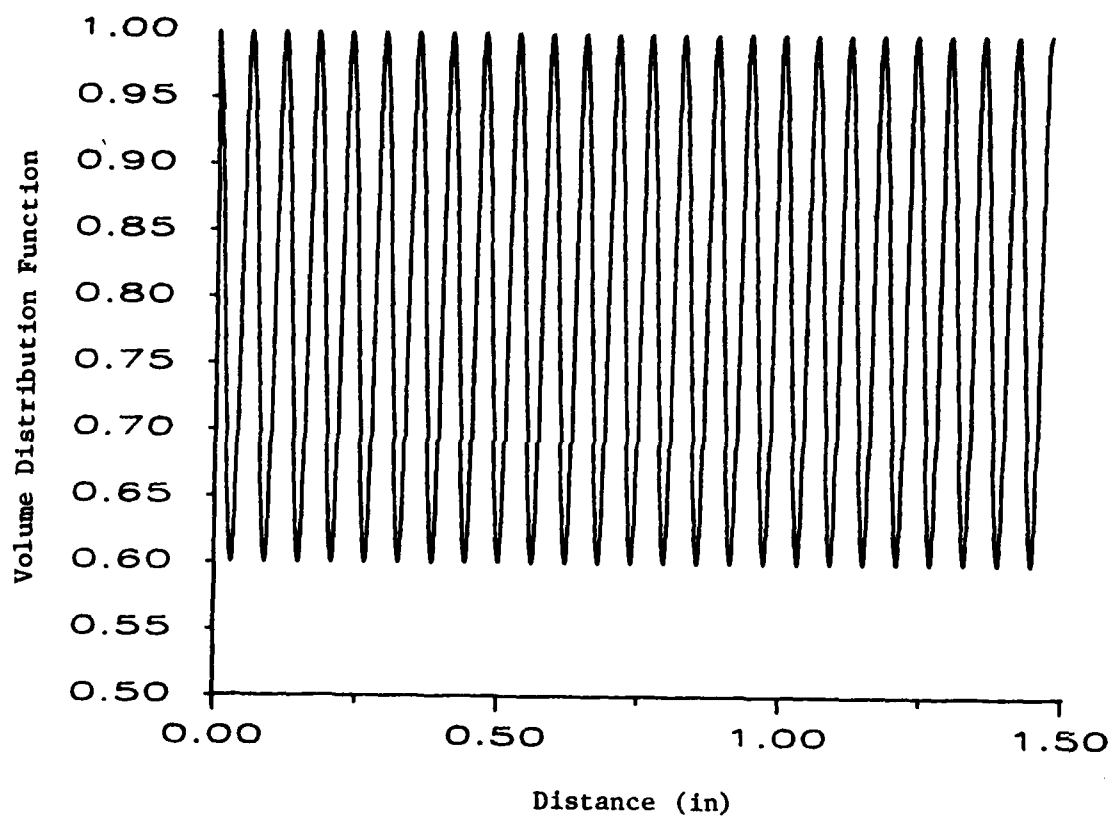


Figure 3.1. Periodic volume distribution function ($v_a = 0.8$,
 $\ell = 0.05$ in).

Some Typical Two-Dimensional Bulk "Voronoi Cells"

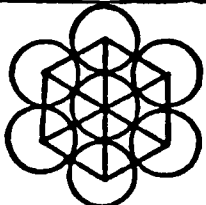
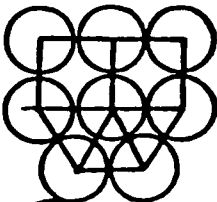
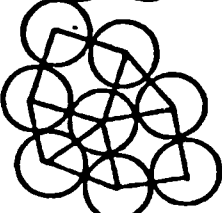
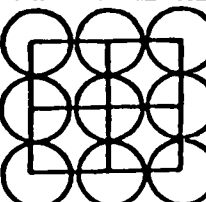
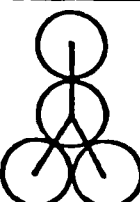
Cellular Structure	Coordination Number	Porosity	Void Ratio	Cell Number
	6	0.0931	0.1027	1
	5	0.1582	0.1879	2
	5	0.1582	0.1879	3
	4	0.2146	0.2732	4
	3	0.3954	0.6540	5

Figure 3.2. Typical two-dimensional Voronoi cells; Reference 77.

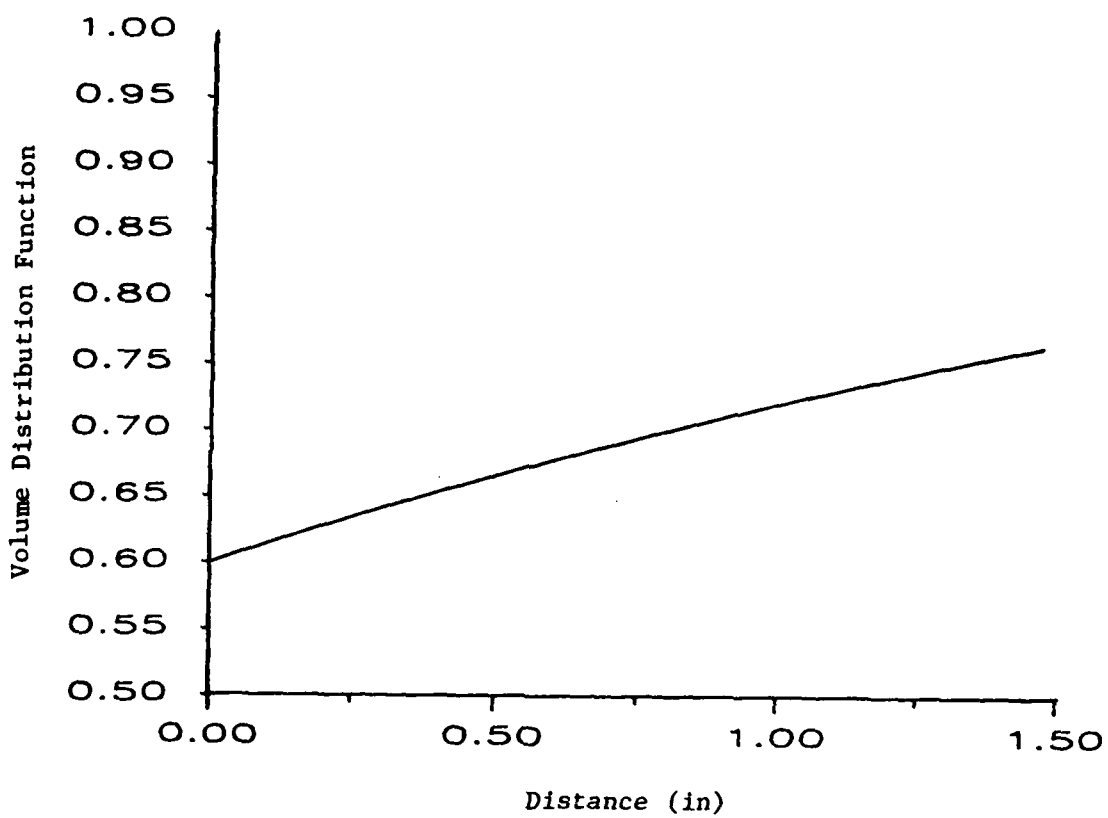


Figure 3.3. Exponential volume distribution function ($v_b = 0.6$,
 $B = 5 \text{ in}^2/\text{lb}$, $\gamma = 7.2 \times 10^{-2} \text{ lb/in}^3$)

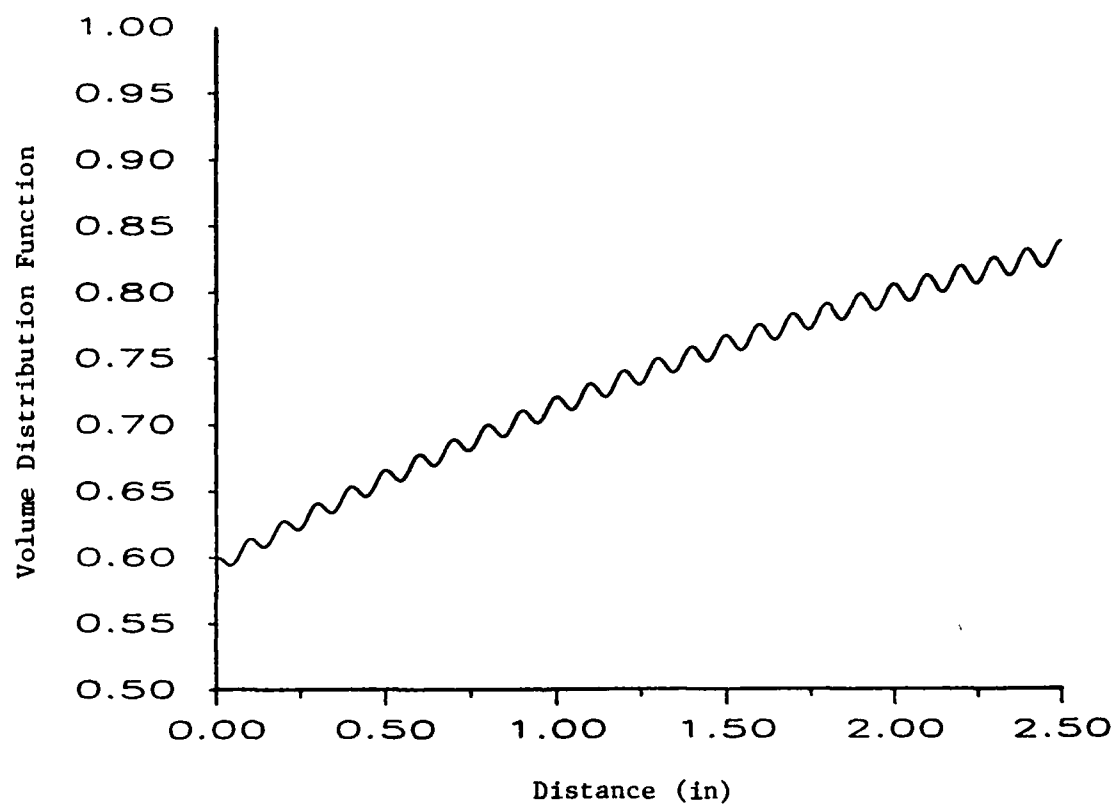
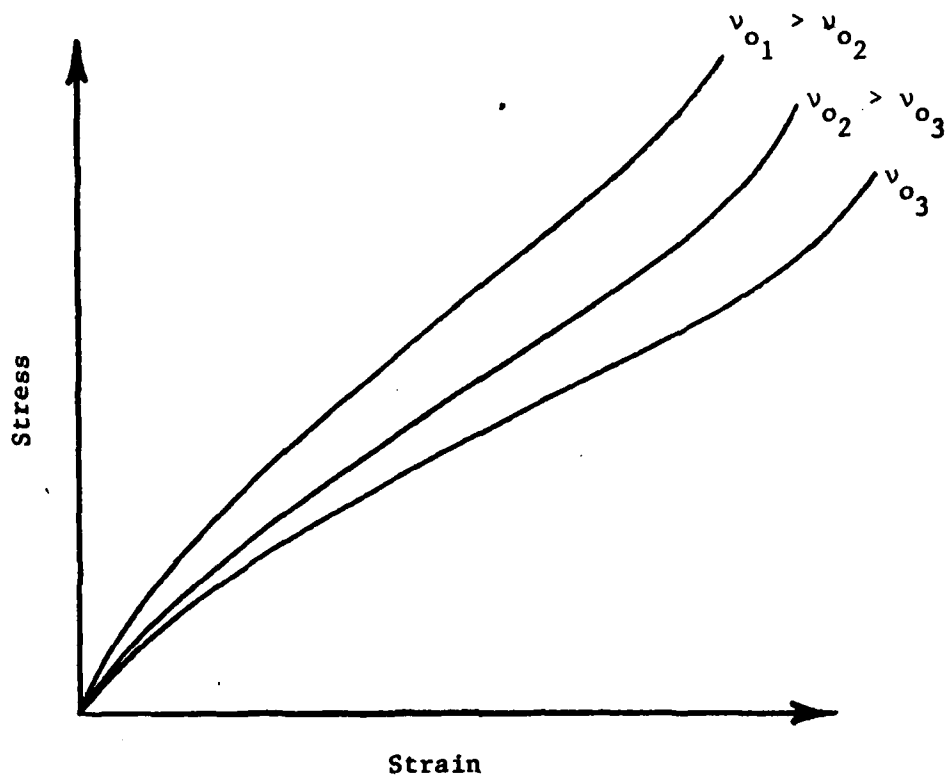


Figure 3.4. Periodic-exponential volume distribution function ($v_a = 0.99$,
 $v_b = 0.6$, $B = 5 \text{ in}^2/\text{lb}$, $\gamma = 7.2 \times 10^{-2} \text{ lb/in}^3$, $\ell = 0.10 \text{ in}$).



$$T = T(X, \epsilon) = T(v_o, v_o, (v_X)_o, \epsilon)$$

$$E = \frac{\partial T}{\partial \epsilon} > 0$$

$$\tilde{E} = \frac{\partial^2 T}{\partial \epsilon^2} > < 0$$

Figure 3.5. Typical stress-strain behavior of granular materials under uniaxial strain conditions.

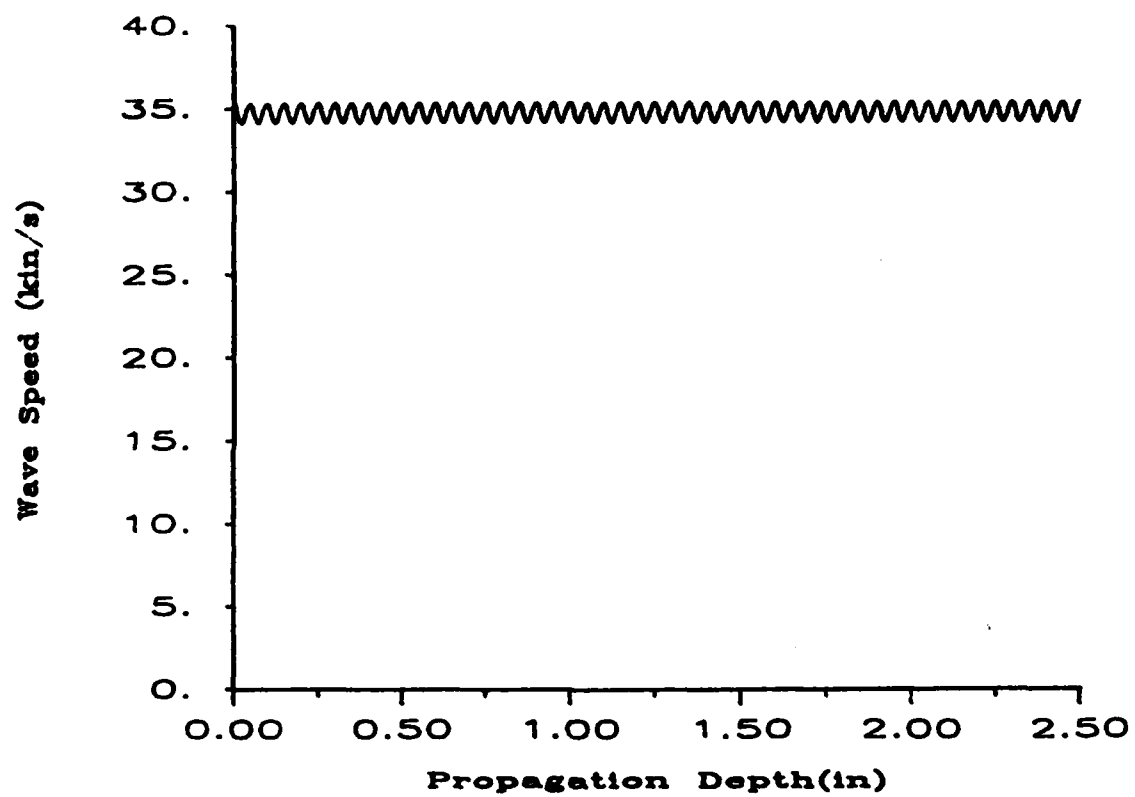


Figure 3.6. Actual wave speed versus distance for periodic volume distribution.

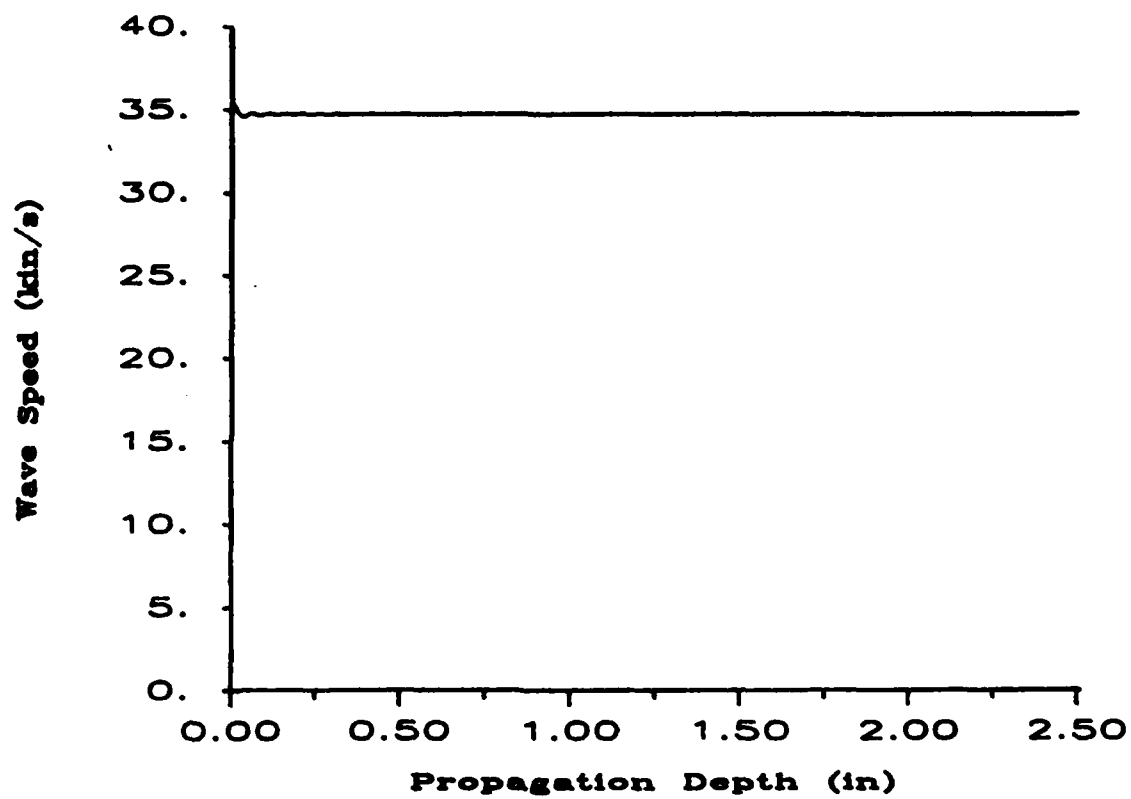


Figure 3.7. Average wave speed versus distance for periodic volume distribution.

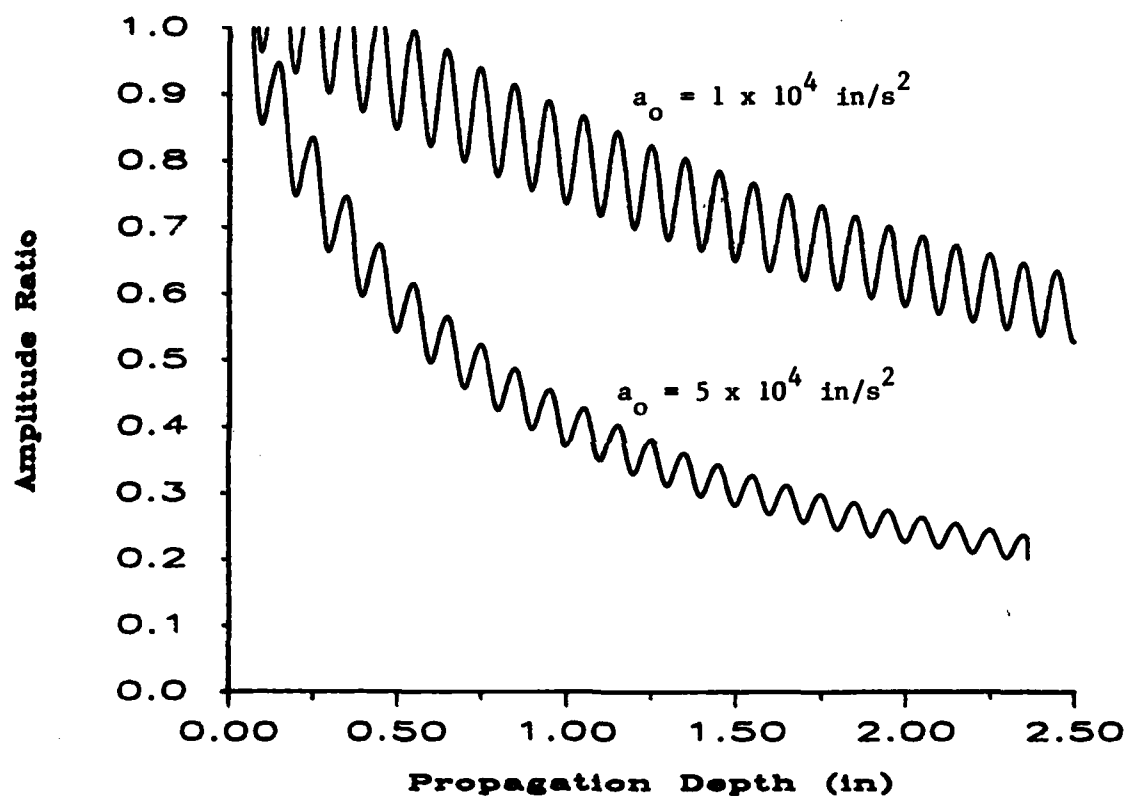


Figure 3.8. Amplitude attenuation versus distance for periodic volume distribution.

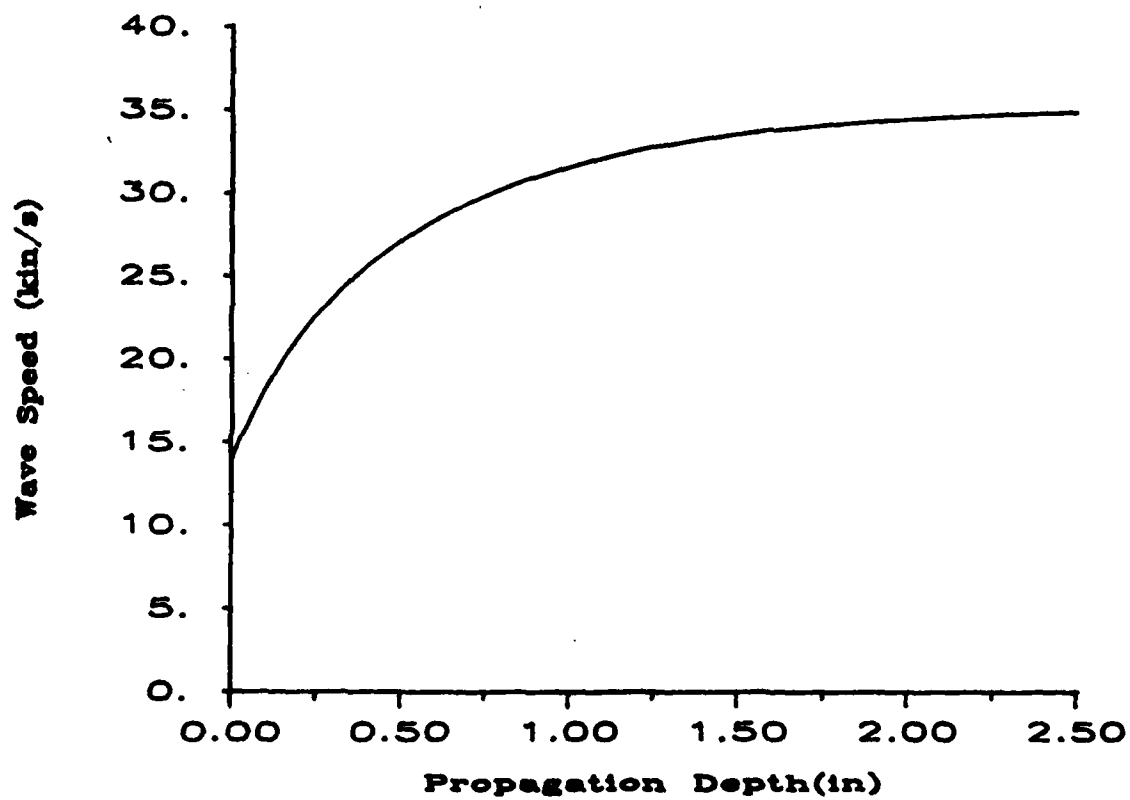


Figure 3.9. Actual wave speed versus distance for exponential volume distribution.

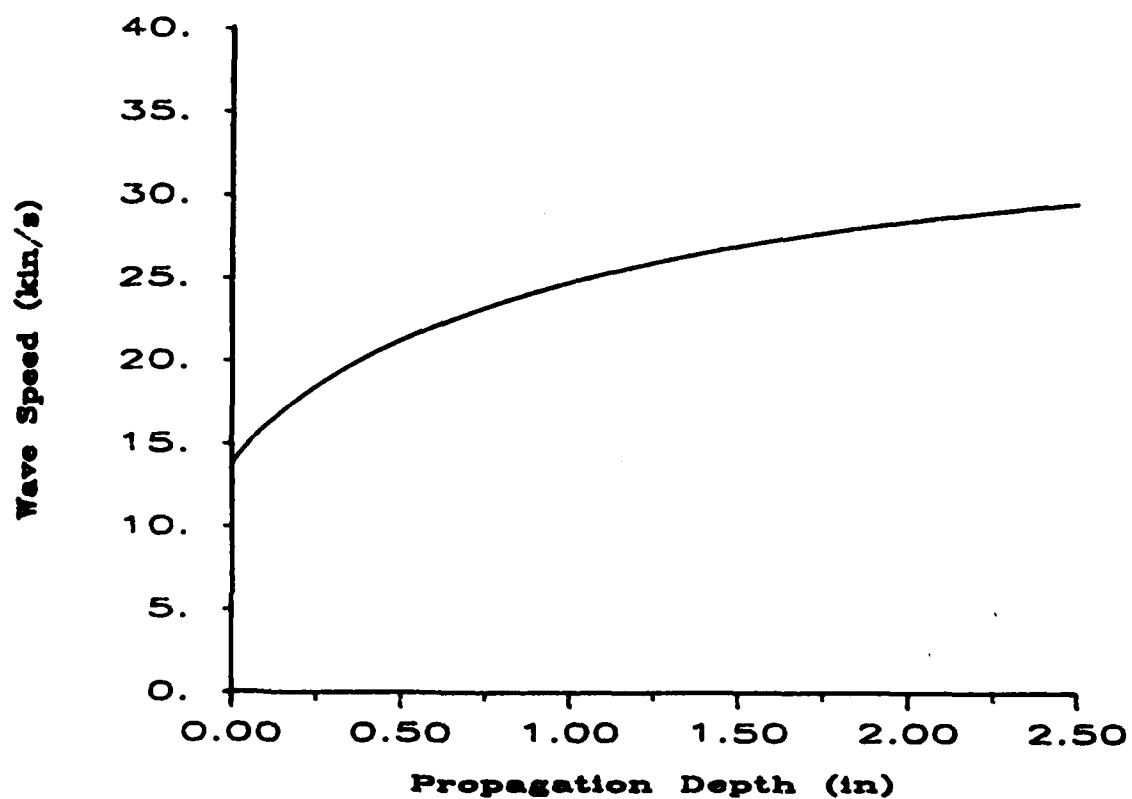


Figure 3.10. Average wave speed versus distance for exponential volume distribution.

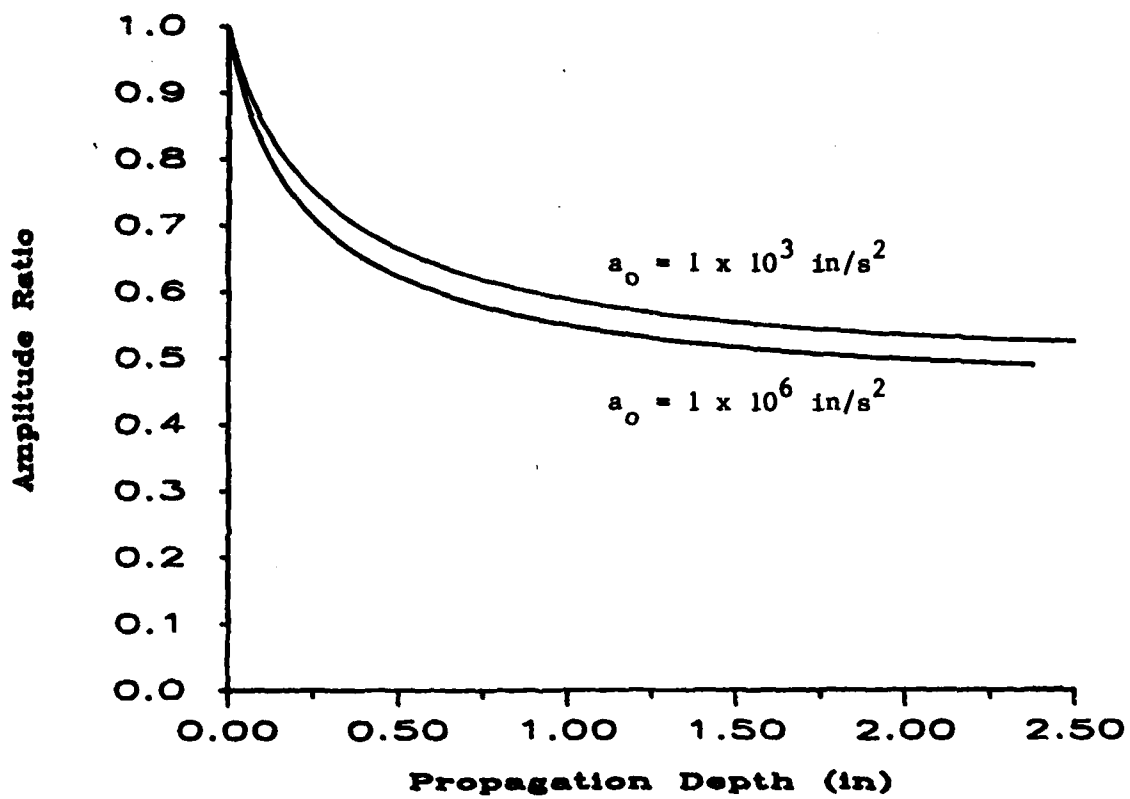


Figure 3.11. Amplitude attenuation versus distance for exponential volume distribution.

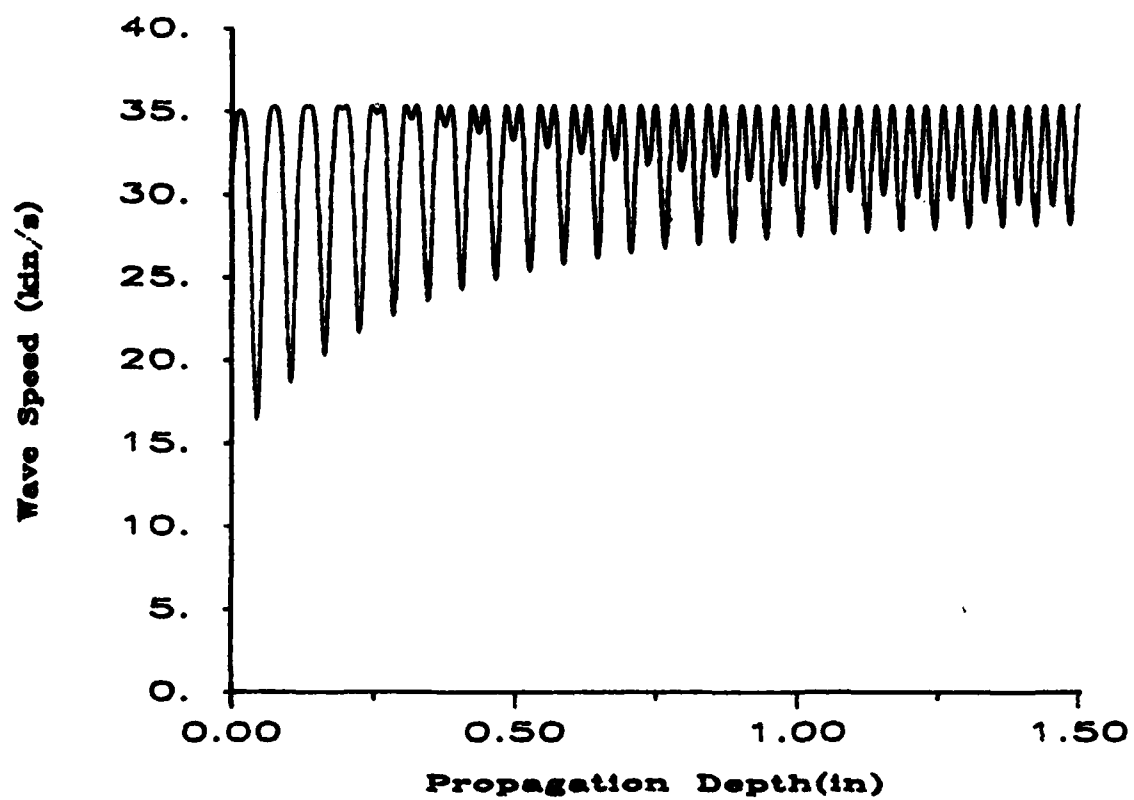


Figure 3.12. Actual wave speed versus distance for combined periodic-exponential volume distribution.

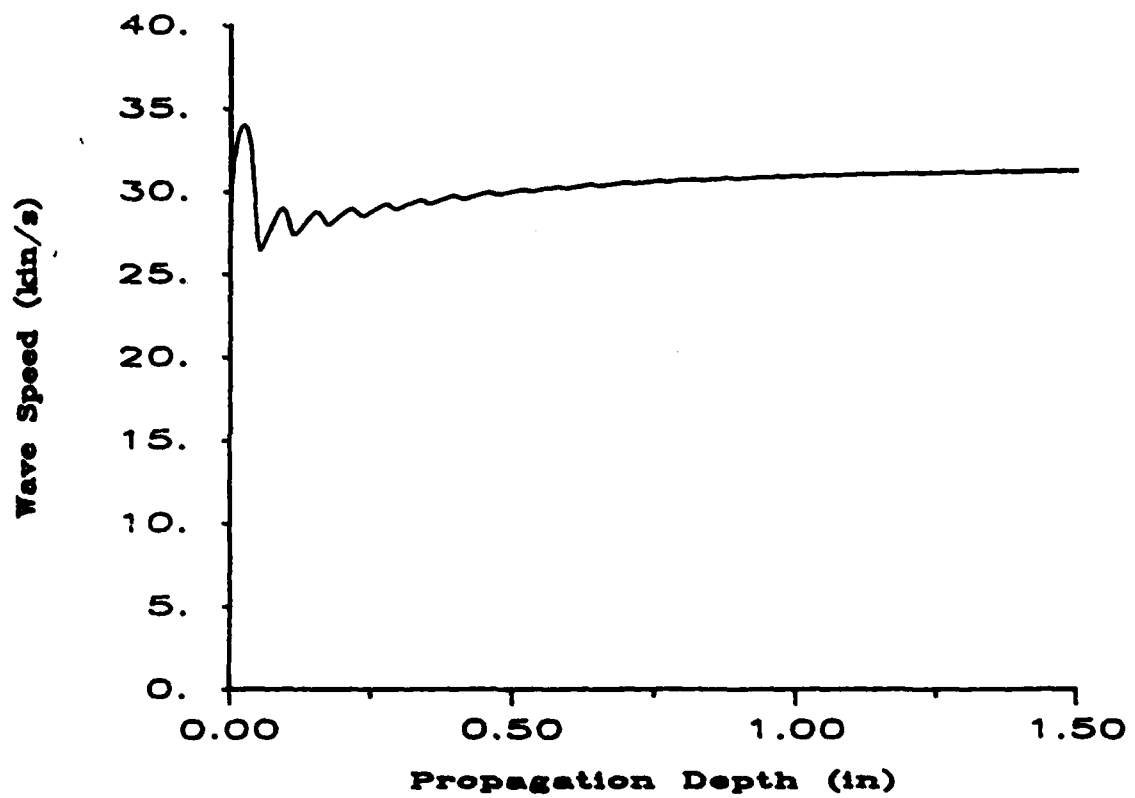


Figure 3.13. Average wave speed versus distance for combined periodic-exponential volume distribution.

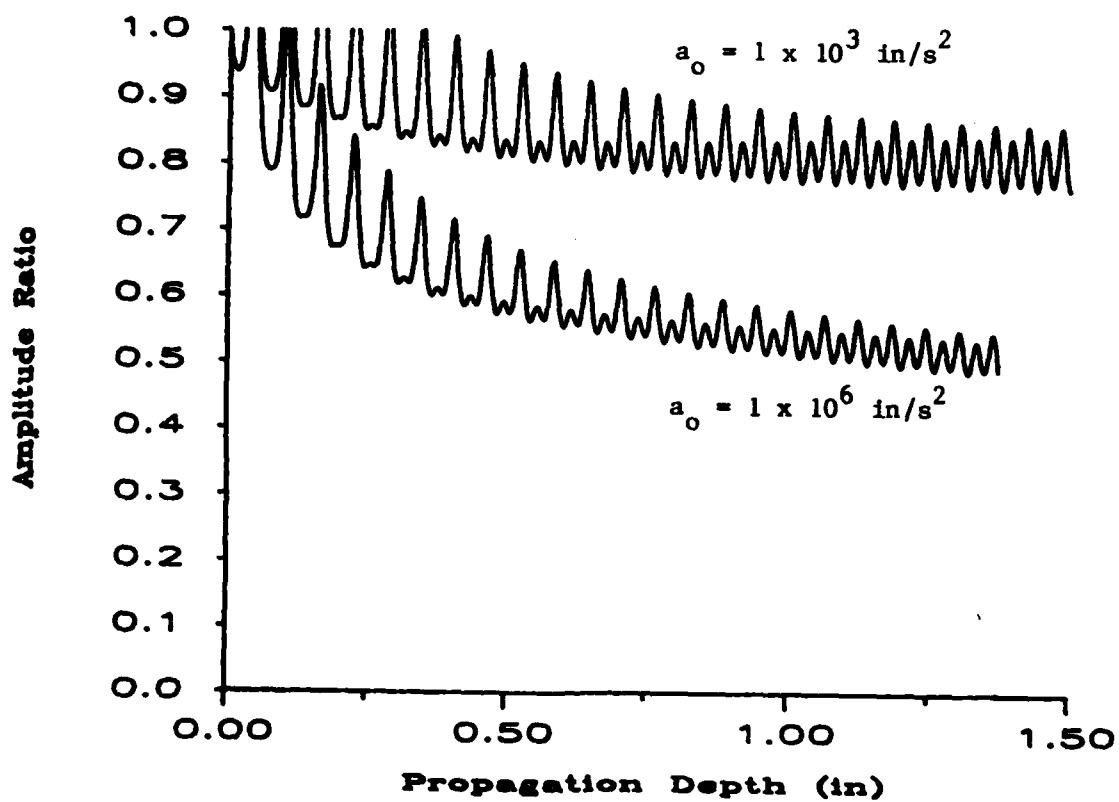


Figure 3.14. Amplitude attenuation versus distance for combined periodic-exponential volume distribution.

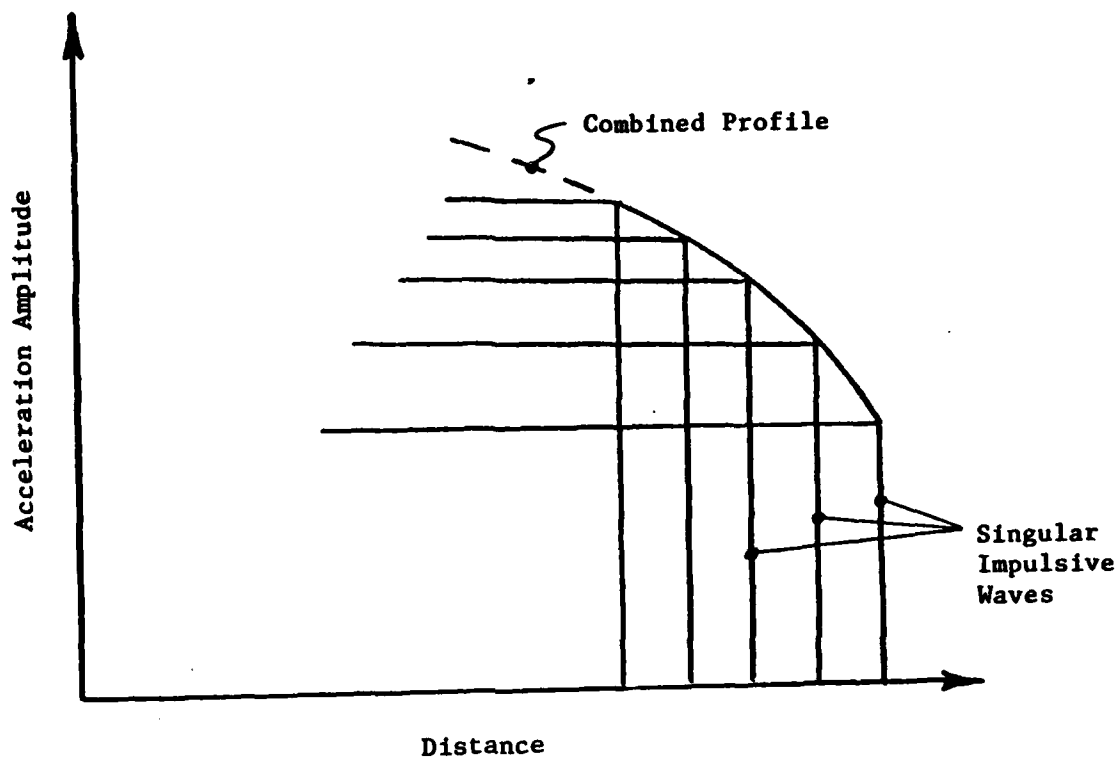


Figure 3.15. Wave profile construction.

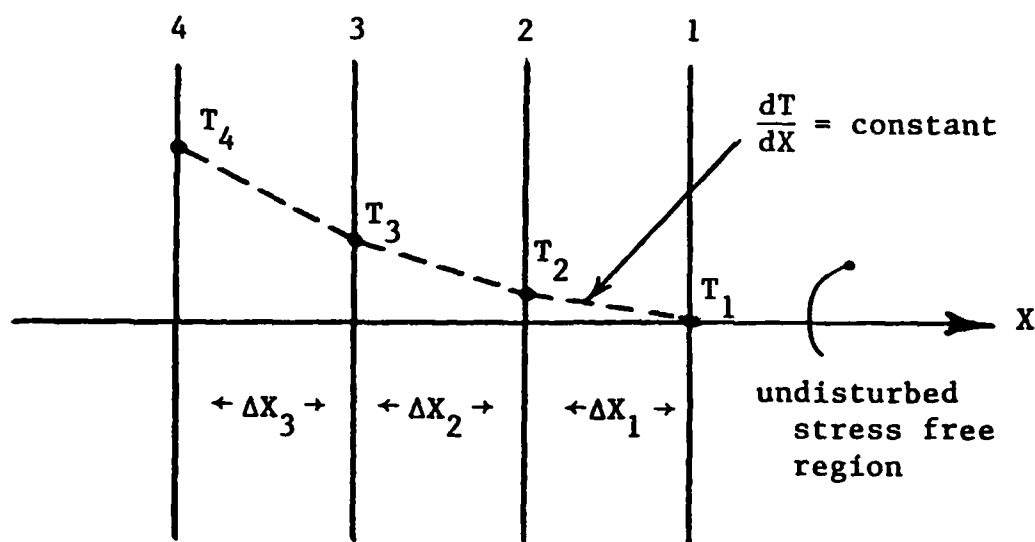


Figure 3.16. Four wave profile example.

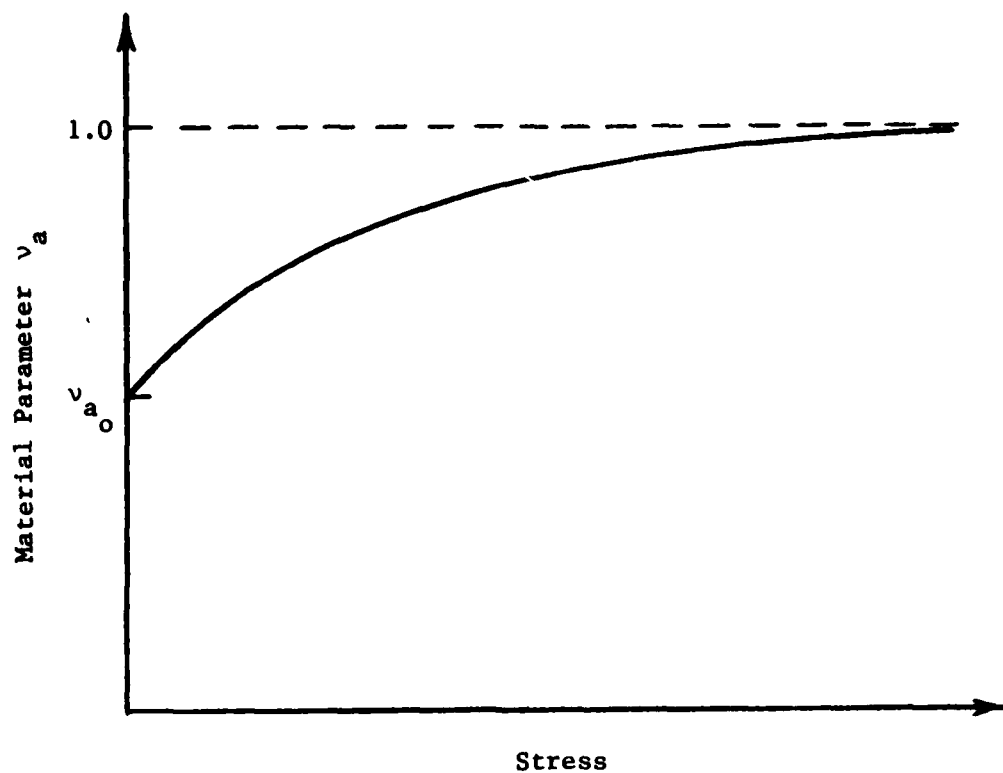


Figure 3.17. Postulated variation of material parameter ν_a as a function of stress.

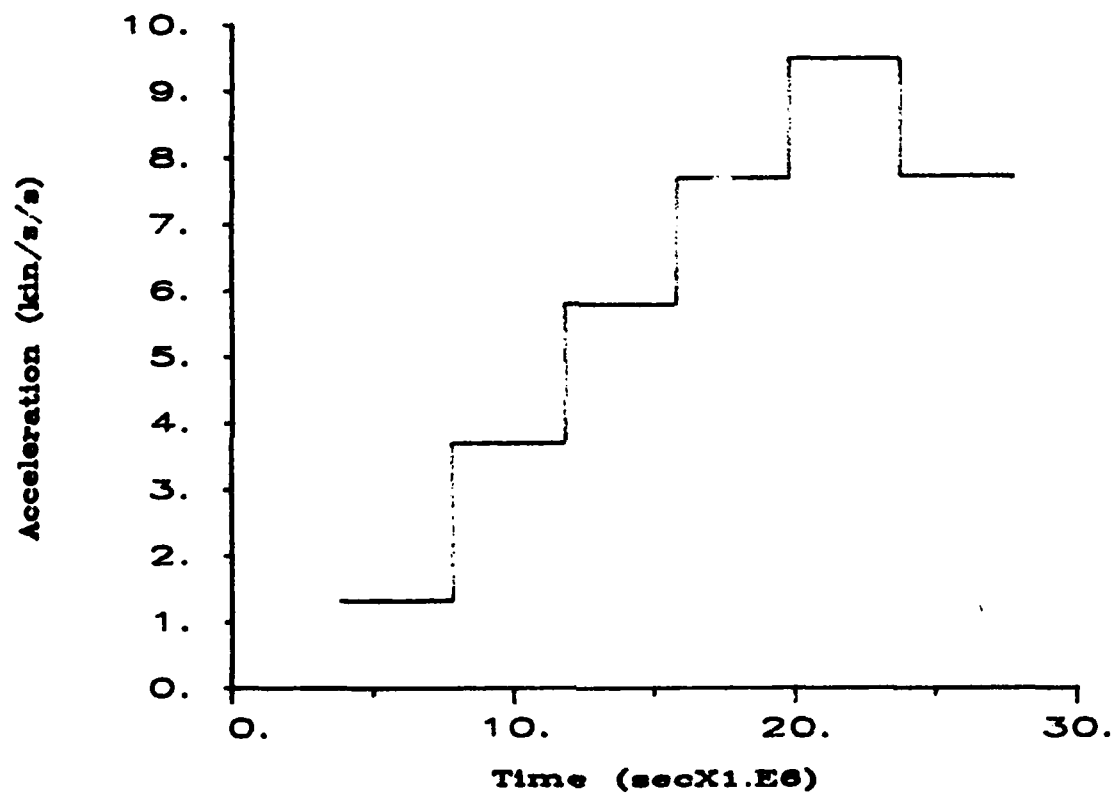


Figure 3.18. Particle acceleration profile for a periodic volume distribution (Material Pl) at $X = 0.125$ in.

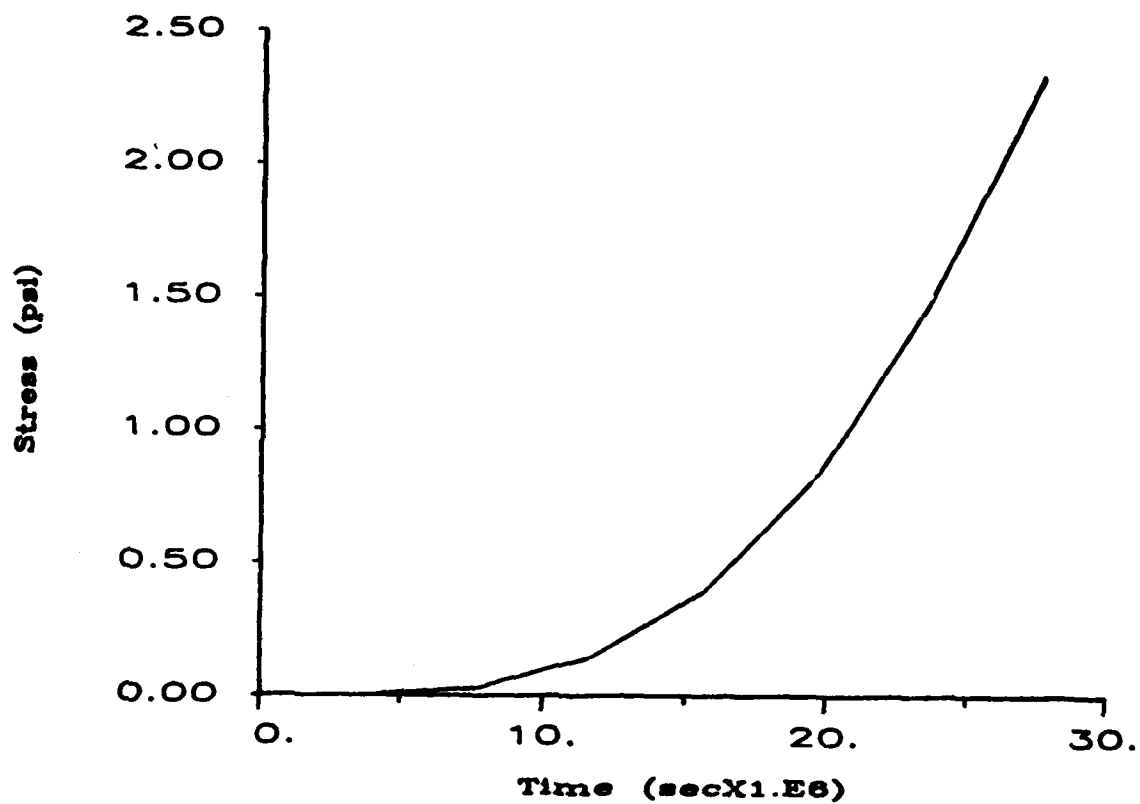


Figure 3.19. Stress profile for a periodic volume distribution (Material P1) at $X = 0.125$ in.

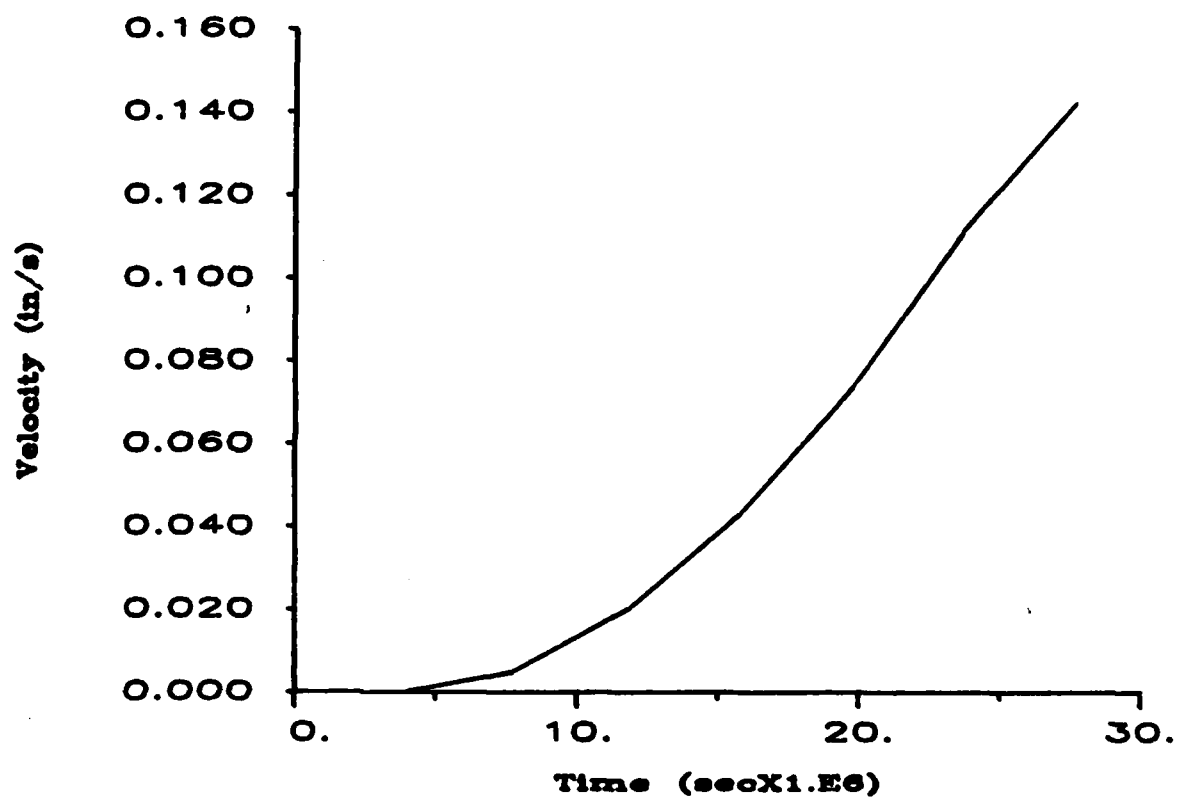


Figure 3.20. Particle velocity profile for a periodic volume distribution (Material P1) at $X = 0.125$ in.

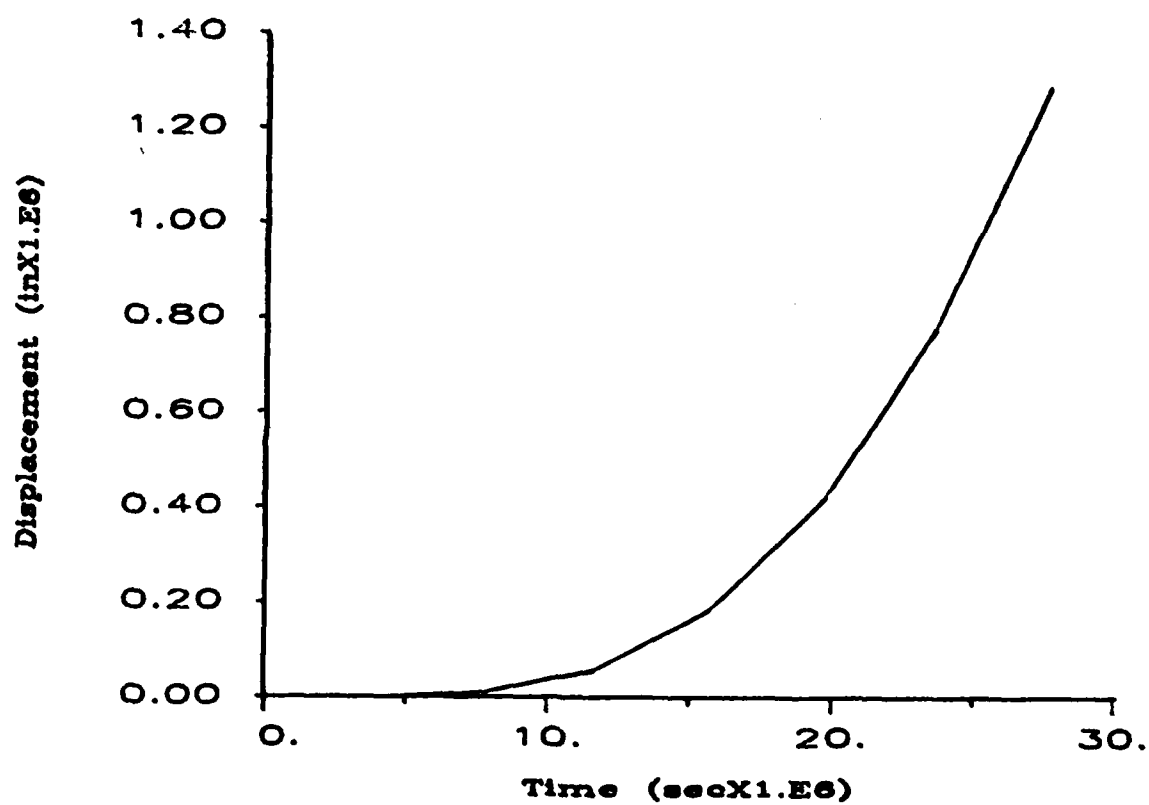


Figure 3.21. Particle displacement profile for a periodic volume distribution (Material P1) at $X = 0.125$ in.

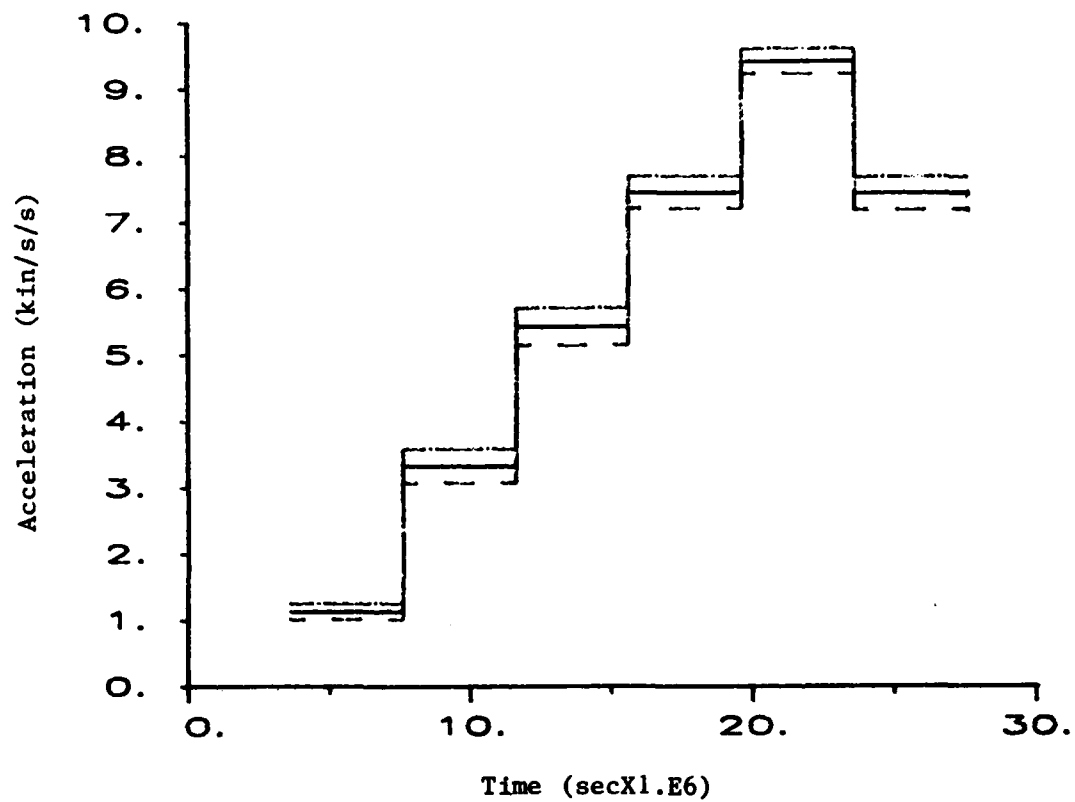


Figure 3.22. Probabilistic results for the particle acceleration profile at $X = 0.125$ in; mean response with its one-standard-deviation bounds. Input variables; $\bar{\ell} = 0.059$ in , $\sigma_{\ell} = 0.02$ in , $\bar{v}_a = 0.85$, and $\sigma_{v_a} = 0.1$.

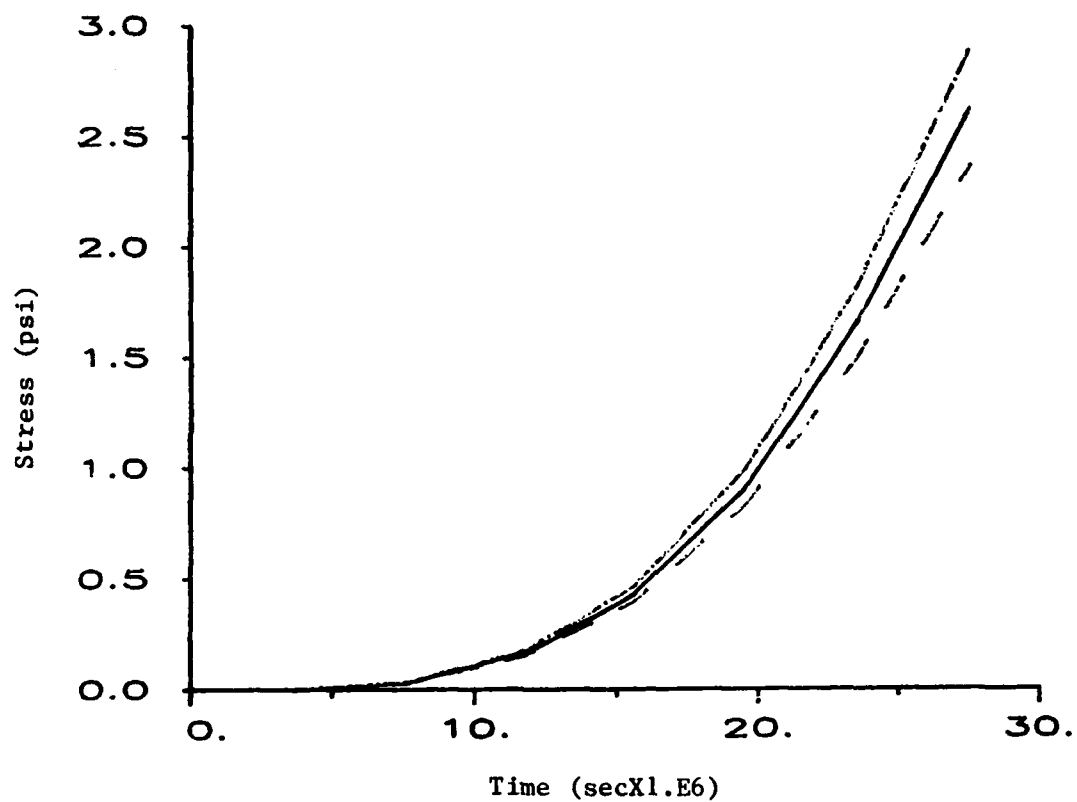


Figure 3.23 Probabilistic results for the stress profile at $X = 0.125$ in ; mean response with its one-standard-deviation bounds. Input variables; $\bar{\ell} = 0.059$ in , $\sigma_{\ell} = 0.02$ in , $\bar{v}_a = 0.85$, and $\sigma_{v_a} = 0.1$.

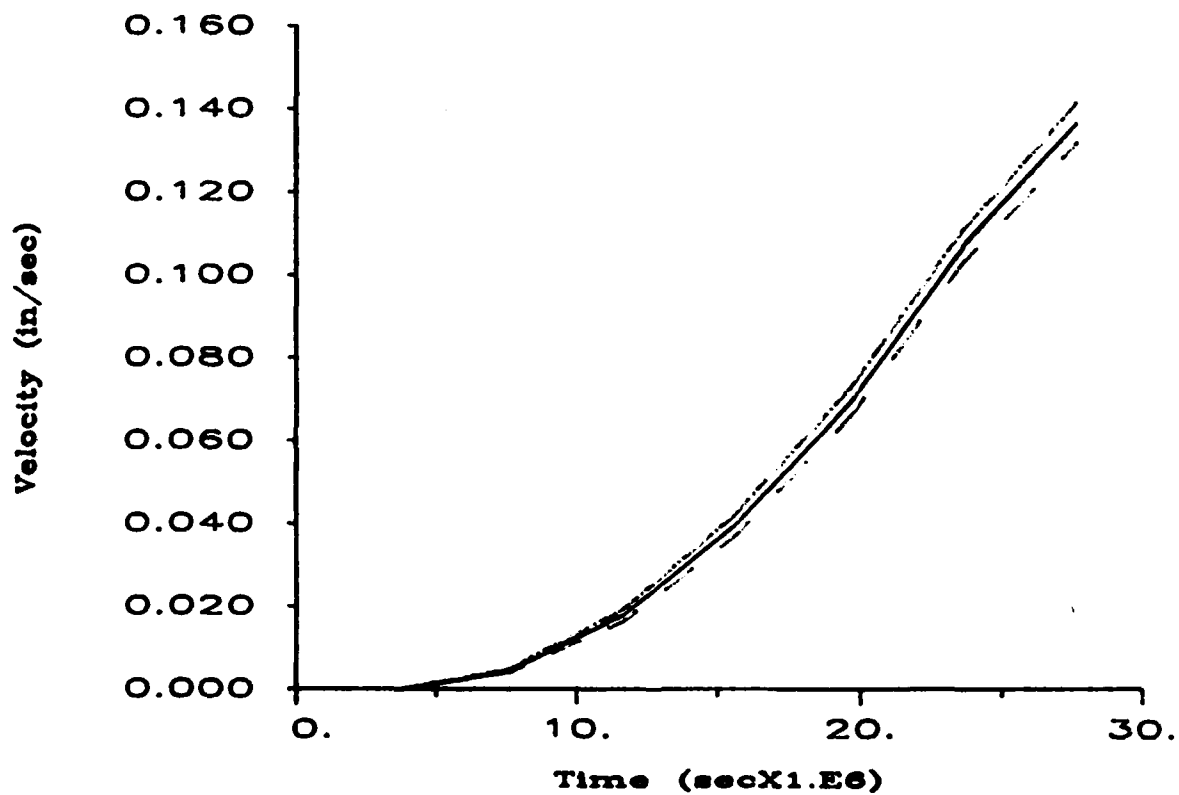


Figure 3.24. Probabilistic results for the velocity profile at $X = 0.125$ in ; mean response with its one-standard-deviation bounds. Input variables; $\bar{\ell} = 0.059$ in , $\sigma_{\ell} = 0.02$ in , $\bar{v}_a = 0.85$ and $\sigma_{v_a} = 0.1$.

CHAPTER 4

PARAMETRIC STUDIES

4.1 GENERAL

This chapter will present a variety of typical results from the developed computer code, MIC1D. Depending upon which volume distribution function is used in the modeling, a wide variety of predicted output can result by varying particular constitutive, microstructural, and input parameters. The constitutive parameters in the wave propagation theory are α_e , α_{ee} , Λ_e , and Λ_{ee} . The microstructural parameters are v_a , v_b , l , B , γ_0 , γ , and M . The input parameters are a_0 and Δt_0 . For the purpose of the parametric calculations, the numerical values of the constitutive parameters were kept constant for each of the three volume distribution functions that were used. The parametric calculations concentrated only on the variation in the microstructural and input parameters. In principle, however, the constitutive parameters would be a function of the microstructural parameters (see Equation 2.6). Explicit relationships for these parameters have not yet been determined. Space limitations in this report preclude presenting many cases; consequently, only major model parameters will be considered. The chapter is divided into three major sections dealing with (1) depth dependent behavior, (2) wave profiles, and (3) probabilistic profiles. Subsections within each of these sections then present specific effects of parametric variation.

4.2 DEPTH DEPENDENT BEHAVIOR

This section will present the effects of the microstructural and input parameters on the variation of the average wave speed and amplitude attenuation with depth. These wave propagational characteristics are for the case of a single wave moving into regions which are at rest in their reference configuration.

4.2.1 Periodic Volume Distribution Case

For the periodic distribution model, the microstructural parameters are the average porosity v_a and the grain or characteristic length l . The basic input parameter is the initial amplitude a_0 . A typical volume distribution plot for this case is shown in Figure 3.1. Figures 4.1-4.6 illustrate typical code output for a variety of parametric variations. Figure 4.1

presents the variation of average wave speed with v_a . As expected, the average wave speed decreases with increasing porosity (i.e., decreasing v_a). Figure 4.2 shows that the wave speed will increase as ℓ increases. This result is apparently related to the fact that, with an increase in ℓ , the wave will see fewer microstructural changes per unit length of travel and, hence, less dispersion. Figure 4.3 illustrates the amplitude behavior for three different initial amplitudes, $a_0 = 5 \times 10^3$, 1×10^3 , and 5×10^2 in/s². Clearly, the expected result can be seen in that higher initial amplitudes decay faster than the lower amplitude waves. Figure 4.3, in conjunction with Figures 4.4 and 4.5, portray the effect of v_a on amplitude attenuation. It is observed that the attenuation rate is strongly dependent on v_a . As v_a decreases (i.e., increasing porosity) the rate of attenuation increases. This result is also consistent with the variation in wave speed with v_a shown in Figure 4.1. Finally, Figures 4.6 and 4.4 demonstrate the effect of ℓ on amplitude attenuation. These figures indicate that larger values of ℓ result in less attenuation, which is consistent with the previous observation regarding the variation of wave speed with ℓ .

4.2.2 Exponential Volume Distribution Case

The exponential volume distribution model contains the microstructural parameters of the free surface porosity v_b and the depth rate of consolidation B . As before, the input parameter is the initial amplitude a_0 . Figures 4.7-4.10 show typical results concerning the effects of these parameters on the wave propagation variables. Figure 4.7 shows the variation of the volume distribution function with distance for two different values of v_b . Figure 4.8 shows the effect of v_b on the average wave speed. For this case, the wave speed increases with depth due to the overall decrease in porosity with depth. It is also apparent that an increase in porosity produces a slower wave speed. Figures 4.9 and 4.10 show the effect of v_b and the initial amplitude on wave attenuation. These results give trends similar to the previous observations for the periodic distribution function. That is, higher initial amplitude waves attenuate faster and the attenuation rate increases with porosity.

4.2.3 Periodic-Exponential Volume Distribution Case

For the combined periodic-exponential distribution model, all four micro-

structural parameters v_a , v_b , l , and B are present. This, along with the initial amplitude a_0 , provides considerable parameter variations. Only a portion of the possible parametric variations will be presented, and these are shown in Figures 4.11-4.14. Figure 4.11 illustrates the variation of volume distribution function with distance for this model for two different values of v_b . This combined function has both oscillatory and monotonic depth-dependent features. Figure 4.12 shows the effect of v_b on the average wave speed. Figures 4.13 and 4.14 show the effect of the initial amplitude and v_b on wave attenuation. These results portray the same trends as observed in the previous sections.

4.3 WAVE PROFILES

Time profiles of the particle acceleration, velocity, and displacement, along with the stress at selected depths into the medium, are presented in this section. The profile construction procedure was discussed earlier in Section 3.4. Only results from the periodic volume distribution case (corresponding to model Material P1) will be presented; however, the other volume distributions will produce similar results. Referring to the wave coupling aspects discussed in Section 3.4, see Equation 3.25, this section will present both uncoupled ($M = 0$) and coupled results ($M \neq 0$). The input acceleration profile used equal time spacing of $\Delta t_0 = 4 \times 10^{-6}$ s for all cases presented here.

4.3.1 Uncoupled Results

Figures 4.15-4.18 illustrate uncoupled results for the four profiles at two different depths, $X = 0.0$ in, $X = 2.5$ in, and $X = 6$ in. The input acceleration wave is shown in Figure 4.15 corresponding to $X = 0.0$ in. It should be pointed out that, for this case, all individual waves in a given profile propagate independently of each other. However, as discussed earlier, in a given profile higher amplitude waves attenuate faster than the lower amplitude waves.

4.3.2 Coupled Results

For the coupled case, Equation 3.25 is in effect and the parameter M plays a significant role in determining the amount of coupling. The wave profile results for the coupled case are shown in Figures 4.19-4.22 for a value of $M = 0.04$ in²/lb and with $v_{a0} = 0.85$. Coupling effects through

variation of v_a (see Equation 3.25) for the periodic distribution case will produce less attenuation than the corresponding uncoupled results. This occurs since increases in v_a produce a material with less average porosity and, hence, dispersive effects will be reduced.

4.4 PROBABILISTIC PROFILES

This final section shows results of some typical probabilistic computer runs. The theoretical development was discussed previously in Section 3.5. The probabilistic results consisting of the expected value and the one-standard-deviation bounds of particle motion and stress are shown in Figures 4.23-4.26 for the case of zero coupling. These results correspond to model Material PE1 (the combined periodic-exponential volume distribution case). Only the parameter l was considered to be random for these calculations. Therefore, the dispersion in the output quantities is only due to uncertainties in l .

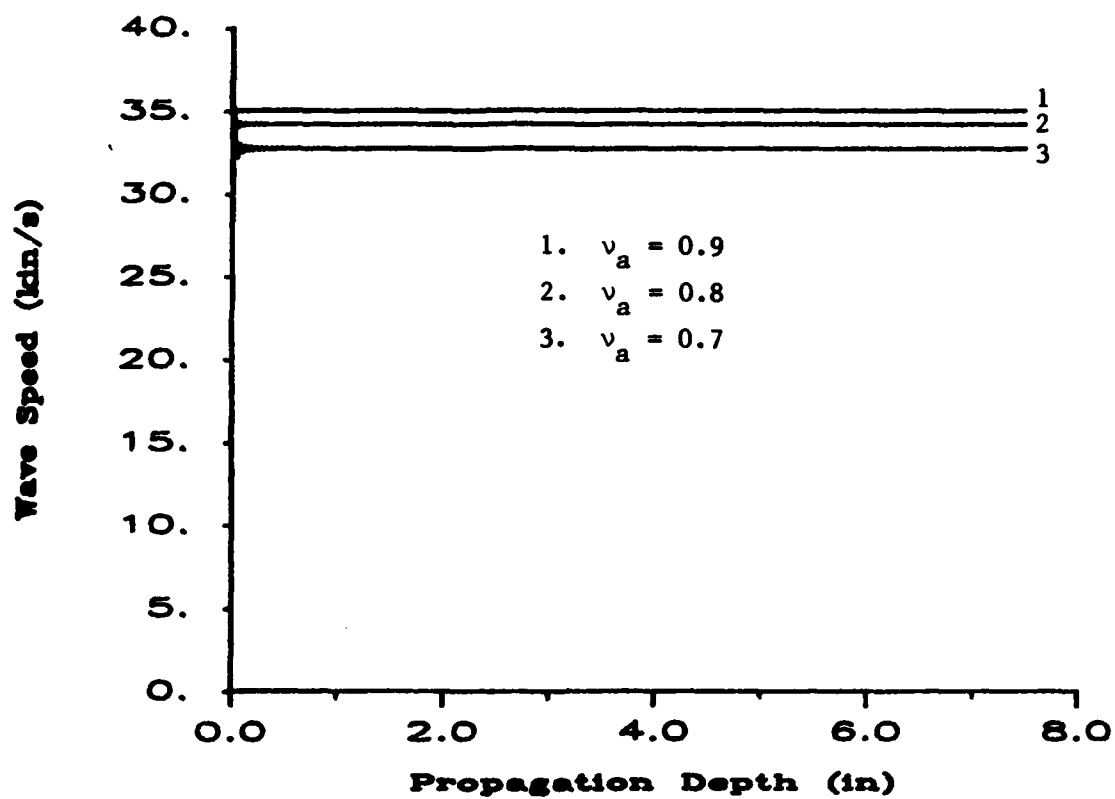


Figure 4.1. The effect of v_a on the average wave speed versus depth for a periodic volume distribution (Material P1 with $\ell = 0.1$ in).

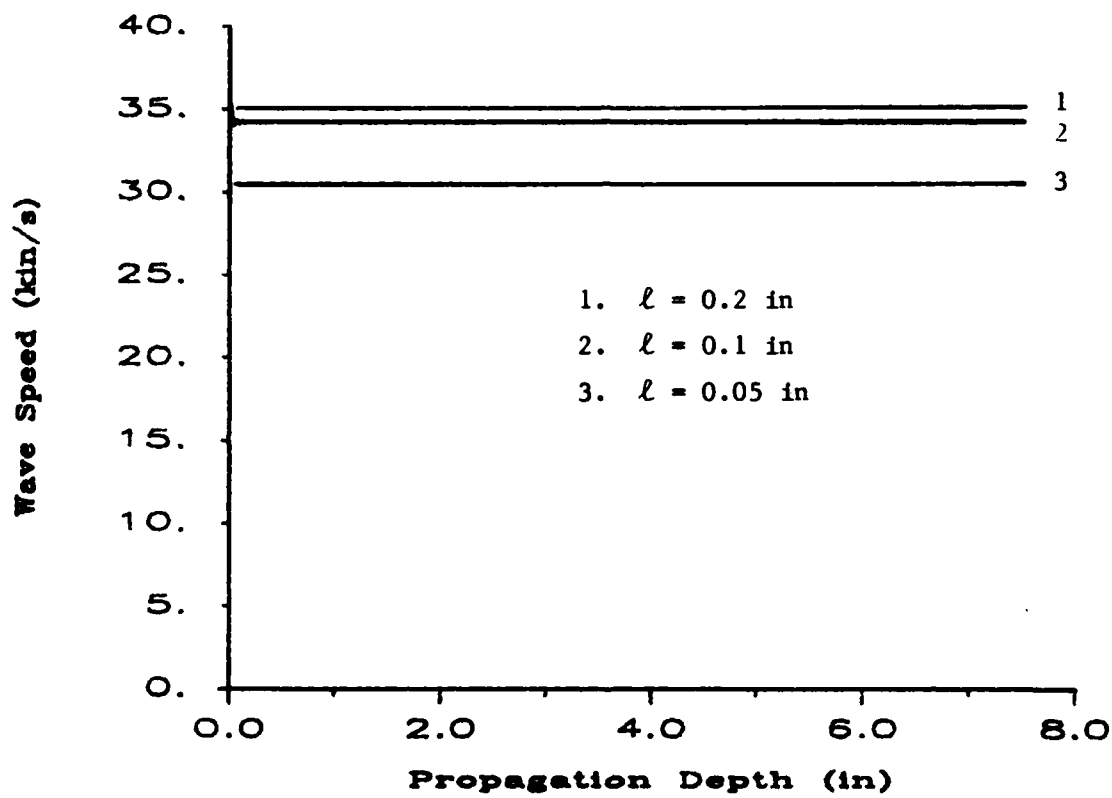


Figure 4.2. The effect of l on the average wave speed versus depth for a periodic volume distribution (Material P1 with $v_a = 0.8$).

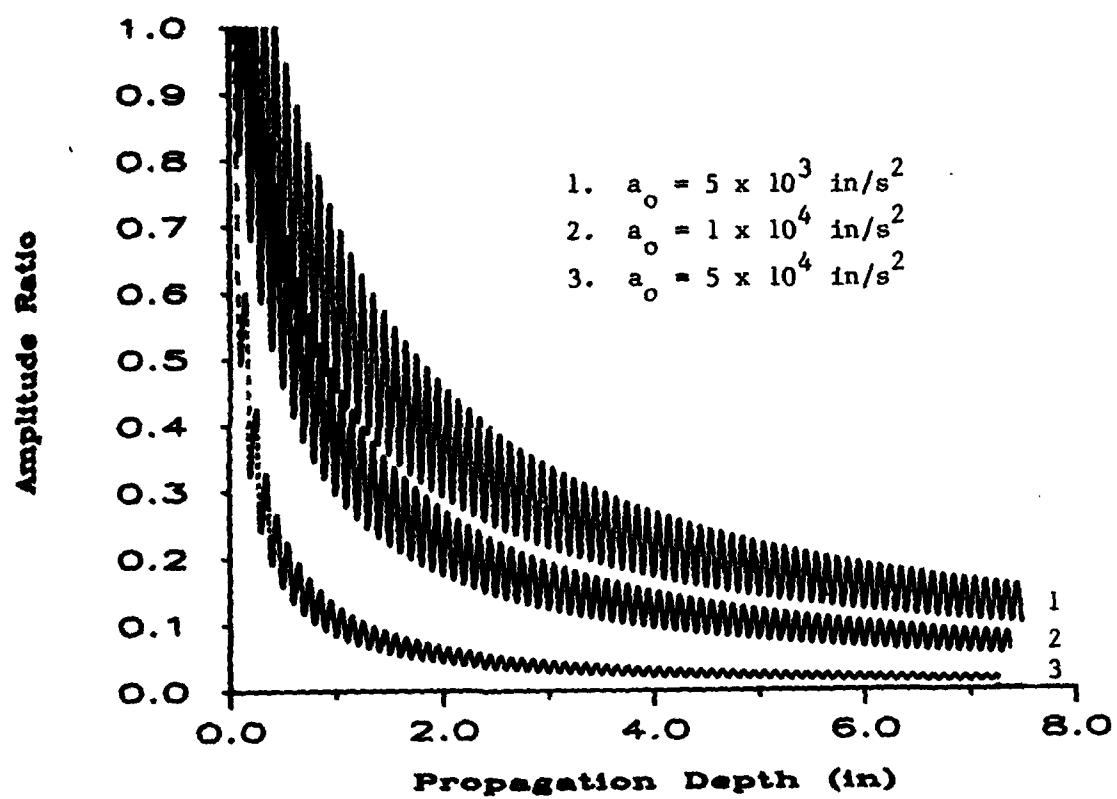


Figure 4.3. Amplitude ratio versus depth for a periodic volume distribution (Material P1 with $\ell = 0.1 \text{ in}$ and $\nu_a = 0.7$).

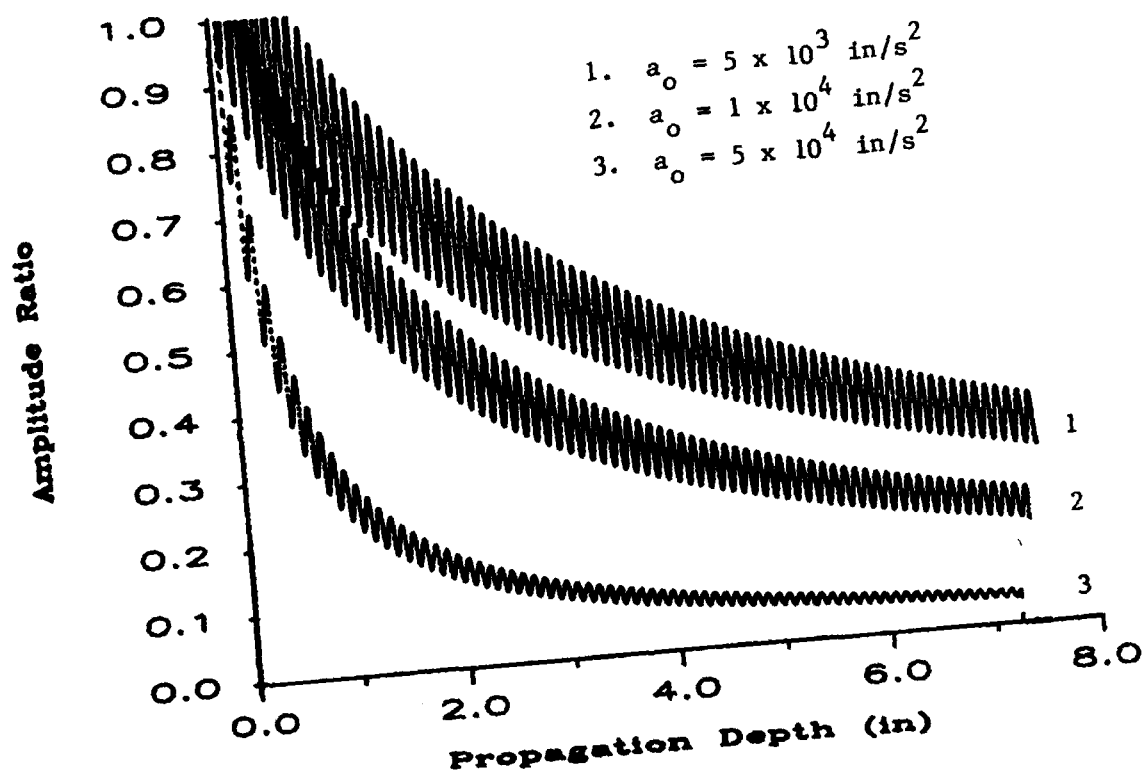


Figure 4.4. Amplitude ratio versus depth for a periodic volume distribution (Material Pl with $\ell = 0.1 \text{ in}$ and $v_a = 0.8$).

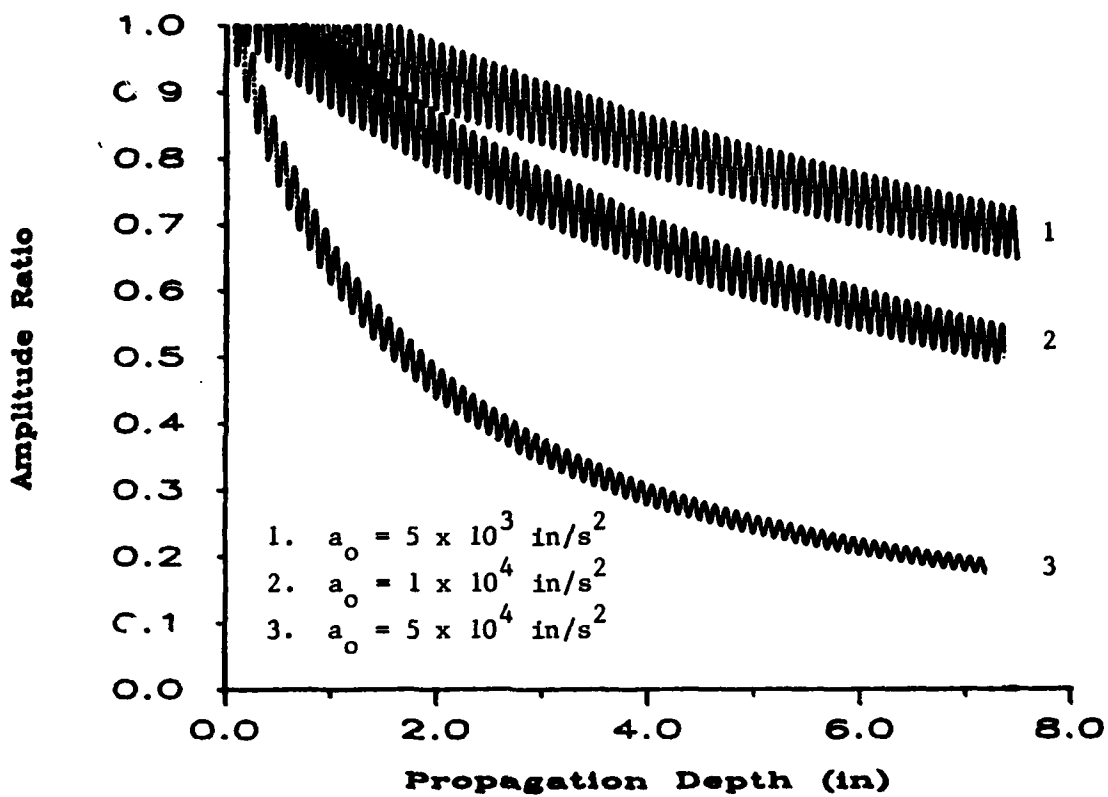


Figure 4.5. Amplitude ratio versus depth for a periodic volume distribution (Material P1 with $\ell = 0.1$ in and $v_a = 0.9$).

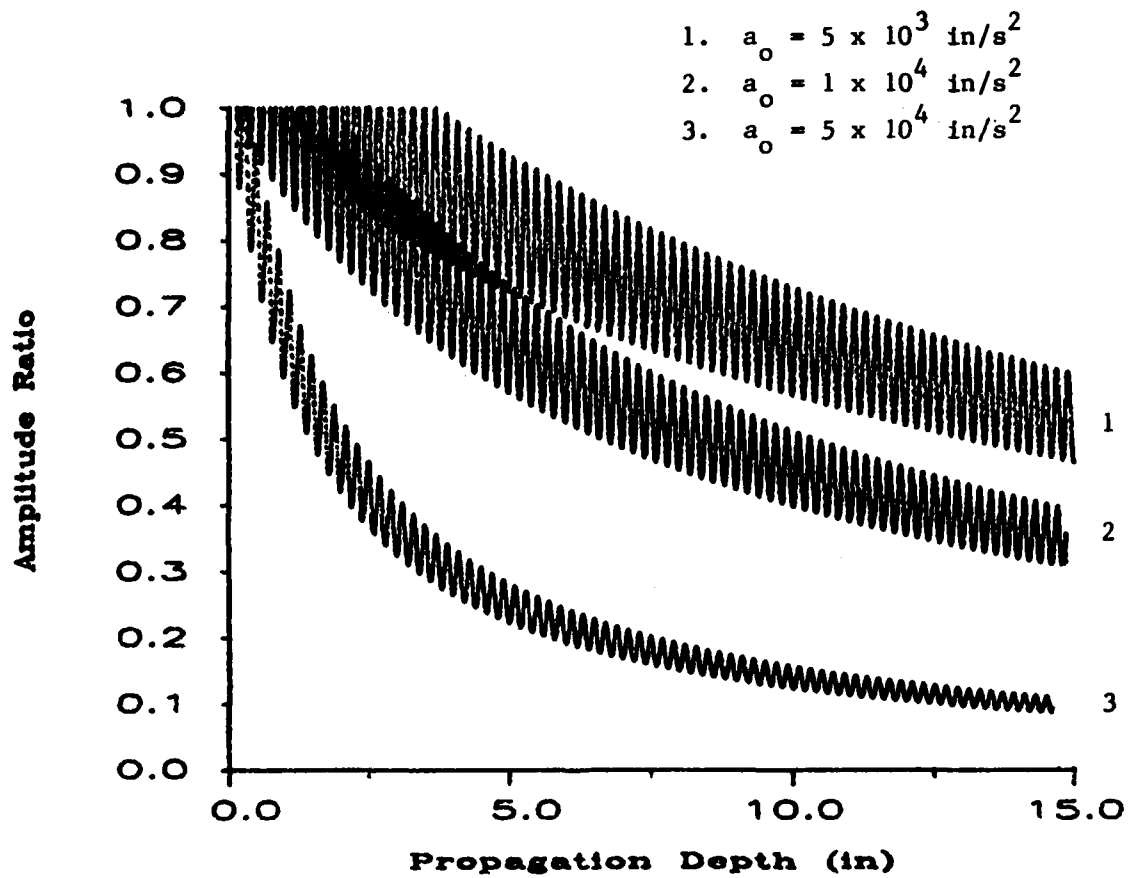


Figure 4.6. Amplitude ratio versus depth for a periodic volume distribution (Material Pl with $\ell = 0.2 \text{ in}$ and $v_a = 0.8$).

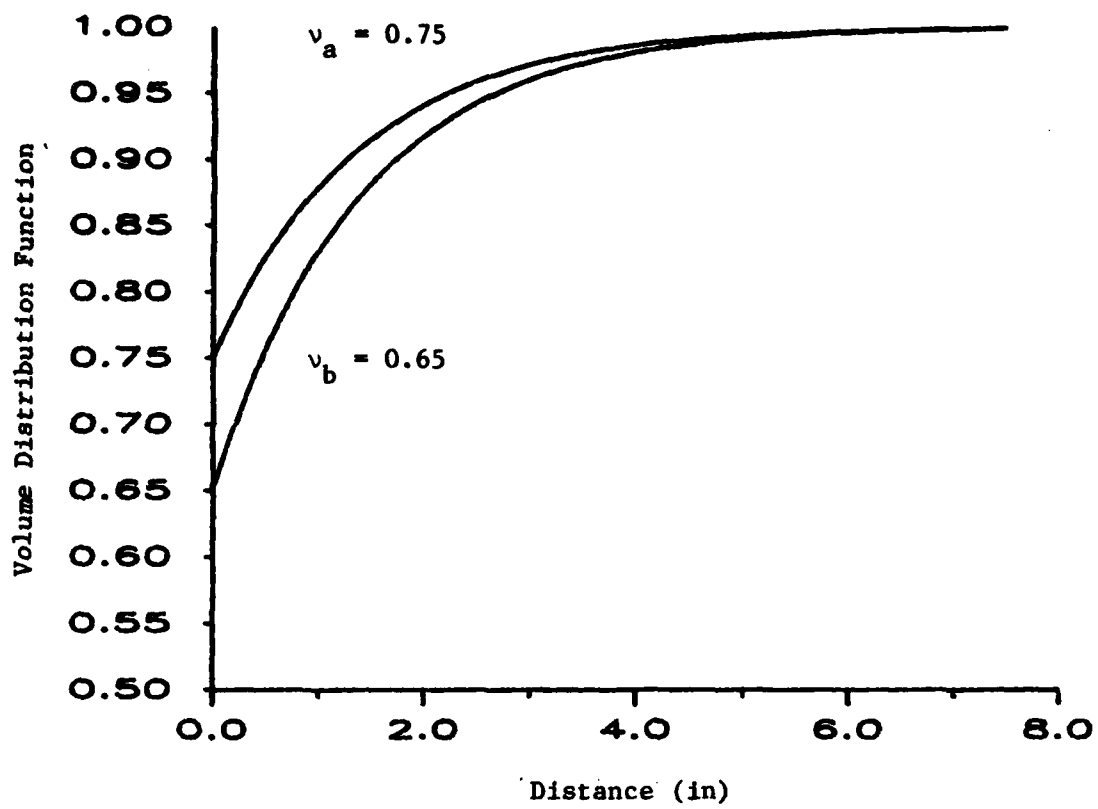


Figure 4.7 Exponential volume distribution function with $B = 10 \text{ in}^2/\text{lb}$.

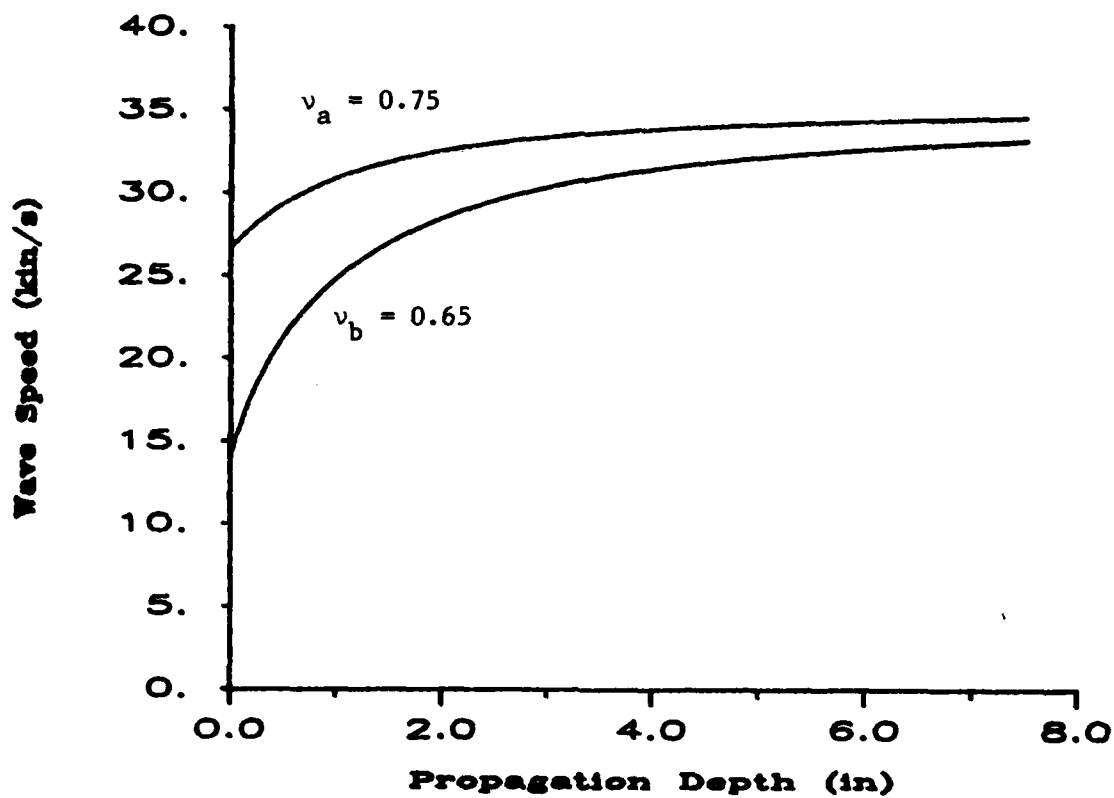


Figure 4.8. Average wave speed versus depth for an exponential volume distribution (Material E1 with $B = 10 \text{ in}^2/\text{lb}$).

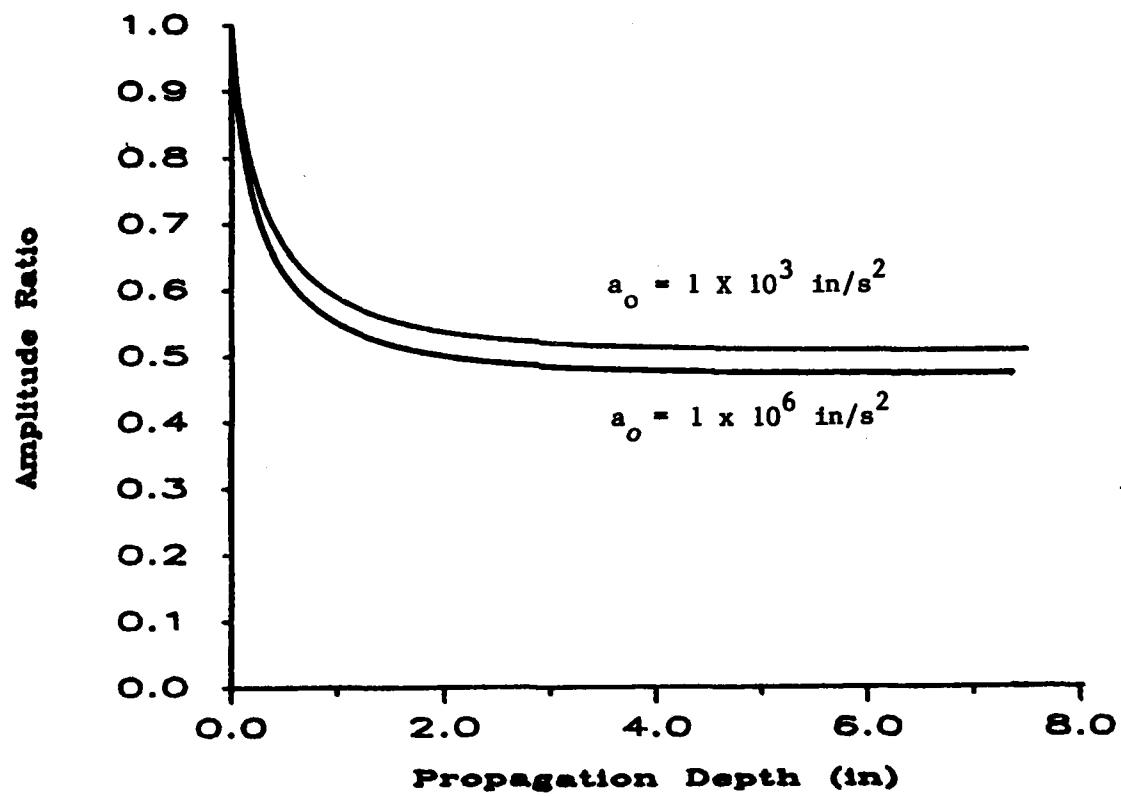


Figure 4.9. Amplitude ratio versus depth for an exponential volume distribution (Material E1 with $B = 10 \text{ in}^2/\text{lb}$ and $\nu_b = 0.65$).

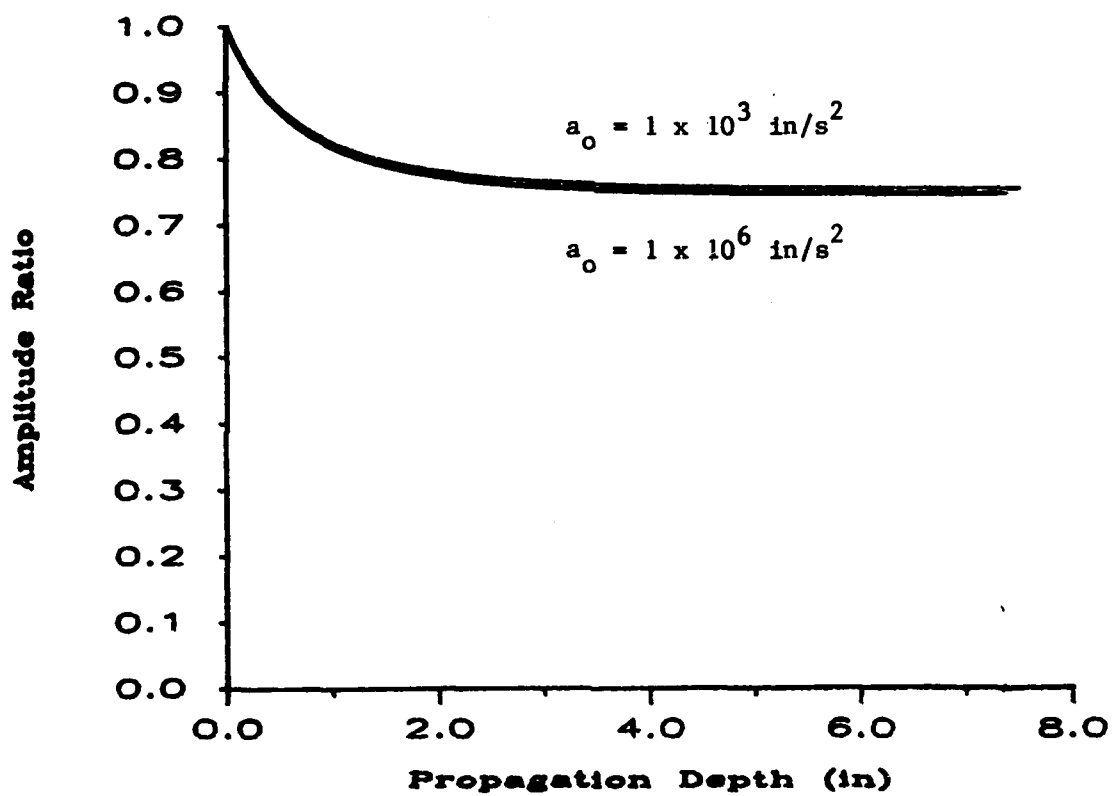


Figure 4.10. Amplitude ratio versus depth for an exponential volume distribution (Material E1 with $B = 10 \text{ in}^2/\text{lb}$ and $\nu_b = 0.75$).

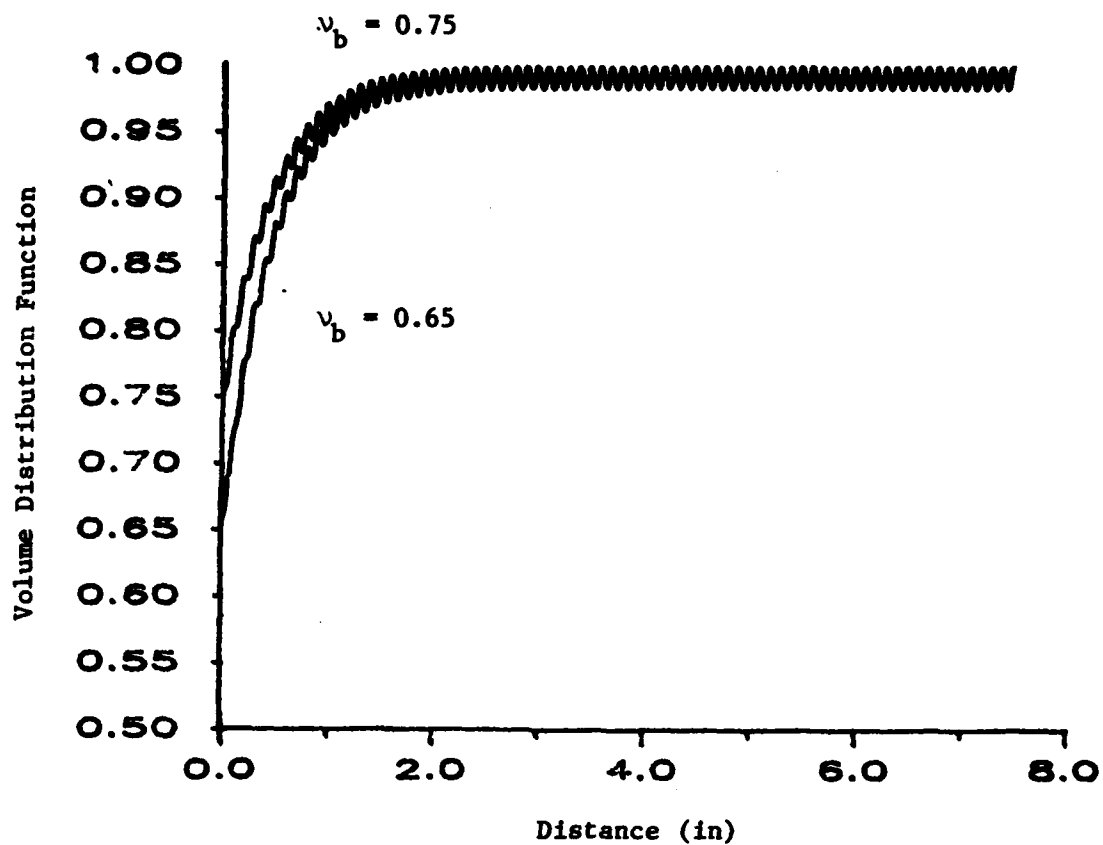


Figure 4.11. Combined periodic-exponential volume distribution function with $v_a = 0.992$, $B = 30 \text{ in}^2/\text{lb}$ and $\ell = 0.10 \text{ in}$.

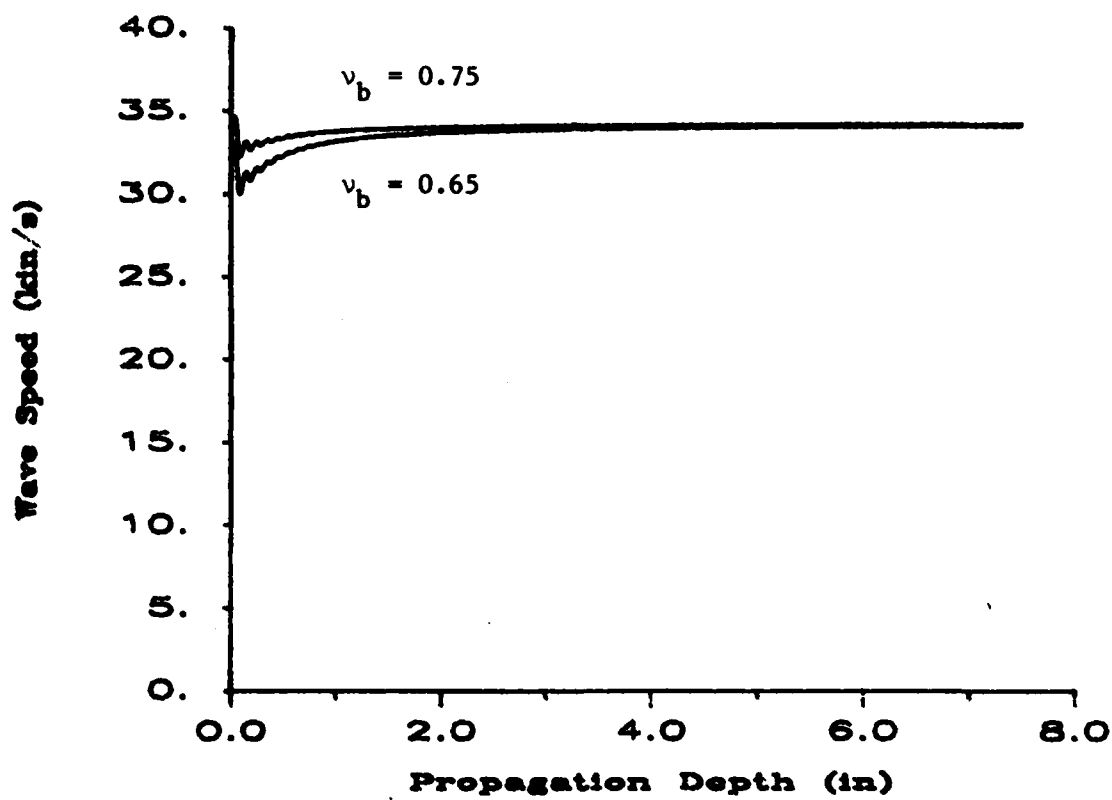


Figure 4.12. Average wave speed versus depth for a periodic-exponential volume distribution (Material PE1 with $\ell = 0.1$ in).

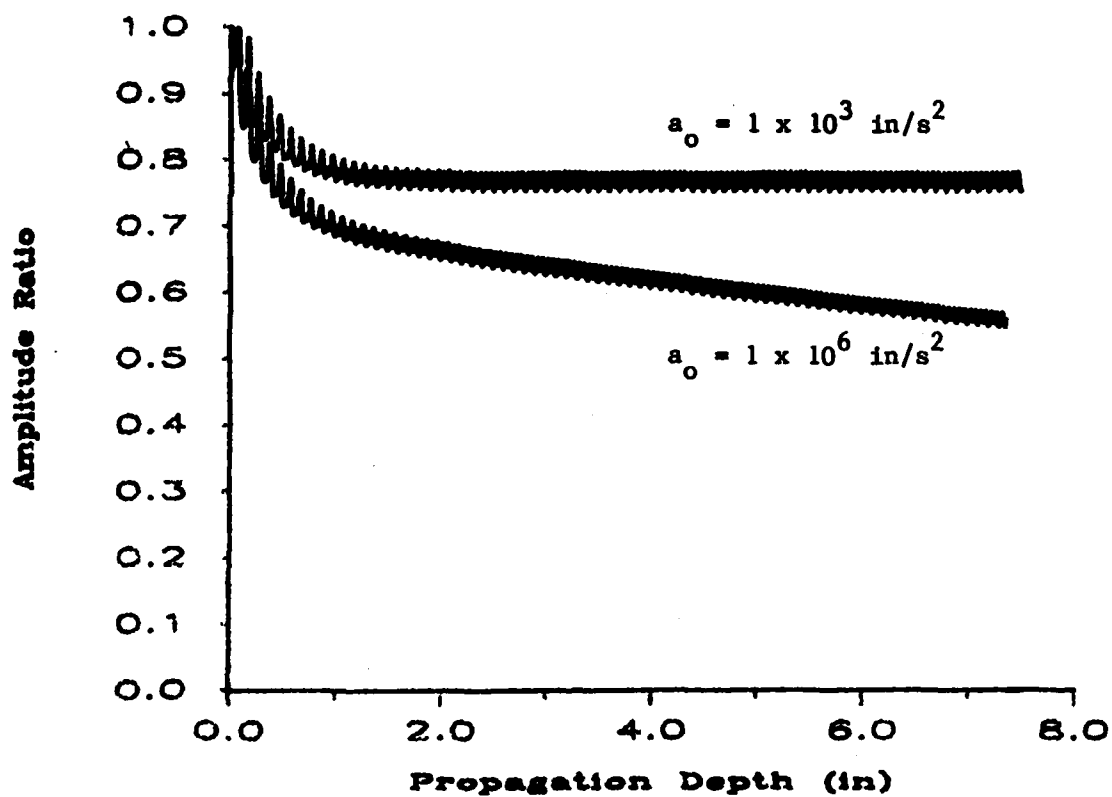


Figure 4.13. Amplitude ratio versus depth for a periodic-exponential volume distribution (Material PEI with $\ell = 0.1$ in and $\nu_b = 0.65$).

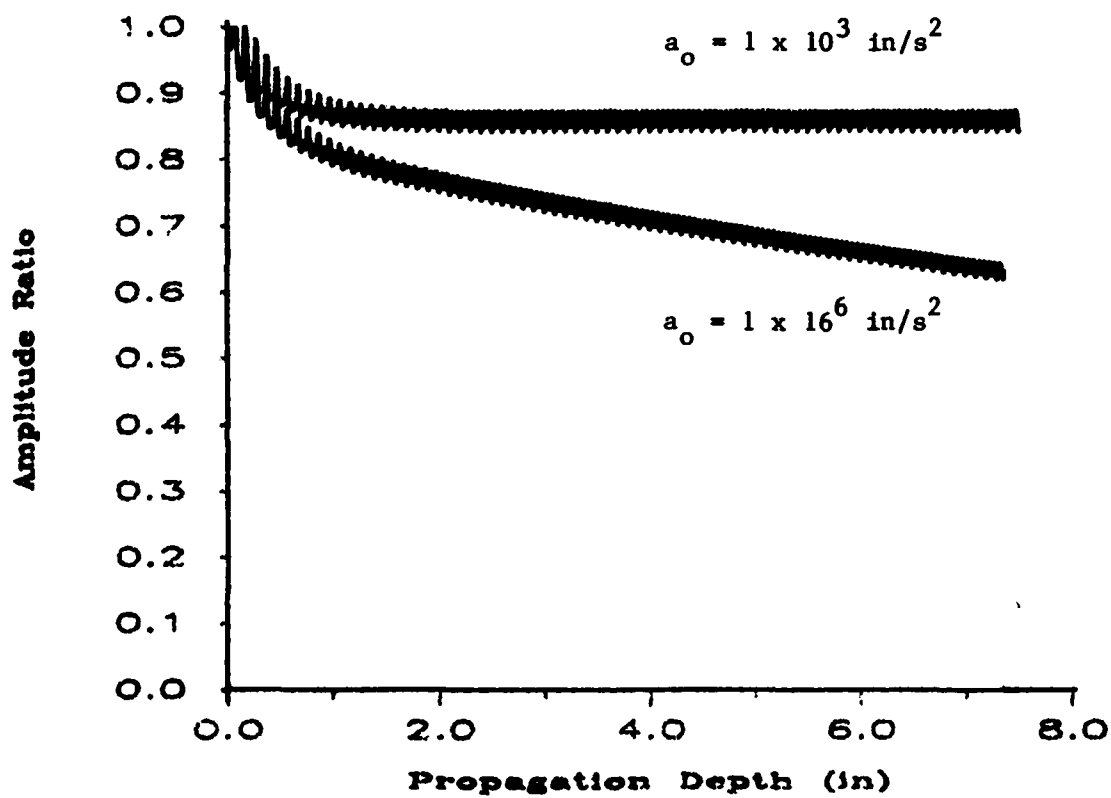


Figure 4.14. Amplitude ratio versus depth for a periodic-exponential volume distribution (Material PEI with $\ell = 0.1 \text{ in}$ and $v_b = 0.75$).

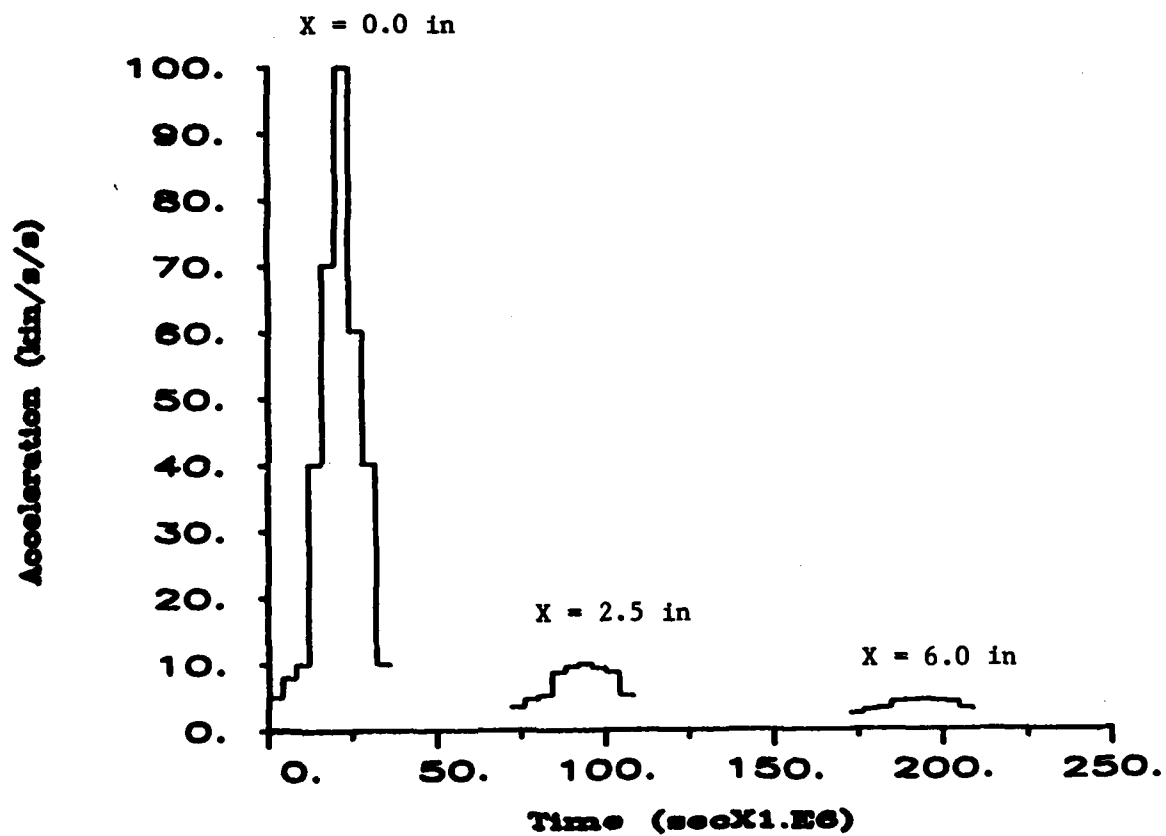


Figure 4.15. Uncoupled particle acceleration profiles at various depths (Material P1 with $v_a = 0.85$ and $l = 0.1$ in).

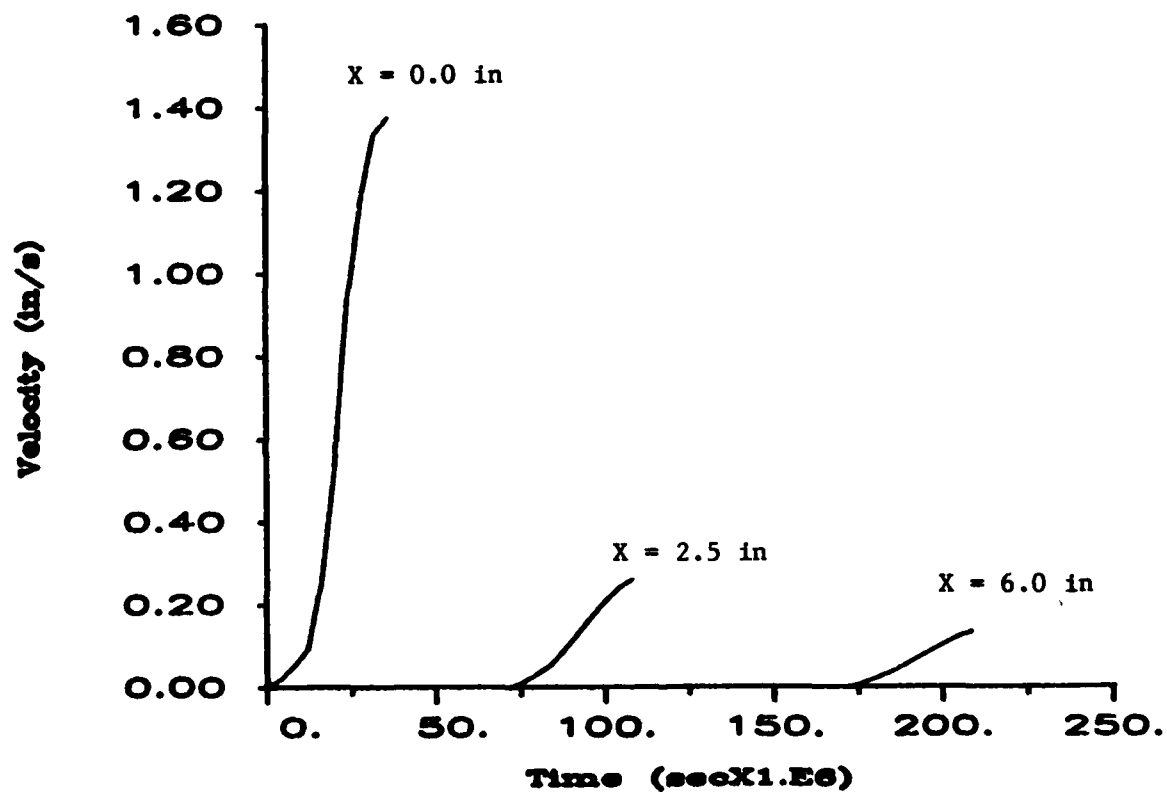


Figure 4.16. Uncoupled particle velocity profiles at various depths (Material P1 with $v_a = 0.85$ and $\ell = 0.1$ in).

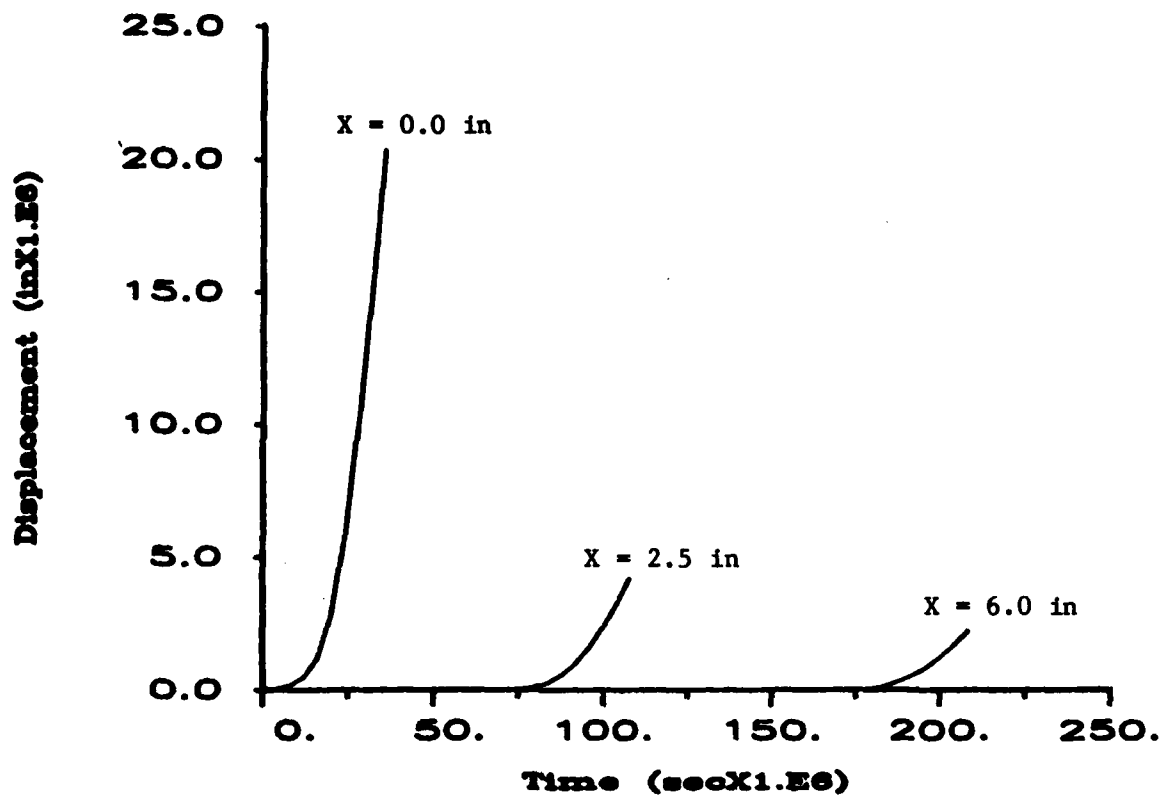


Figure 4.17. Uncoupled particle displacement profiles at various depths (Material P1 with $\nu_a = 0.85$ and $\ell = 0.1$ in).

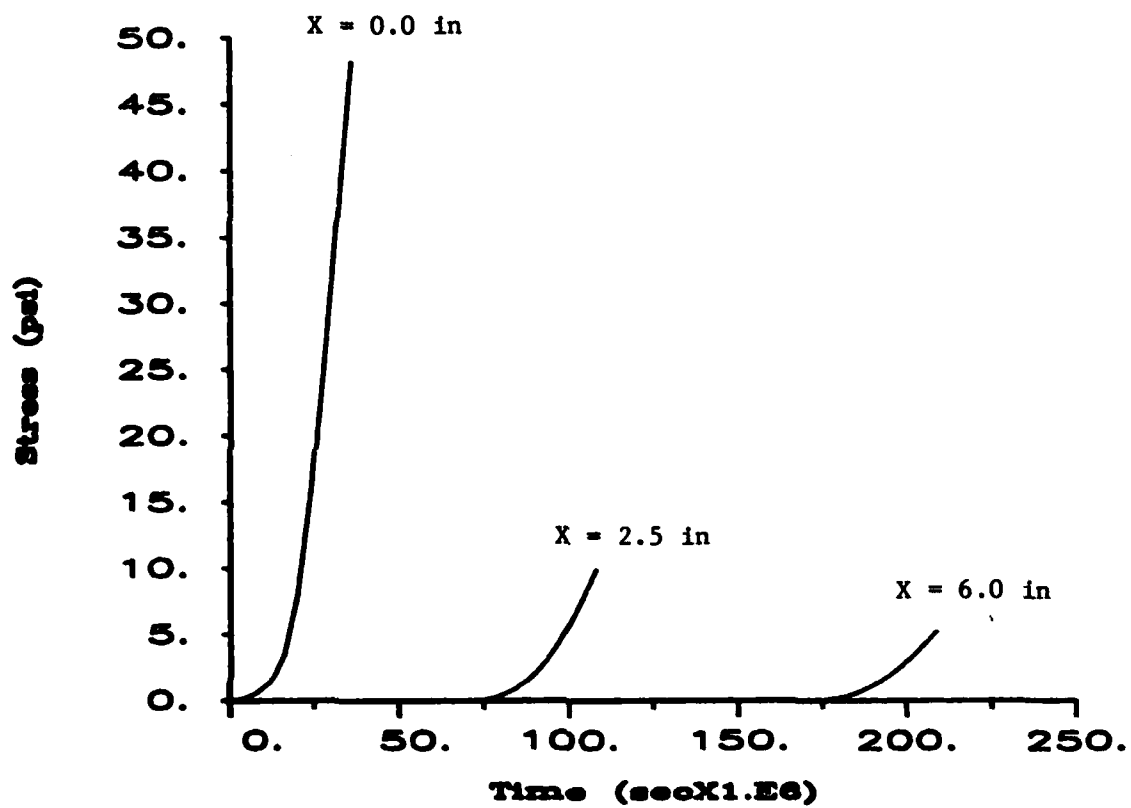


Figure 4.18. Uncoupled stress profiles at various depths (Material P1 with $\nu_a = 0.85$ and $\ell = 0.1$ in).

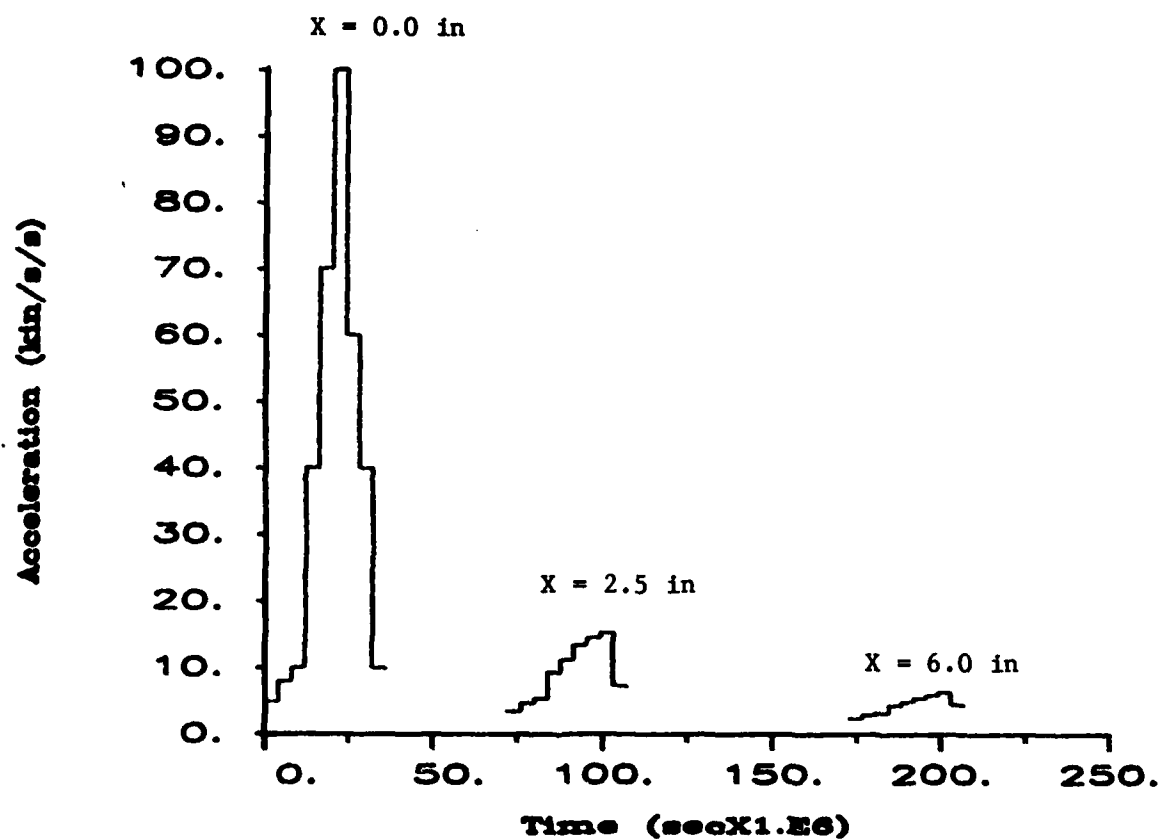


Figure 4.19. Coupled particle acceleration profiles at various depths (Material P1 with $v_a = 0.85$, $\ell = 0.1$ in, and $M = 0.04 \text{ in}^2/\text{lb}$). a_o

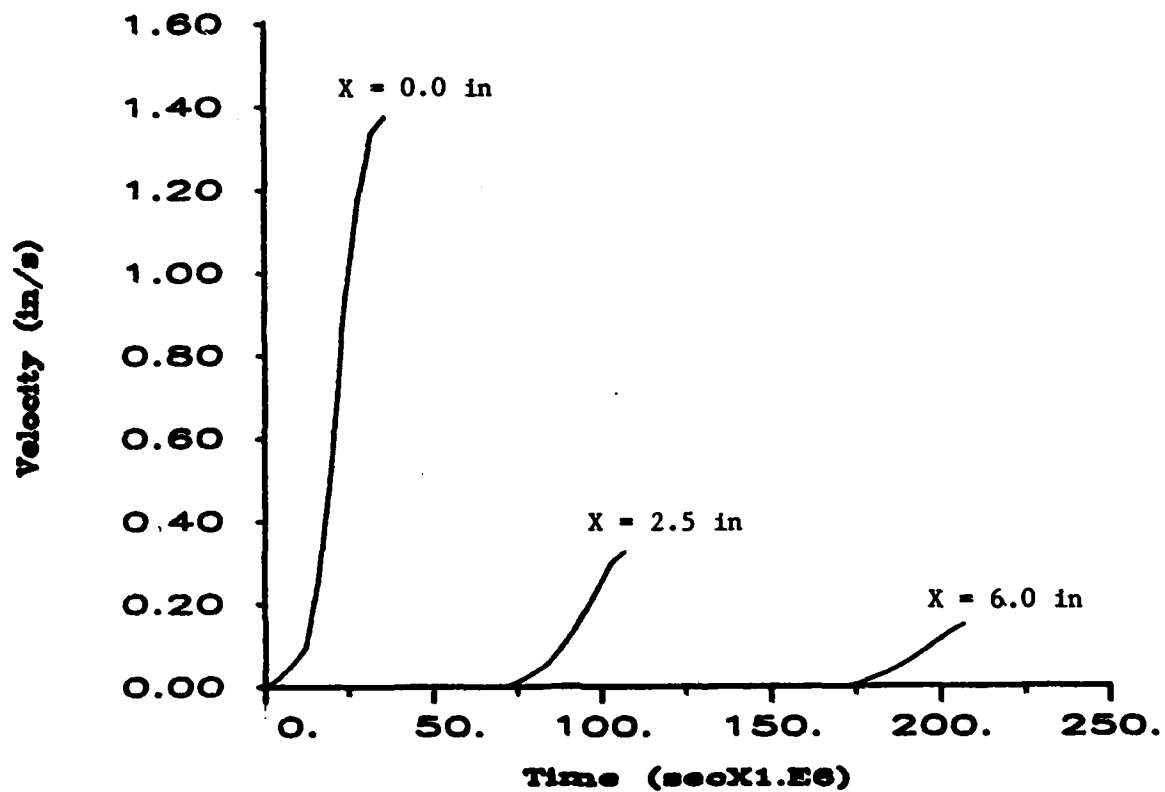


Figure 4.20. Coupled particle velocity profiles at various depths (Material P1 with $v_a = 0.85$, $l = 0.1$ in, and $M = 0.04$ in²/lb). v_a

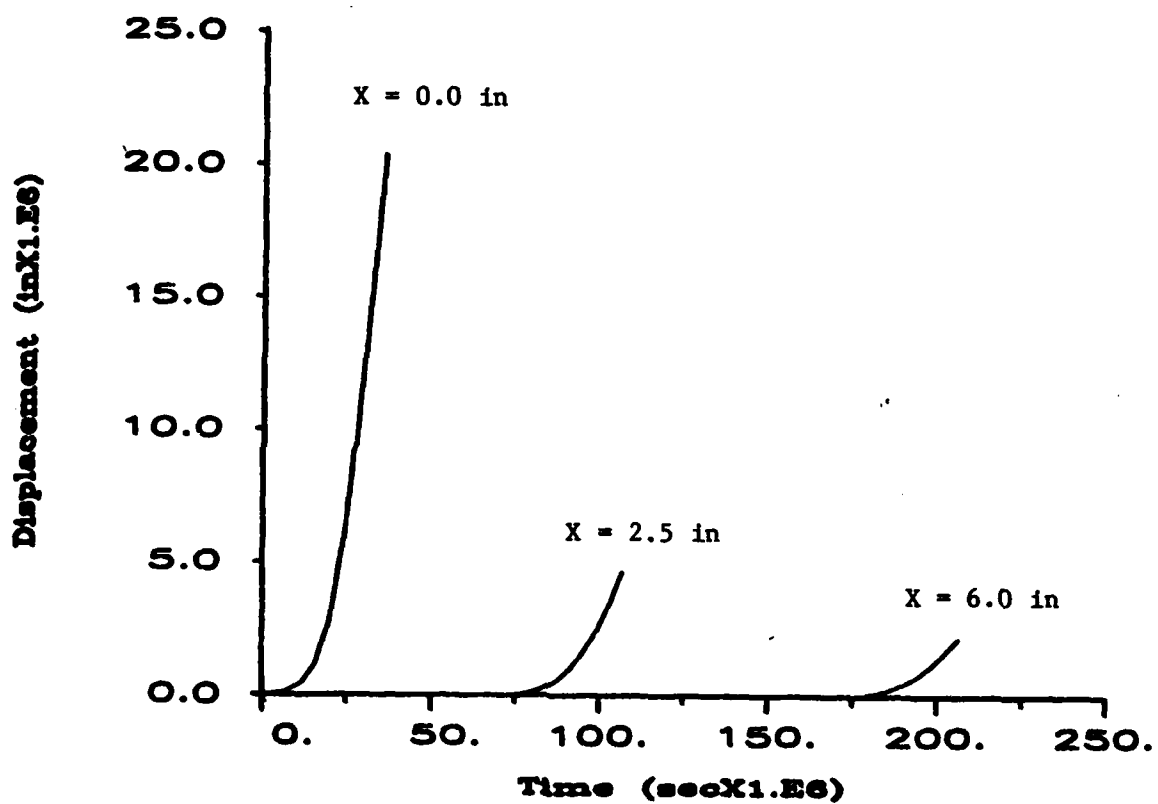


Figure 4.21. Coupled particle displacement profiles at various depths (Material Pl with $\nu_a = 0.85$, $\ell = 0.1$ in, and $M = 0.04$ in²/lb). a_o

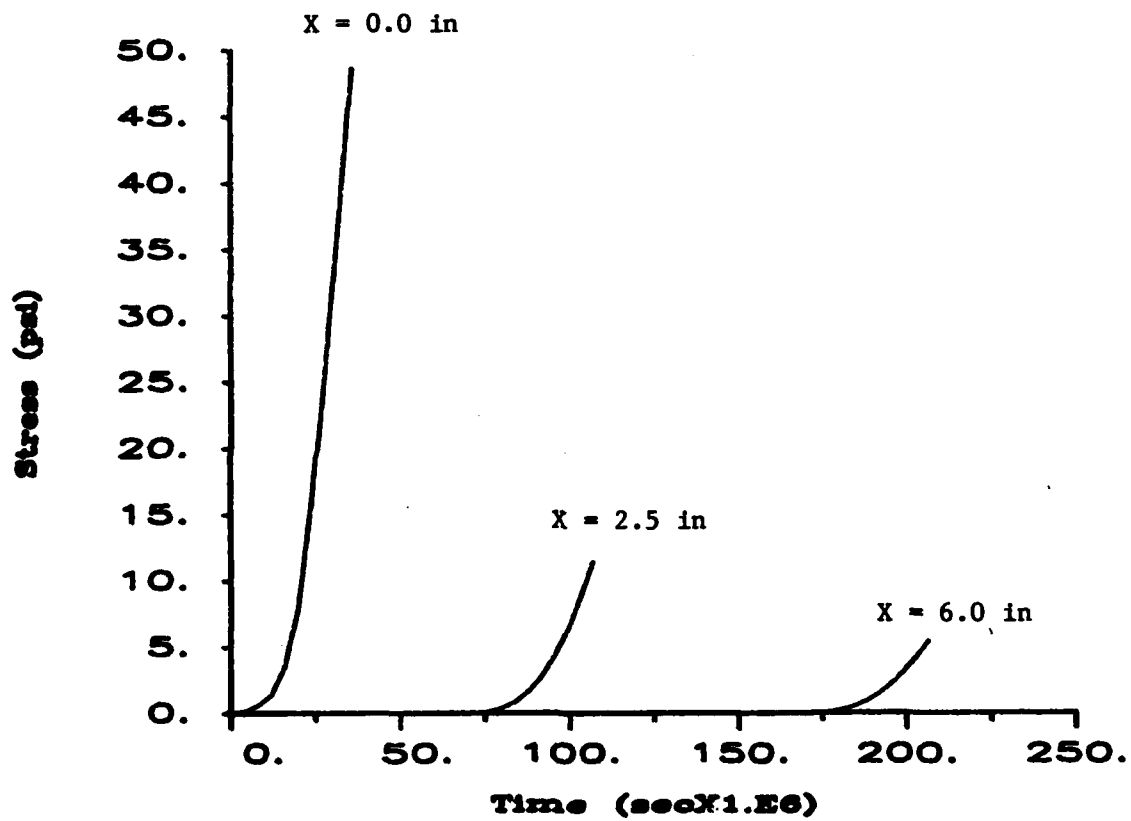


Figure 4.22. Coupled stress profiles at various depths (Material P1 with $\nu_{a_0} = 0.85$, $\ell = 0.1$ in, and $M = 0.04$ in²/lb).

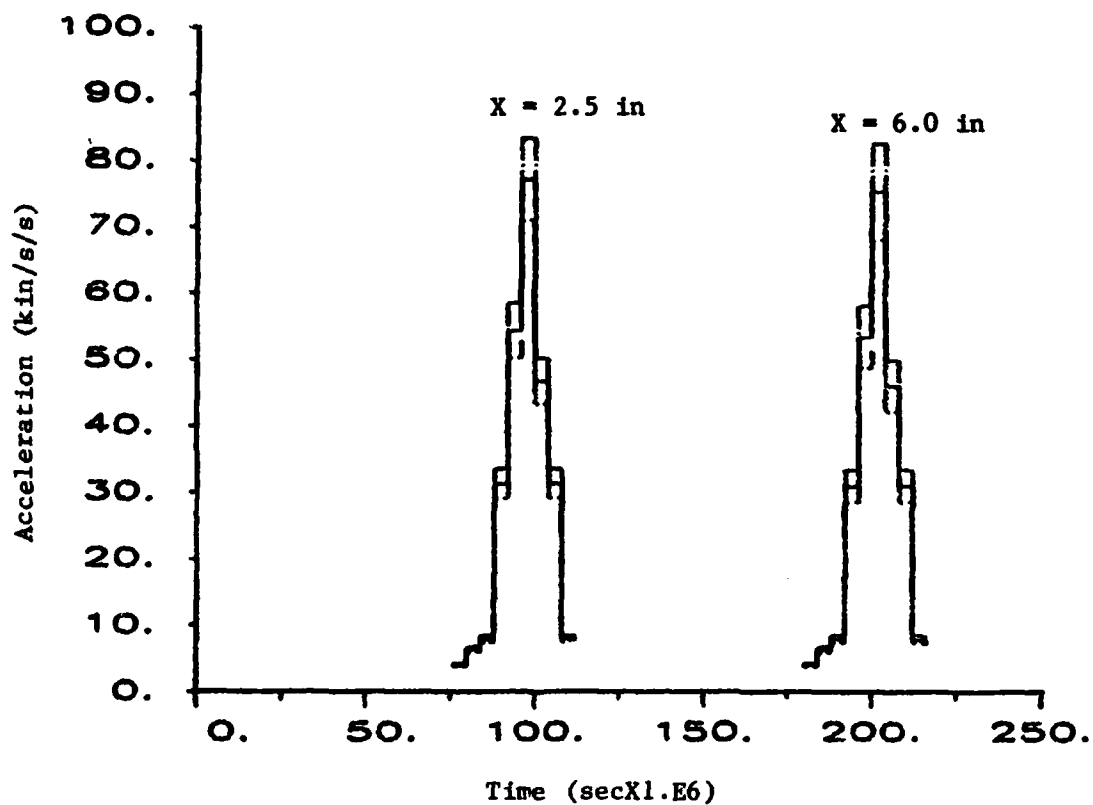


Figure 4.23. Probabilistic acceleration profiles at various depths; mean response with its one-standard-deviation bounds for $\bar{z} = 0.1$ in and $\sigma_z = 0.03$ in.

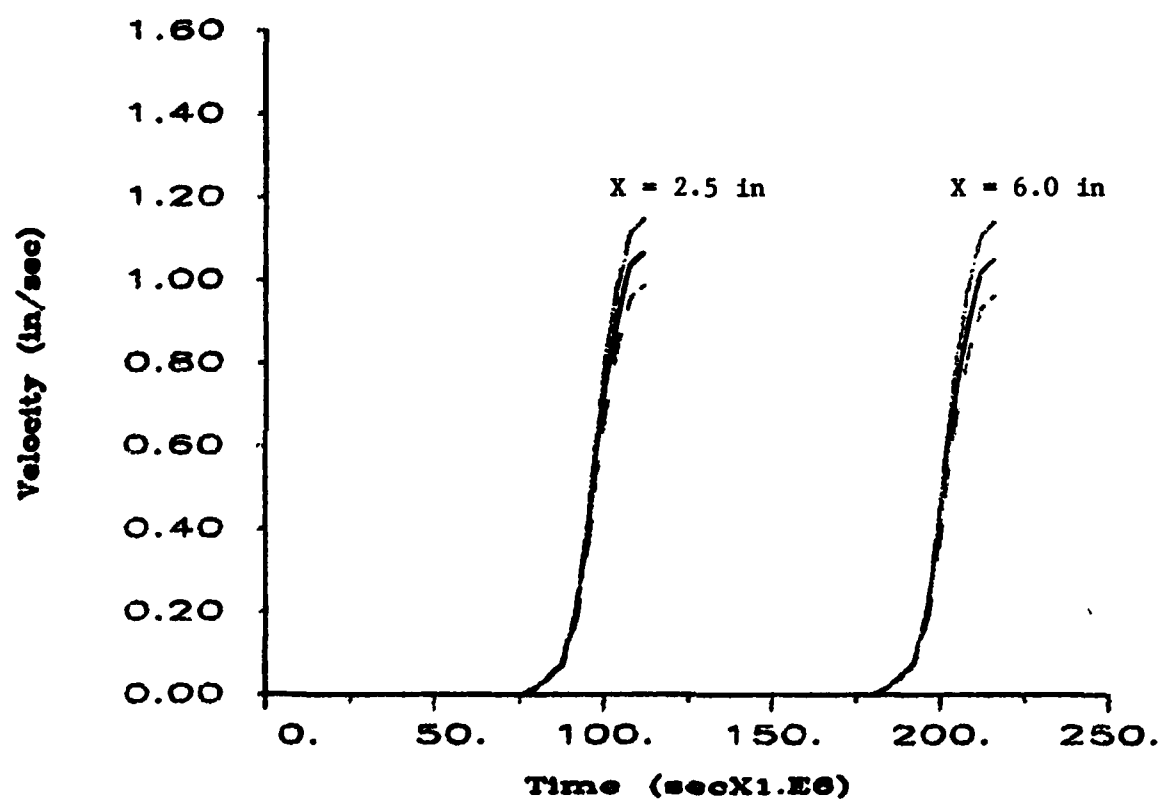


Figure 4.24. Probabilistic velocity profiles at various depths; mean response with its one-standard-deviation bounds for $\bar{\ell} = 0.1$ in and $\sigma_{\ell} = 0.03$ in.

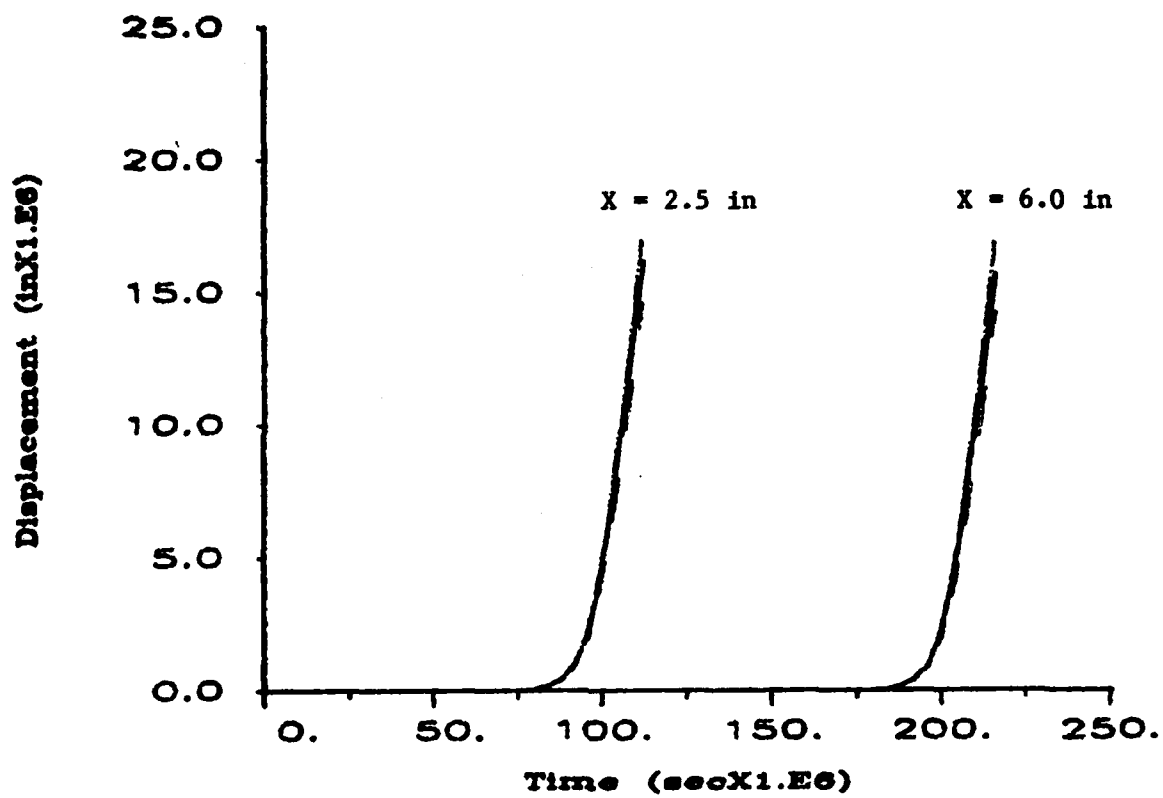


Figure 4.25. Probabilistic displacement profiles at various depths; mean response with its one-standard-deviation bounds for $\bar{\ell} = 0.1$ in and $\sigma_{\ell} = 0.03$ in.

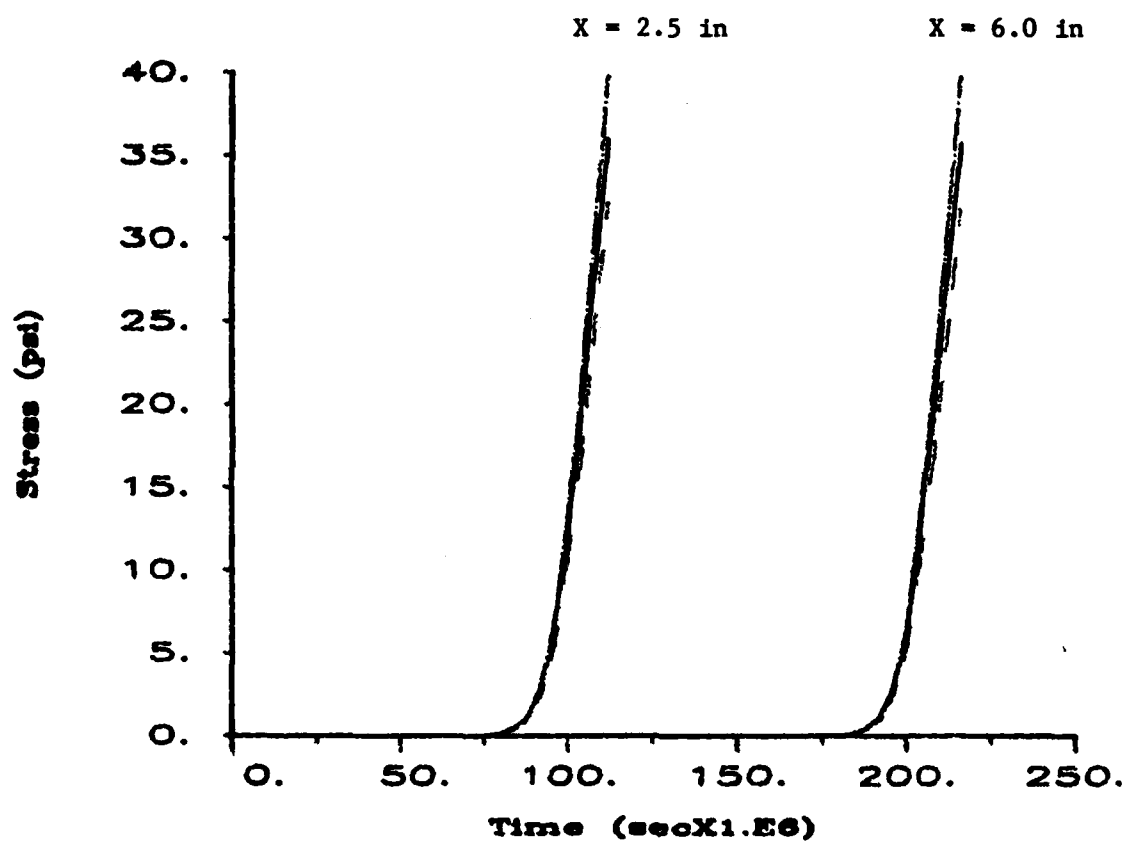


Figure 4.26. Probabilistic stress profiles at various depths; mean response with its one-standard-deviation bounds for $\bar{\ell} = 0.1$ in and $\sigma_{\ell} = 0.03$ in.

CHAPTER 5

SUMMARY AND RECOMMENDATIONS

5.1 SUMMARY

A one-dimensional computer program (referred to as MIC1D) has been developed for analyses of explosive wave propagation in granular materials with microstructure. The theoretical foundation of the computer program is based on the distributed body concept advanced by Goodman and Cowin (Reference 31) and the associated wave propagation studies conducted by Nunziato, Walsh, et al. (References 57-63). The computer program allows for (1) arbitrary surface airblast loading, (2) depth-dependent volume distribution function simulating gravity effects in a granular mass, and (3) treatment of grain size and local porosity as random variables. Three forms of depth-dependent volume distribution functions are incorporated in the program, i.e., a periodic form, an exponential form, and a combined periodic-exponential formulation. The user can select any of these forms for the particular application at hand. Probabilistic treatment of grain size and local porosity is accomplished by using a moment-generating procedure due to Rosenblueth (Reference 73). The computer program calculates the expected value and the variance of the output quantities, such as stress, particle motion, etc., due to the randomness in these variables.

Application of the computer program is demonstrated by presenting the results of a series of parametric calculations dealing with propagation of acceleration waves in granular media. It is shown that, within the range of variables studied, local porosity and grain size characteristics (which are reflected in the microstructural parameters v_a , v_b , B , l , γ_0 , γ) play an important role in wave attenuation in such materials. The effect of grain size parameter l on wave attenuation during short propagation distances (less than a hundred grains) is interesting and requires experimental verification.

5.2 RECOMMENDATIONS

Several recommendations are made for further development in the analytical aspects and for the experimental validation of the present work. First, the wave propagation model should be validated with an experimental setup that captures the dynamic load transfer and wave motion across several grain

boundaries. This can be accomplished via dynamic photoelasticity as described by Rossmannith and Shukla (Reference 75). For example, the dynamic photoelastic laboratory at the University of Rhode Island can take data at a rate of 10^6 frames/sec. It is possible to measure wave speed and amplitude attenuation as the dynamic loads are transferred across a finite number of particles. Second, the coupling effects for constructing wave profiles from a group of traveling waves should be examined further. In the present formulation, the coupling effects due to spatial redistribution of local porosity as the waves propagate through the medium were neglected. The consequence of this assumption needs to be examined. Third, in the present study the constitutive moduli were taken to be constant, but, in actuality, they depend on the basic microstructural parameters. Attempts should be made to relate these moduli to some basic microstructural variables of the granular medium. Studies in fabric tensor models proposed by Oda, Nemat-Nasser, et al., (Reference 67) may provide some direction for developing the desired relationships. Fourth, the probabilistic analysis in this study was only relevant to the periodic aspects of the volume distribution model since only v_a and l were treated as random variables. The present probabilistic analysis should be extended to treat v_b in the exponential distribution model also as a random variable. Finally, the wave propagation model should be extended to two-dimensional geometry. The variation in local porosity in two dimensions can then be incorporated in such a formulation without recourse to a probabilistic analysis.

REFERENCES

1. Atkin, R. J., Cowin, S. C., and Fox, N. 1977. "On Boundary Conditions for Polar Materials," Journal of Applied Mathematics and Physics (ZAMP), Vol 28, pp 1017-1026.
2. Bazant, Z. P., Krizek, R. J., and Sheih, C. L. 1983. "Hystertic Endochronic Theory for Sand," Journal of Engineering Mechanics, Vol 109, pp 1073-1095.
3. Bleich, H. H., Matthews, A. T., and Wright J. P. 1968. "Moving Step Load on the Surface of a Half-Space of Granular Material," International Journal of Solids and Structures, Vol 4, pp 243-286.
4. Brandt, H. 1955. "A Study of the Speed of Sound of Porous Granular Media," Journal of Applied Mechanics, Vol 22, pp 479-486.
5. Brown, J. W., Murnell, D. W., and Stout, J. H. July 1980. "Propagation of Explosive Shock Through Rubble Screens," Miscellaneous Paper SL-80-7, US Army Engineer Waterways Experiment Station, Vicksburg, MS.
6. Butcher, B. M., Carroll, M. M., and Holt, A. C. 1974. "Shock Wave Compaction of Porous Aluminum," Journal of Applied Physics, Vol 45, pp 3864-3875.
7. Carroll, M. M., and Holt, A. C. 1972. "Suggested Modification of the P- α Model for Porous Materials," Journal of Applied Physics, Vol 43, pp 759-761.
8. Carroll, M. M., and Holt, A. C. 1972. "Static and Dynamic Pore-Collapse Relations for Ductile Porous Materials," Journal of Applied Physics, Vol 43, pp 1626-1636.
9. Chambre, P. L. 1984. "Speed of a Plane Wave in a Gross Mixture," Journal of the Acoustical Society of America, Vol 26, pp 329-331.
10. Chen, P. J. 1984. "Growth and Decay of Waves in Solids," Mechanics of Solids, Vol III, Springer, pp 303-401.
11. Christoffersen, J., Mehrabadi, M. M., and Nemat-Nasser, S. 1981. "A Micromechanical Description of Granular Material Behavior," Journal of Applied Mechanics, Vol 48, pp 339-344.
12. Cowin, S. 1974. "A Theory for the Flow of Granular Materials," Powder Technology, Vol 9, pp 61-69.
13. Cowin, S. C. 1974. "Constitutive Relations That Imply a Generalized Mohr-Coulomb Criterion," Acta Mechanica, Vol 20, pp 41-46.
14. Cowin, S., and Goodman, M. A. 1976. "A Variational Principle for Granular Materials," Journal of Applied Mathematics and Physics (ZAMP), Vol 56, pp 281-286.

15. Cowin, S. 1978. "Microstructural Continuum Models for Granular Materials," Proceedings of US-Japan Seminar on Continuum Mechanical and Statistical Approaches in the Mechanics of Granular Materials, Tokyo, pp 162-170.
16. Cowin, S. C., and Satake, M. June 1978. "Continuum Mechanical and Statistical Approaches in the Mechanics of Granular Materials," Proceedings of US-Japan Seminar, Gakujutsu Bunken Fukyu-Kai, Tokyo.
17. Cowin, S. C., and Leslie, F. M. 1980. "On Kinetic Energy and Momenta in Cosserat Continua," Journal of Applied Mathematics and Physics (ZAMP), Vol 31, pp 247-260.
18. Cowin, S., and Nunziato, J. 1983. "Linear Elastic Materials with Voids," Journal of Elasticity, Vol 13, pp 125-147.
19. Cristescu, N. 1967. Dynamic Plasticity, North Holland.
20. Cundall, P., Marti, J., Beresford, P., Last, N., and Asgian, M. August 1978. "Computer Modelling of Jointed Rock Masses," Technical Report N-78-4, US Army Engineer Waterways Experiment Station, Vicksburg, MS.
21. Cundall, P. A., and Strack, D. L. 1979. "A Discrete Numerical Model for Granular Assemblies," Geotechnique, Vol 29, pp 47-65.
22. Deresiewicz, H. 1958. "Mechanics of Granular Matter," Advances in Applied Mechanics, Vol V, Academic Press Inc.
23. Drescher, A., and De Josselin De Jong, G. 1972. "Photoelastic Verification of a Mechanical Model for the Flow of a Granular Material," Journal of the Mechanics and Physics of Solids, Vol 20, pp 337-351.
24. Drescher, A. 1979. "Application of Photoelasticity to Investigation of Constitutive Laws for Granular Materials," Proceedings of IUTAM-Symposium on Optical Methods in Solid Mechanics, Poltiers, France.
25. Drumheller, D. S. 1978. "The Theoretical Treatment of a Porous Solid Using a Mixture Theory," International Journal of Solids and Structures, Vol 14, pp 441-456.
26. Duffy, J., and Mindlin, R. D. 1957. "Stress-Strain Relations and Vibration of a Granular Medium," Journal of Applied Mechanics, pp 585-593.
27. Durelli, A. J., and Wu, D. 1983. "Use of Coefficients of Influence to Solve Some Inverse Problems in Plane Elasticity," Journal of Applied Mechanics, Vol 50, pp 288-296.
28. Endley, S. N., and Peyrot, H. 1977. "Load Distribution in Granular Media," Journal of the Engineering Mechanics Division, pp 99-111.
29. Fletcher, E. H. 1971. "Random Walk Model of Ideal Granular Mass," Journal of the Soil Mechanics and Foundations Division, American Society of Civil Engineers, Vol 98, No. SM10, Proceedings Paper 8444, pp 1379-1392.

30. Fu, L. S. 1984. "A New Micro-Mechanical Theory for Randomly Inhomogeneous Media," Wave Propagation in Homogeneous Media and Ultrasonic Non-Destructive Evaluation, AMD, Vol 62, Ed. G. C. Johnson, American Society of Mechanical Engineers.
31. Goodman, M. A., and Cowin, S. C. 1972. "A Continuum Theory for Granular Materials," Archive for Rational Mechanics and Analysis, Vol 44, pp 249-266.
32. Garg S. K., Brownell, D. H., Pritchett, J. W., and Hermann, R. G. 1975. "Shock Wave Propagation in Fluid-Saturated Porous Media," Journal of Applied Physics, Vol 46, pp 702-713.
33. Gassman, F. 1951. "Elastic Waves Through a Packing of Spheres," Geophysics, Vol 16, pp 673-685.
34. Hendron, A. J., Jr. July 1963. "The Behavior of Sand in One-Dimensional Compression," Ph.D. Dissertation, University of Illinois.
35. Herrmann, W. 1969. "Constitutive Equation for the Dynamic Compaction of Ductile Porous Materials," Journal of Applied Physics, Vol 40, pp 2490-2499.
36. Hill, J. M., and Harr, M. E. 1982. "Elastic and Particulate Media," Journal of the Engineering Mechanics Division, American Society of Civil Engineers, Vol 108, pp 596-604.
37. Hsieh, L., and Yew, C. H. 1973. "Wave Motions in a Fluid Saturated Porous Medium," American Society of Mechanical Engineers Paper No. 73-APMW-16.
38. Hudson, J. A. 1968. "The Scattering of Elastic Waves by Granular Media," Quarterly Journal of Mechanics and Applied Mathematics, Vol 21, pp 487-502.
39. Hughes, D. S., and Cross, J. H. 1951. "Elastic Wave Velocities in Rocks at High Pressures and Temperatures," Geophysics, Vol XVI No. 4, pp 577-593.
40. Hughes, D. S., and Kelly, J. L. 1952. "Variation of Elastic Wave Velocity with Saturation in Sandstone," Geophysics, Vol 17, pp 739-752.
41. Iida, K. 1939. "The Velocity of Elastic Waves in Sand," Bulletin Earthquake Research Institute, Vol 17, pp 783-807.
42. Iida, K. 1939. "Velocity of Elastic Waves in a Granular Substance," Bulletin Earthquake Research Institute, Japan, Vol 17, pp 783-808.
43. Jackson, J. G., Ehrgott, J. Q., and Rohani, B. 1980. "Loading Rate Effects on Compressibility of Sand," Journal of the Geotechnical Engineering Division, American Society of Civil Engineers, Vol 106, pp 839-852.
44. Jenkins, J. T. 1975. "Static Equilibrium of Granular Materials," Journal of Applied Mechanics, Vol 42, pp 603-606.

45. Jenkins, J. T., and Satake, M. August 1982. "Mechanics of Granular Materials-New Models and Constitutive Relations," Proceedings of US-Japan Seminar on New Models and Constitutive Relations in the Mechanics of Granular Materials, Elsevier, Cornell University.
46. Junger, M. C. 1981. "Dilational Waves in an Elastic Solid Containing Lined, Gas Filled, Spherical Cavities," Journal of the Acoustical Society of America, Vol 69, pp 1573-1576.
47. Kipp, M. E., and Lawrence, R. J. June 1982. "WONDY V- A One-Dimensional Finite-Difference Wave Propagation Code," Sandia Laboratories Report SAND18-0930.
48. Krizek, R. J. 1971. "Rheologic Behavior of Cohesionless Soils Subjected to Dynamic Load," Transactions. Society of Rheology, Vol 15, pp 491-540.
49. Kuo, C. L. May 1983. "Modeling of Dynamic Deformation Mechanisms for Granular Material," Ph.D. Dissertation, University of Massachusetts.
50. Lin, H. C., and Wu, H. C. 1976. "Strain Rate Effect in the Endochronic Theory of Viscoplasticity," Journal of Applied Mechanics, Vol 43, pp 92-96.
51. Mal, A. K., and Bose, S. K. 1974. "Dynamic Elastic Moduli of a Suspension of Imperfectly Bonded Spheres," Proceedings of Cambridge Philological Society, Vol 76, pp 587-600.
52. Morland, L. W. 1976. "Elastic Anisotropy of Regularly Jointed Media," Rock Mechanics, Vol 8, pp 35-48.
53. Mroz, A. 1980. "Deformation and Flow of Granular Materials," IUTAM Conference Proceedings, pp 119-132.
54. Mullenger, G. 1978. "A Condition for a Continuum Model of Granular Structure," Proceedings of US-Japan Seminar on Continuum Mechanical and Statistical Approaches in the Mechanics of Granular Materials, Tokyo, pp 282-290.
55. Nachlinger, R. R., and Nunziato, J. W. 1976. "Wave Propagation and Uniqueness Theorems for Elastic Materials with Internal State Variables," International Journal of Engineering Science, Vol 14, pp 31-38.
56. Nemat-Nasser, S., and Mehrabadi, M. M. 1984. "Micromechanically Based Rate Constitutive Descriptions for Granular Materials," Mechanics of Engineering Materials, ed. Desai, C. S., and Gallagher, R. H., John Wiley.
57. Nunziato, J., Walsh, E. 1977. "On the Influence of Void Compaction and Material Non-uniformity on the Propagation of One-Dimensional Acceleration Waves in Granular Materials," Archive for Rational Mechanics and Analysis, Vol 64, pp 299-316.
58. Nunziato, J., and Walsh, E. 1977. "Small-Amplitude Wave Behavior in One-Dimensional Granular Solids," Journal of Applied Mechanics, Vol 44, pp 559-564.

AD-A173 015

A STUDY OF EXPLOSIVE WAVE PROPAGATION IN GRANULAR
MATERIALS WITH MICROSTR (U) RHODE ISLAND UNIV KINGSTON
DEPT OF MECHANICAL ENGINEERING AND M H SADD ET AL

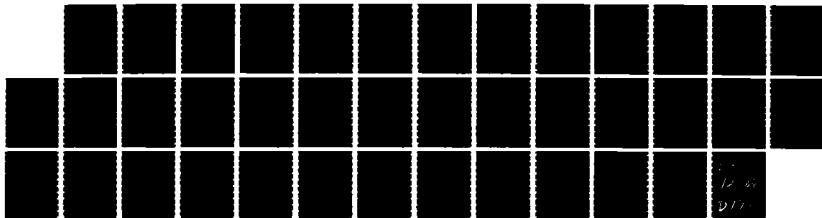
2/2

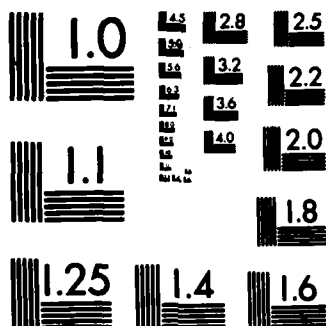
UNCLASSIFIED

SEP 86 WES/TR/SL-86-35 DACA39-85-C-0023

F/G 19/4

NL





MICROCOPY RESOLUTION TEST CHART
NATIONAL BUREAU OF STANDARDS-1963-A

59. Nunziato, J. W., and Yarrington, P. 1977. "A Continuum Theory of Porous Materials with Application to Wave Propagation Calculations," Sandia National Laboratories Report.
60. Nunziato, J. 1978. "The Propagation of Plane Waves in Granular Media," Proceedings of US-Japan Seminar on Continuum Mechanical and Statistical Approaches in the Mechanics of Granular Materials, Tokyo, pp 291-300.
61. Nunziato, J., Kennedy, J. E., and Walsh, E. 1978. "The Behavior of One-Dimensional Acceleration Waves in an Inhomogeneous Granular Solid," International Journal of Engineering Science, Vol 16, pp 647-648.
62. Nunziato, J., and Walsh, E. 1978. "One-Dimensional Shock Waves in Uniformly Distributed Granular Materials," International Journal of Solids and Structures, Vol 14, pp 681-689.
63. Nunziato, J., and Cowin, S. 1979. "A Nonlinear Theory of Elastic Materials with Voids," Archive for Rational Mechanics and Analysis, Vol 72, pp 175-201.
64. Nunziato, J., and Walsh, E. 1980. "On Ideal Multiphase Mixtures with Chemical Reactions and Diffusion," Archive for Rational Mechanics and Analysis, Vol 73, pp 285-311.
65. Nunziato, J. 1983. "A Multiphase Mixture Theory for Fluid-Particle Flows," Theory of Dispersive Multiphase Flow, Academic Press.
66. Nunziato, J. W. 1983-84. "Initiation and Growth-to-Deformation in Reactive Mixtures," Shock Waves in Condensed Matter, Eds. Asay, J. R., Graham, G. K., and Straub, G. K., Elsevier, pp 581-588.
67. Oda, M., Nemat-Nasser, S., and Mehrabadi, M. M. 1982. "A Statistical Study of Fabric in a Random Assembly of Spherical Granules," International Journal for Numerical and Analytical Methods in Geomechanics, Vol 6, pp 77-94.
68. Passman, S. 1983. "Consequences of a Theory for Flowing Granular Materials," Mechanics of Granular Materials: New Models and Constitutive Relations, ed. by Jenkins and Satake, Elsevier, pp 255-260.
69. Passman, S. L., and Batra, R. C. August 1984. "A Three-Dimensional Model for a Porous Elastic Anisotropic Solid with Inclusions, Taking into Account Dissipation, Heat Flux, Radiation and Thermal Stress," Sandia National Laboratories Report SAND84-0847.
70. Read, H. E., and Valanis, K. C. 1979. "An Endochronic Constitutive Model for General Hysteretic Response of Solids," Final Report Research Project 810, Electric Power Research Institute, Palo Alto, CA.
71. Rohani, B. July 1970. "Theoretical Studies of Stress Wave Propagation in Laterally Confined Soils," US Army Engineer Waterways Experiment Station Working Draft Report.

72. Rohani, B., and Cargile, J. D. April 1984. "A Probabilistic One-Dimensional Ground Shock Code for Layered Nonlinear Hysteretic Materials," Miscellaneous Paper SL-84-6, US Army Engineer Waterways Experiment Station, Vicksburg, MS.
73. Rosenblueth, E. 1975. "Point Estimates for Probability Moments," Proceedings. National Academy of Sciences (USA), Vol 72, No. 10, pp 3812-3814.
74. Rosenblueth, E. 1981. "Two-Point Estimates in Probabilities," Applied Mathematical Modelling, Vol 5, pp 329-335.
75. Rossmanith, H. P., and Shukla, A. 1982. "Photoelastic Investigation of Dynamic Load Transfer in Granular Media," Acta Mechanica, Vol 42, pp 211-225.
76. Sadd, M. H. October 1984. "A Preliminary Investigation of Wave Propagation in Granular Materials with Microstructure," Final Report, US Army Engineer Waterways Experiment Station, Vicksburg, MS.
77. Shahinpoor, M. 1983. "Frequency Distribution of Voids in Randomly Packed Monogranular Layers," Mechanics of Granular Materials: New Models and Constitutive Relations, ed by Jenkins, J. T., and Satake, M., Elsevier.
78. Soo, S. L. 1983. "Dynamic Interactions of Granular Materials," Advances in the Mechanics and Flow of Granular Materials, Ed. Shahinpoor, M., Vol II, Trans. Tech. Pub., pp 675-698.
79. Takahashi, T., and Sato, Y. 1949. "On the Theory of Elastic Waves in Granular Substance," Bulletin Earthquake Research Institute, Japan, Vol 27, pp 11-16.
80. Toupin, R. A. 1964. "Theories of Elasticity with Couple-Stress," Archive for Rational Mechanics and Analysis, Vol 17, pp 85-112.
81. Varadan, V. K., Varadan, V. V., and Ma, Y. August 1983. "Propagation and Scattering of Elastic Waves in Discrete Random Media," Proceedings of the 20th Annual Meeting of Society of Engineering Science, University of Delaware, p 310.
82. Vardoulakis, I. G., and Beskos, D. E. 1983. "On the Dynamic Behavior of Nearly Saturated Granular Media," Geomechanics, AMD-Vol 57, American Society of Mechanical Engineers Publications.
83. Vermeer, P. A., and Luger, H. J. September 1982. "Deformation and Failure of Granular Materials," IUTAM Symposium on Deformation and Failure of Granular Materials, Delft, A. A. Balkema.
84. Zienkiewicz, O. C., and Shiomi, T. 1984. "Dynamic Behavior of Saturated Porous Media; The Generalized Biot Formulation and Its Numerical Solution," International Journal for Numerical and Analytical Methods in Geomechanics, Vol 8, pp 71-96.

APPENDIX A
WAVE PROPAGATION COMPUTER CODE

APPENDIX A

WAVE PROPAGATION
COMPUTER CODE

GLOSSARY OF MAJOR VARIABLE NAMES

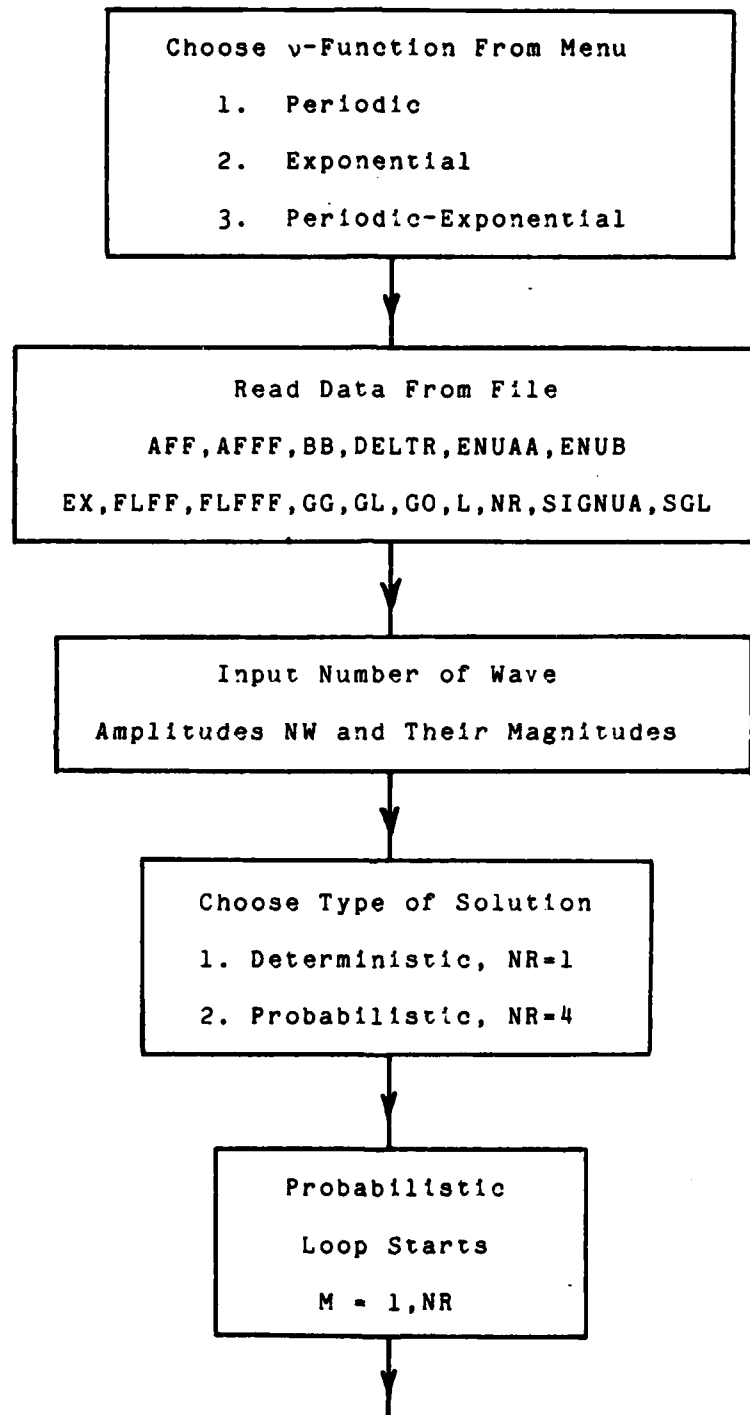
<u>NAME</u>	<u>DEFINITION</u>
A(N,J)	Acceleration array for N depths and J waves
A1(N,J)	Acceleration array for probabilistic calculations
A2(N,J)	Acceleration array for probabilistic calculations
A3(N,J)	Acceleration array for probabilistic calculations
A4(N,J)	Acceleration array for probabilistic calculations
AB(2J)	Amplitude array for acceleration plotting
AFF	α_e , material constant
AFFF	α_{ee} , material parameter
AM(2J)	Acceleration profile minus one-standard-deviation
AP(2J)	Acceleration profile plus one-standard-deviation
APLOT(2J,..)	Acceleration array for probabilistic plotting
AR(N,J)	Normalized amplitude array
BB	B, power of exponential volume distribution function
C1(N,J)	μ coefficient in amplitude equation
C2(N,J)	κ coefficient in amplitude equation
C3(N,J)	Array for volume distribution function
DD(J,..)	Particle displacement array for probabilistic plotting
DELTR	Initial time increment between input acceleration waves
DELX(N,J)	Distance between two consecutive waves.
DISP(N,J)	Array for particle displacement
DM(J)	Particle displacement profile minus one-standard-deviation

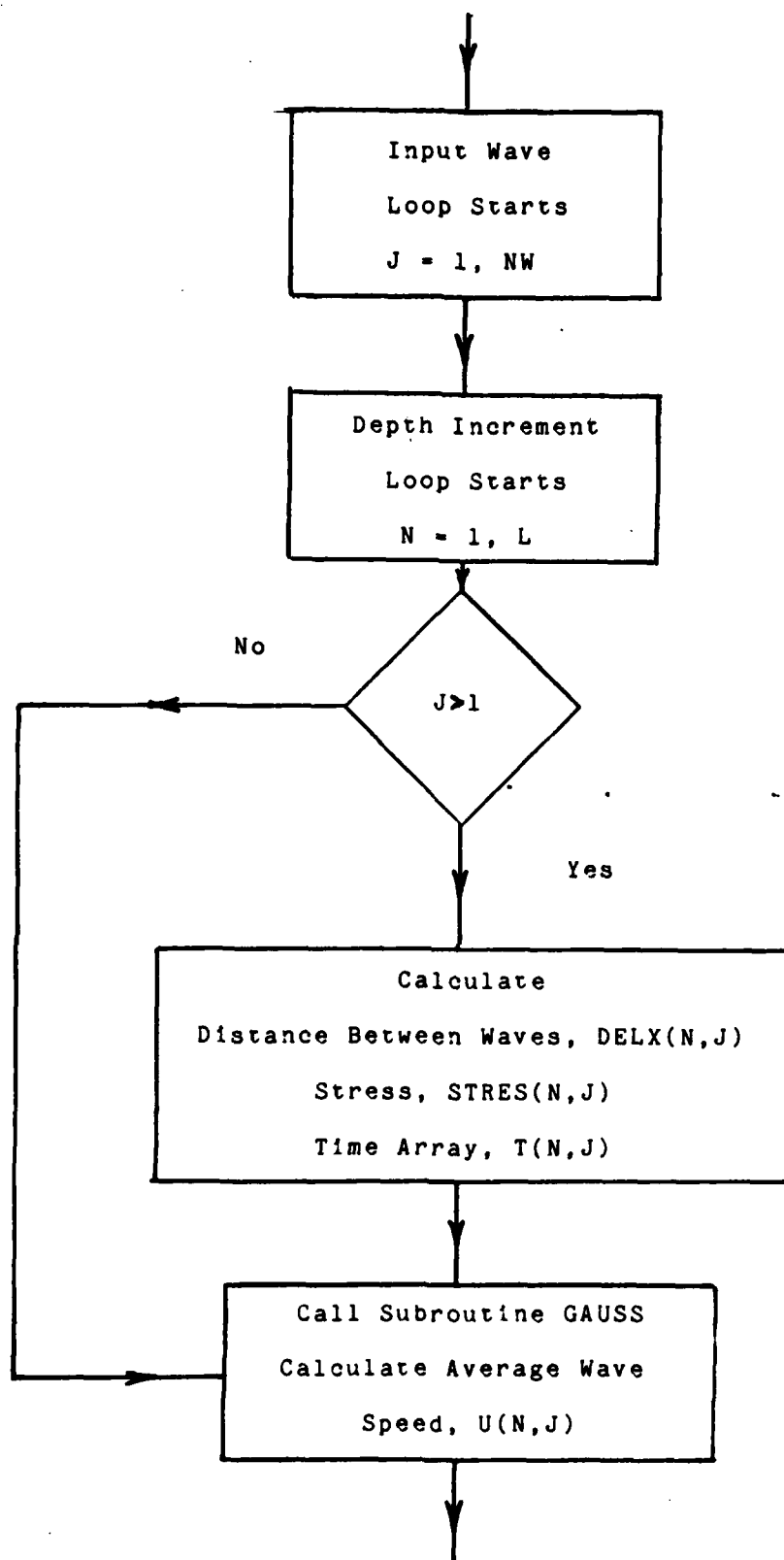
DP(J)	Particle displacement profile plus one-standard-deviation
DPLOT(J)	Displacement array for plotting
D1(N,J)	Displacement array for probabilistic calculations
D2(N,J)	Displacement array for probabilistic calculations
D3(N,J)	Displacement array for probabilistic calculations
D4(N,J)	Displacement array for probabilistic calculations
EA(2J)	Expected acceleration profile array
ED(J)	Expected particle displacement profile array
ENUAA	$(v_a)_0$ value of v_a in the reference state
ENUB	v_b material function for exponential volume distribution function
ES(J)	Expected stress profile array
EV(J)	Expected particle velocity profile array
EX	M, material constant in equation (3.25)
FLFF	Λ_e , material constant
FLFFF	Λ_{ee} , material constant
GG	γ , specific weight of the material used in equation (3.2)
GL	l , characteristic length for periodic distribution form (3.1)
GO	γ_0 , weight density of the material
H	$l/40$, interval measure for numerical integration
J	Looping index for number of input waves
L	Maximum limit of the looping parameter N for propagation depth
M	Looping index for probabilistic calculations
N	Looping index for depth incrementing
NR	Maximum number of runs for probabilistic calculations. (NR=1 yields deterministic case)

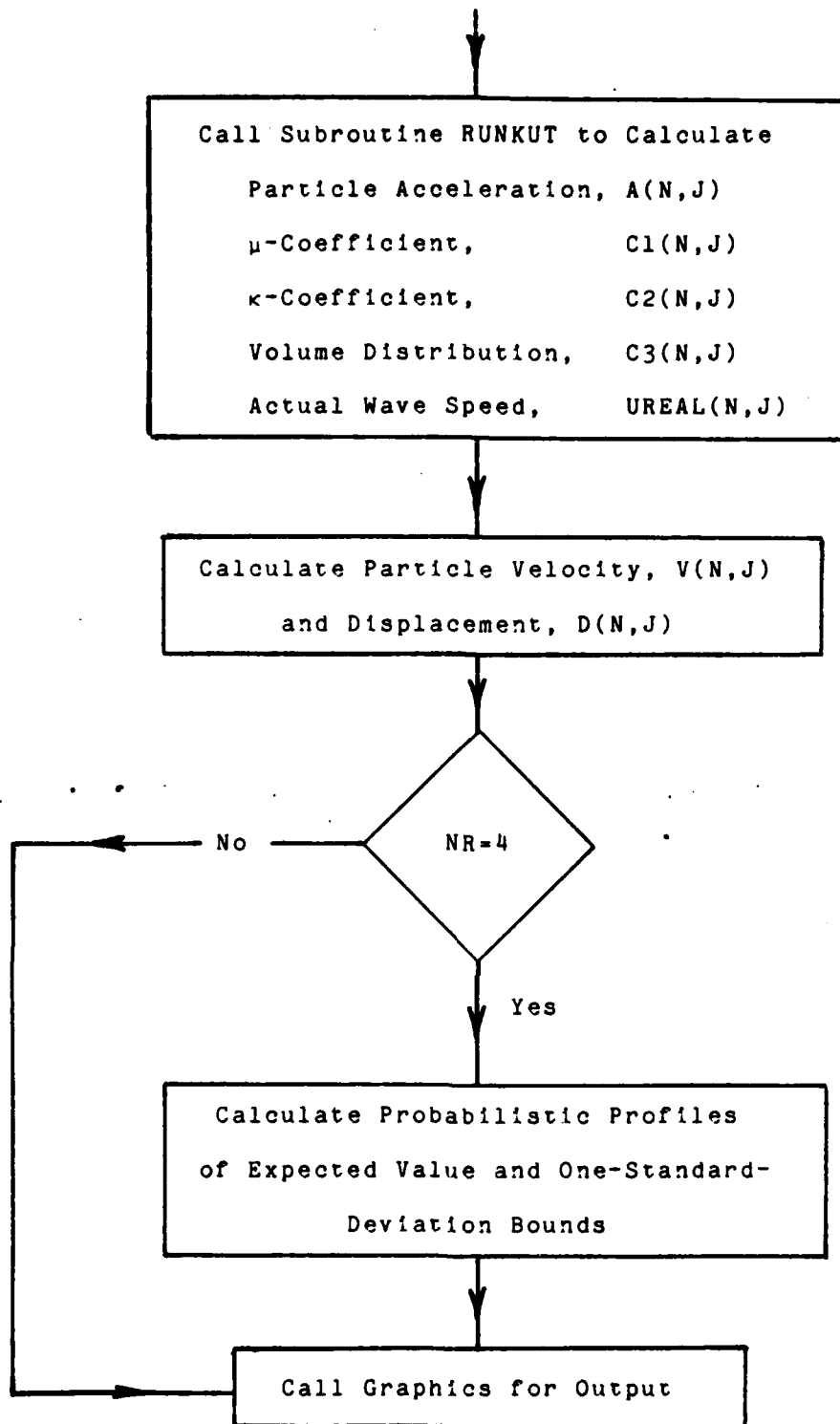
NV	Value of looping parameter at a desired depth
NW	Number of initial input wave amplitudes used to construct a profile
PSTRES(J)	Array used for plotting of stress profile
SIGNUA	σ_{va} , the standard deviation for volume distribution parameter v_a
SGL	σ_l , the standard deviation for characteristic length, l
SM(J)	Stress profile minus one-standard-deviation
SP(J)	Stress profile plus one-standard-deviation
SPLOT(J,..)	Stress array for probabilistic plotting
STRES(N,J)	Wave front stress array
S1(N,J)	Stress array for probabilistic calculations
S2(N,J)	Stress array for probabilistic calculations
S3(N,J)	Stress array for probabilistic calculations
S4(N,J)	Stress array for probabilistic calculations
TAVG(J)	Average time for probabilistic run
T(N,J)	Time of propagation
TSUM(N,J)	Arrival time increment
TP(J)	Time array used for profile plotting
TPLOT(J)	Time array used for profile plotting
T1(N,J)	Time array for probabilistic calculations
T2(N,J)	Time array for probabilistic calculations
T3(N,J)	Time array for probabilistic calculations
T4(N,J)	Time array for probabilistic calculations
UBAR	Average wave speed as calculated in subroutine Gauss
UF(N)	Fast wave speed
UGRN	Initial wave speed on the free surface of the medium at $X=0$. Also equal to granule wave speed.

U(N,J)	Average wave speed
UREAL(N,J)	Actual wave speed
V(N,J)	Particle velocity
VM(J)	Particle velocity profile minus one-standard-deviation
VP(J)	Particle velocity profile plus one-standard-deviation
VPART(J)	Particle velocity for profile plotting
VV(J,..)	Particle velocity array for probabilistic plotting
V1(N,J)	Particle velocity array for probabilistic calculations
V2(N,J)	Particle velocity array for probabilistic calculations
V3(N,J)	Particle velocity array for probabilistic calculations
V4(N,J)	Particle velocity array for probabilistic calculations
X(N)	Depth into the media
YAM(J)	Initial input amplitudes

MICID
WAVE PROPAGATION CODE
FLOW CHART







EXAMPLE RUN

As an example of the use of the program MIC1D, a typical run will now be presented. The first prompt from the program which will appear on the CRT screen will be a menu for the type of volume distribution to be used, i.e.

```
-----  
| CHOOSE THE TYPE OF VOLUME DISTRIBUTION |  
| FUNCTION TO BE USED IN THE ANALYSIS FOR |  
| THE GRANULAR MEDIUM IN CONSIDERATION |  
-----
```

ENTER THE PROPER SELECTION NUMBER PLEASE

```
-----  
| 1. PERIODIC VOLUME DISTRIBUTION FUNCTION |  
| 2. EXPONENTIAL VOLUME DISTRIBUTION FUNCTION |  
| 3. PERIODIC-EXPONENTIAL COMBINED FUNCTION |  
-----
```

The user should respond with the appropriate choice.

The name of the input data file is requested next through the prompt

```
ENTER NAME OF THE DATA FILE. (NAME.DAT)  
PEDAT.
```

The program requires the input data AFF, AFFF, BB, DELTR, ENUAA, ENUB, EX, FLFF, FLFFF, GG, GL, GO, L, NR, SIGNUA, SGL (see glossary for description of each of these quantities). The data is read in an unformatted fashion, and a typical data file would look like

```
-3.E5.5.E8.30.0,4.E-6,0.996,0.7,0.0,3.E5,-750.0,7.2E-2,0.1,  
2.4E-4,1000,1,0.0,0.03
```

Depending upon which volume distribution that is selected and whether the run is deterministic or not, some of the input data will not actually be used.

Next the number of initial wave amplitudes are requested by

INPUT NUMBER OF INITIAL WAVE AMPLITUDES TO BE USED

Finally the code requests the values of each of the initial input waves

ENTER INITIAL VALUES OF THE WAVE AMPLITUDES

The input is now complete and the code will print out all of this data so that the user can check to see if the input has been done correctly. A typical output of this step is shown below for the case of the previous data file and with three initial amplitudes

INPUT DATA

```
AFF = -300000.0
AFFF = 5.0000000E+08
BB = 30.00000
DELTR = 4.0000000E-06
ENUAA = 0.9960000
ENUB = 0.7000000
EX = 0.0000000E+00
FLFF = 300000.0
FLFFF = -750.0000
GG = 7.1999997E-02
GL = 0.1000000
GO = 2.3999999E-04
L = 1000

AMPLITUDE( 1) = 0.10000E+04
AMPLITUDE( 2) = 0.50000E+04
AMPLITUDE( 3) = 0.10000E+05
```

PRESS RETURN TO CONTINUE...

Once the "return key" has been depressed, the program will start its computation and the following will typically be seen on the screen

PROGRAM IS NOW RUNNING

COMPUTATION OF DELTA X BETWEEN WAVES ENDS

J= 2

N= 944

T(N,J)= 7.3260060E-05

MAXIMUM LIMIT = 7.3219308E-05

COMPUTATION OF DELTA X BETWEEN WAVES ENDS

J= 3

N= 888

T(N,J)= 7.3226467E-05

MAXIMUM LIMIT = 7.3219308E-05

The message concerning the computation of DELTA X is related to the theory in section 3.4 dealing with the stress calculations. This computation will stop before the completion of the entire N-loop, and this comment lets the user know when this occurs. The above example is for the case of three initial wave amplitudes with L=1000.

When the code is finished with its calculations, the user is prompted with the following menu for output results

CHOOSE THE TYPE OF GRAPHICS OPTION

1. DETERMINISTIC PROFILE PLOT
2. PROBABILISTIC PROFILE PLOT
3. DEPTH DEPENDENT PLOT

Selecting for example item #3, depth dependent plots, the final plotting menu will appear.

ENTER ITEM NUMBER FOR DEPTH DEPENDENT PLOT

1. ACTUAL WAVE SPEED
2. AVERAGE WAVE SPEED
3. AMPLITUDE BEHAVIOR WITH DEPTH
4. VOLUME DISTRIBUTION FUNCTION
5. MU-COEFFICIENT
6. KAPPA-COEFFICIENT
7. NO GRAPHICS i.e. DATA OUTPUT IN A FILE

Specifics on the final stages of plotting will not be given since these will be system and software dependent and thus will vary from system to system. An example output corresponding to the example input data shown previously, is given in Figure A.1.

VOLUME DISTRIBUTION FUNCTION

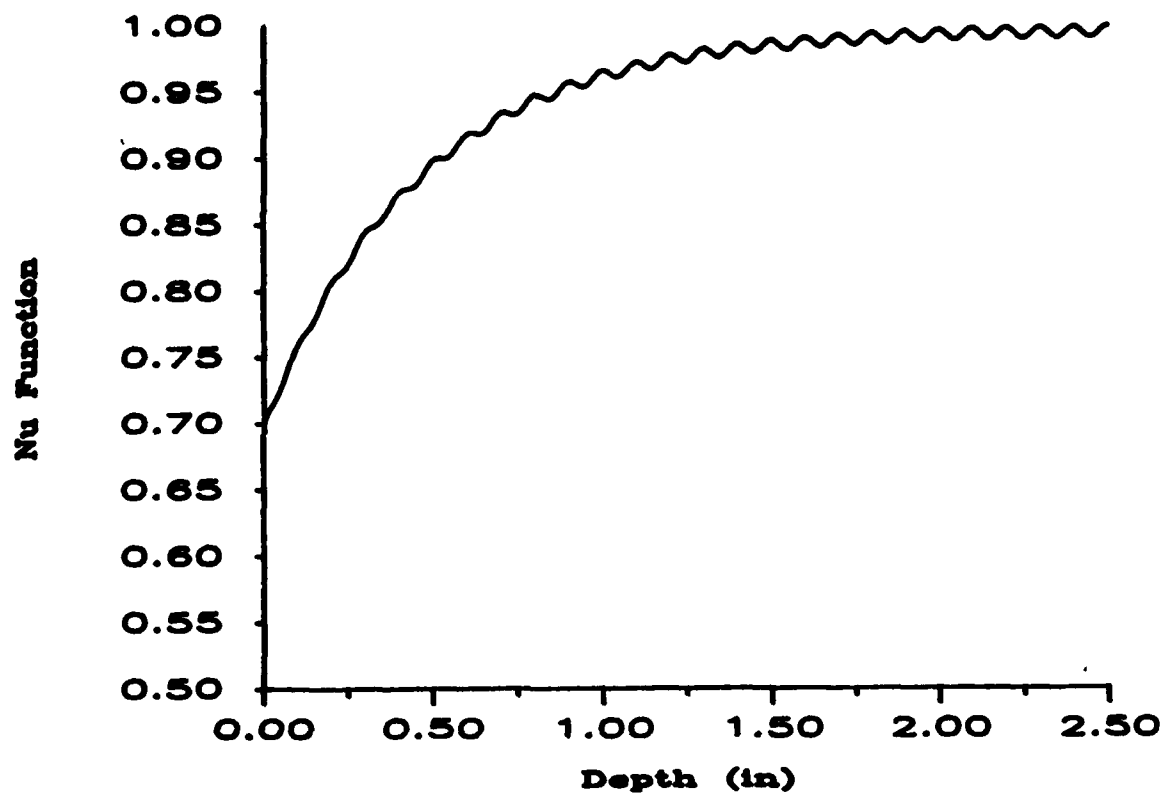


Figure A-1. Plotted output for example run (continued).

AVERAGE WAVE SPEED

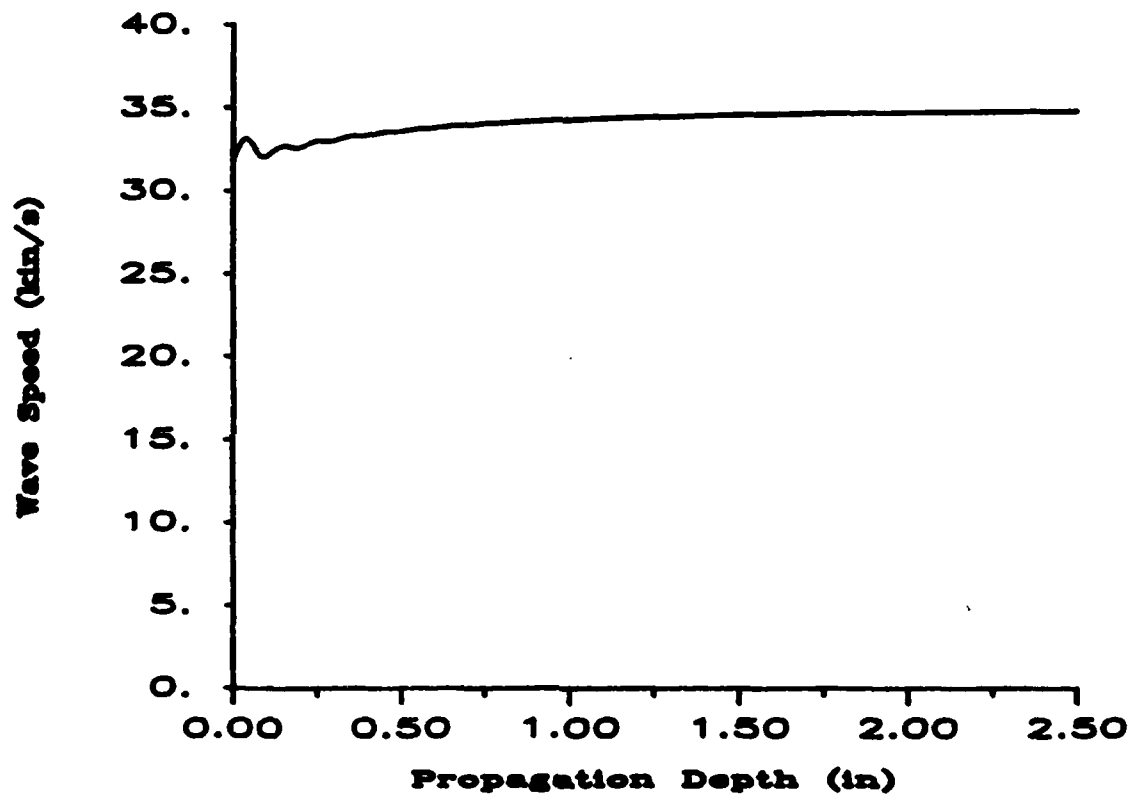


Figure A-1. Plotted output for example run (continued).

AMPLITUDE BEHAVIOR WITH DEPTH

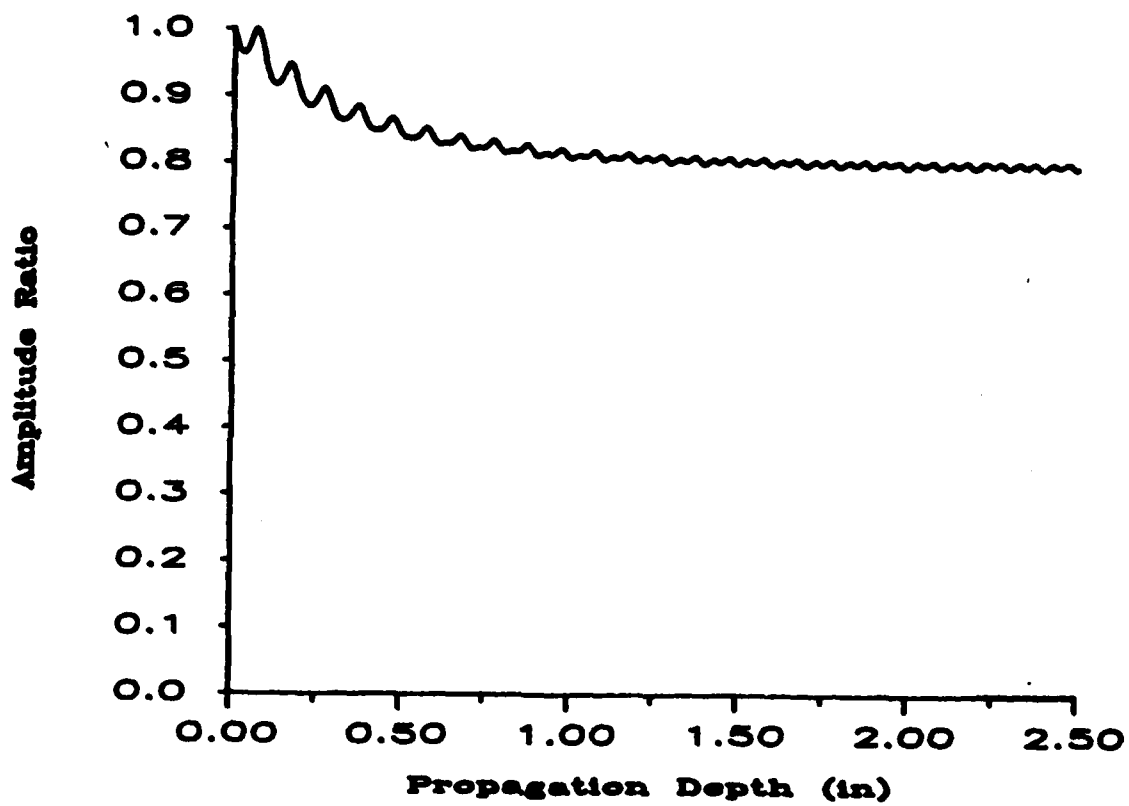


Figure A-1. Plotted output for example run (concluded).

```

C*****
C
C          PROGRAM M I C I D
C
C          ONE DIMENSIONAL WAVE PROPAGATION CODE FOR MICROSTRUCTURAL
C          MATERIALS MODELLED BY GOODMAN-COWIN DISTRIBUTED BODY
C          THEORY. CODE EMPLOYS SINGULAR SURFACE WAVE THEORY
C          ORIGINALLY DEVELOPED BY NUNZIATO et al.
C
C          WRITTEN BY
C
C          PROFESSOR MARTIN H. SADD
C
C          AND
C
C          MOHAMMAD N. HOSSAIN
C
C          DEPARTMENT OF MECHANICAL
C          ***** ENGINEERING & APPLIED MECHANICS *****
C          ***** UNIVERSITY OF RHODE ISLAND *****
C          ***** KINGSTON, RI 02881 *****
C          ***** SEPTEMBER, 1986 *****
C
C          WRITTEN FOR
C
C          DR. BEHZAD ROHANI
C
C          U. S. ARMY ENGINEER
C
C          WATERWAYS EXPERIMENT STATION
C          VICKSBURG, MS 39180
C*****
C
C          DIMENSION SIZES ARE RELATED TO DEPTH COUNTER "N" (1<N<L) AND
C          NUMBER OF WAVES COUNTER "J" (1<J<N*W); MAXIMUM L=3000 AND
C          MAXIMUM J=15
C
C          DIMENSION A(3000,15), A1(3000,15), A2(3000,15), A3(3000,15), A4
C          * (3000,15), AB(30), AM(30), AP(30), APL0T(30,3), AR(3000,15), C1(3000,
C          * 15), C2(3000,15), C3(3000,15), D1(3000,15), D2(3000,15), D3(3000,15),
C          * D4(3000,15), DELX(3000,15), DD(15,3), DISP(3000,15), DPL0T(15),
C          * DP(15), DM(15), EA(30), ED(15), ES(15), EV(15), NMAX(15),
C          * PSTRES(15), STRES(3000,15), S1(3000,15), S2(3000,15), S3(3000,15),
C          * S4(3000,15), SM(15), SP(15), SPL0T(15,3), T(3000,15),
C          * TAVG(15), T1(3000,15), T2(3000,15), T3(3000,15), T4(3000,15), TSUM
C          * (3000,15), TP(15), TPL0T(30), V1(3000,15), V2(3000,15), V3(3000,15),
C          * V4(3000,15), V(3000,15), VP(20), VPART(15), VM(15), VV(15,3), UREAL
C          * (3000,15), U(3000,15), X(3000), YAM(15)
C          CHARACTER ANS*8, DATNAME*8, DATA*8, TITLE*50, XLABEL*50, YLABEL*50,
C          * LINLABEL(10)*25, LINE*25, PANS*5
C          INTEGER JJ, KK, IANS
C          REAL ALD, AHI, AMP, H, U, UL, UH, X, Y, YAM, YO
C          COMMON /GRAIN/ AFFO, AFFF, BB, DUM, ENUB, FLFFO, FLFFF, GG, GL, GO, TIME
C          COMMON /CONTRL/ P, P1, Q, Q1
C          P = 1.0
C          P1 = 0.0

```

```

      G = 1.0
      G1 = 0.0
      WRITE(6,2)
2    FORMAT('1'////)
      PRINT*, '-----'
      PRINT*, '1  CHOOSE THE TYPE OF VOLUME DISTRIBUTION 1'
      PRINT*, '1  FUNCTION TO BE USED IN THE ANALYSIS FOR 1'
      PRINT*, '1  THE GRANULAR MEDIUM IN CONSIDERATION 1'
      PRINT*, '-----'
      PRINT*, ' '
1    PRINT*, '1  ENTER THE PROPER SELECTION NUMBER PLEASE'
      PRINT*, ' '
      PRINT*, '-----'
      PRINT*, '1  1. PERIODIC VOLUME DISTRIBUTION FUNCTION 1'
      PRINT*, '1  '
      PRINT*, '1  2. EXPONENTIAL VOLUME DISTRIBUTION FUNCTION 1'
      PRINT*, '1  '
      PRINT*, '1  3. PERIODIC-EXPONENTIAL COMBINED FUNCTION 1'
      PRINT*, '-----'
      PRINT*, ' '
      READ(5,5) KK
5    FORMAT(I2)
      IF((KK.NE.1).AND.(KK.NE.2).AND.(KK.NE.3)) GO TO 1
      IF(KK.EQ.1) THEN
        G = 0.0
        G1 = 1.0
      END IF
      IF(KK.EQ.2) THEN
        P = 0.0
        P1 = 1.0
      END IF
      READ INPUT DATA FROM THE EXISTING DATA FILE
      WRITE(6,*) 'ENTER NAME OF THE DATA FILE. (NAME.DAT)'
      READ(5,10) DATNAME
10   FORMAT(1A8)
      OPEN(UNIT=2, FILE=DATNAME, STATUS='OLD')
      READ(2,*) AFF, AFFF, BB, DELTR, ENUAA, ENUB, EX, FLFF, FLFFF, GG, GL, GO, L,
      * NR, SENUA, SQL
15  CLOSE(UNIT=2)

      AMPLITUDE INPUT SECTION.  ENTER THE (NW) INITIAL WAVE AMPLITUDES.
      FINAL WAVE (J=NW) IS USED ONLY AS AN END MARKER AND WILL NOT
      BE PLOTTED IN PROFILE RESULTS.

      PRINT*, ' '
      PRINT*, 'INPUT NUMBER OF INITIAL WAVE AMPLITUDES TO BE USED'
      READ(5,*) NW
      PRINT*, ' '
      PRINT*, 'ENTER INITIAL VALUES OF THE WAVE AMPLITUDES'
      READ(5,*) (YAM(J), J=1, NW)
      PRINT*, ' '
      PRINT*, '1  INPUT DATA'
      PRINT*, ' '
      WRITE(6,*) 'AFF = ', AFF
      WRITE(6,*) 'AFFF = ', AFFF
      WRITE(6,*) 'BB = ', BB
      WRITE(6,*) 'DELTR = ', DELTR
      WRITE(6,*) 'ENUAA = ', ENUAA

```

```

WRITE(6,*) 'ENUB = ', ENUB
WRITE(6,*) 'EX = ', EX
WRITE(6,*) 'FLFF = ', FLFF
WRITE(6,*) 'FLFFF = ', FLFFF
WRITE(6,*) 'GO = ', GO
WRITE(6,*) 'OL = ', OL
WRITE(6,*) 'OO = ', OO
WRITE(6,*) 'L = ', L
PRINT*, ' '
DO I=1,NW
WRITE(6,800) I, YAM(I)
END DO
PRINT*, ' '
PRINT*, 'PRESS RETURN TO CONTINUE... '
READ(5,*)
PRINT*, ' '
PRINT*, 'PROGRAM IS NOW RUNNING'
AFFO=AFF/GO
FLFFO=FLFF/GO
UGRN = SQRT(FLFFO)
TAVG(1)=0.0
H=OL/40.0

C
C
C
PROBABILISTIC LOOP STARTS

IF (NR.EQ.1) GO TO 17
PRINT*, ' '
PRINT*, 'PROBABILISTIC RUN WITH DATA'
PRINT*, ' '
WRITE(6,*) 'ENUAA = ', ENUAA
WRITE(6,*) 'EX = ', EX
WRITE(6,*) 'NR = ', NR
WRITE(6,*) 'SIGNUA = ', SENUA
WRITE(6,*) 'SQL = ', SQL
PRINT*, ' '
PRINT*, 'PRESS RETURN TO CONTINUE... '
READ(5,*)
ENUAP=ENUAA+SENUA
ENUAM=ENUAA-SENUA
OLP = OL + SQL
OLM = OL - SQL
DO 71 M=1,NR
IF (NR.EQ.1) GO TO 18
IF (M.EQ.1) THEN
    ENUAA=ENUAP
    OL = OLP
END IF
IF (M.EQ.2) THEN
    ENUAA=ENUAP
    OL = OLM
END IF
IF (M.EQ.3) THEN
    ENUAA = ENUAM
    OL = OLP
END IF
IF (M.EQ.4) THEN
    ENUAA = ENUAM
    OL = OLM
END IF
18 ENUA = ENUAA

```



```

NMAX(1)=L
DO 70 J = 1,NW
DUM=0.0
YO=YAM(J)
DO 65 N = 1,L
X(N)=N*QL/40.
Y=X(N)

C
C
C
C
PERFORM NUMERICAL INTEGRATION FOR THE TRANSIT TIME
AND CALCULATE THE AVERAGE WAVE SPEED

XL=INT((N-1)/20.)*QL/2.0
NN=INT((L-20.)/20.)
DO 20 I=1,NN
LL=20.*I+1
IF (N.EQ.LL) GOTO 30
20 CONTINUE
GOTO 40
30 DUM=TIME
40 IF (N.EQ.1) TSUM(1,J) = H/UORN
IF (N.GT.1) TSUM(N,J) = TSUM(N-1,J)+H/(U(N-1,J)*1000.)
T(N,J) = (J-1)*DELTR+TSUM(N,J)
IF (J.EQ.1) GO TO 50
IF (T(N,J).GT.T(L-1,1)) THEN
PRINT*, ' '
PRINT*, 'CAN NO LONGER COMPUTE DELTA X BETWEEN WAVES'
PRINT*, 'J=',J
PRINT*, 'N=',N
PRINT*, 'T(N,J)=',T(N,J)
PRINT*, 'MAXIMUM LIMIT = ',T(L-1,1)
GO TO 70
END IF
DO NC=N,N+200
NT=NC
IF (T(N,J).LE.T(NC,J-1)) GO TO 45
END DO
PRINT*, 'M=',M
PRINT*, 'N=',N
PRINT*, 'J=',J
PRINT*, 'ERROR IN THE AMPLITUDE TIME-TEST'
GO TO 630
45 DELX(N,J-1)=(NT-1)*H+(T(N,J)-T(NT-1,J-1))*(H/(T(NT,J-1)
*-T(NT-1,J-1)))-N*H
NMAX(J) = NT
MAXN=NMAX(J)
ASUM=0.0
DO JK=1,J-1
ASUM=ASUM+A(N,JK)
END DO
SIGMA=C3(N,1)*GO*ASUM*DELX(N,J-1)
STRES(N,J)=SIGMA+STRES(N,J-1)
ENUA = 1. - (1.-ENUAA)*EXP(-EX*STRES(N,J))
50 CALL GAUSS (ENUA,J,KK,N,XL,Y,UBAR)
U(N,J)=UBAR/1000.

C
C
C
SOLUTION OF THE WAVE AMPLITUDE BY FOURTH ORDER RUNGE-KUTTA METHOD

CALL RUNKUT(AMP,ENUA,H,J,N,PKAPA,PMU,VDFUN,RWSPD,Y,YO)
A(N,J) = AMP
AR(N,J) = A(N,J)/YAM(J)

```

```

C1(N,J) = PMU
C2(N,J) = PKAPA
C3(N,J) = VDFUN
UREAL(N,J) = RWSPD
ASUM=ASUM+A(N,J)
IF (J.EQ.1) THEN
  STRES(N,J)=0.0
  V(N,J)=0.0
  DISP(N,J)=0.0
  GO TO 55
END IF
V(N,J)=V(N,J-1)+A(N,J-1)*(T(N,J)-T(N,J-1))
DISP(N,J)=.5*(V(N,J)+V(N,J-1))*(T(N,J)-T(N,J-1))+DISP(N,J-1)
55 IF (NR.EQ.1) GO TO 65
  IF (M.EQ.1) THEN
    A1(N,J) = A(N,J)
    T1(N,J) = T(N,J)
    S1(N,J)=STRES(N,J)
    V1(N,J)=V(N,J)
    D1(N,J)=DISP(N,J)
  END IF
  IF (M.EQ.2) THEN
    A2(N,J) = A(N,J)
    T2(N,J) = T(N,J)
    S2(N,J)=STRES(N,J)
    V2(N,J)=V(N,J)
    D2(N,J)=DISP(N,J)
  END IF
  IF (M.EQ.3) THEN
    A3(N,J) = A(N,J)
    T3(N,J) = T(N,J)
    S3(N,J)=STRES(N,J)
    V3(N,J)=V(N,J)
    D3(N,J)=DISP(N,J)
  END IF
  IF (M.EQ.4) THEN
    A4(N,J) = A(N,J)
    T4(N,J) = T(N,J)
    S4(N,J)=STRES(N,J)
    V4(N,J)=V(N,J)
    D4(N,J)=DISP(N,J)
  END IF
65 CONTINUE
70 CONTINUE
71 CONTINUE
72 PRINT*, ' '

```

C
C
C

START OF FRIENDLY INTERACTIVE OPTIONS

```

PRINT*, 'CHOOSE THE TYPE OF GRAPHICS OPTION'
PRINT*, ' '
PRINT*, '1. DETERMINISTIC PROFILE PLOT'
PRINT*, ' '
PRINT*, '2. PROBABILISTIC PROFILE PLOT'
PRINT*, ' '
PRINT*, '3. DEPTH DEPENDENT PLOT'
PRINT*, ' '
READ(5,*) IANS
IF ( IANS.EQ.1 ) GO TO 75
IF ( IANS.EQ.2 ) GO TO 135

```

```

      IF ( IANS.EQ.3 ) GO TO 80
      IF (( IANS.NE.1 ).AND.( IANS.NE.2 ).AND.( IANS.NE.3 )) GO TO 72
75  PRINT 760
      PRINT 600, MAXN
      READ(5,650) NV
      XCURNT=NV*GL/40
      PRINT 680, XCURNT

C
C      TIME PROFILE PLOTTING OPTIONS
C
      PRINT*, ' '
      PRINT*, 'ENTER OPTION NUMBER FOR DETERMINISTIC PROFILE PLOT'
      PRINT*, ' '
      PRINT*, '1. PARTICLE-DISPLACEMENT PROFILE'
      PRINT*, ' '
      PRINT*, '2. PARTICLE-VELOCITY PROFILE'
      PRINT*, ' '
      PRINT*, '3. PARTICLE-ACCELERATION PROFILE'
      PRINT*, ' '
      PRINT*, '4. STRESS PROFILE'
      PRINT*, ' '
      READ(5,580) JF
      GO TO (112,115,120,125) JF

C
C      DEPTH-DEPENDENT PLOTTING OPTIONS
C
80  PRINT*, 'ENTER ITEM NUMBER FOR DEPTH DEPENDENT PLOT'
      PRINT*, ' '
      PRINT*, '1. ACTUAL WAVE SPEED'
      PRINT*, ' '
      PRINT*, '2. AVERAGE WAVE SPEED'
      PRINT*, ' '
      PRINT*, '3. AMPLITUDE BEHAVIOR WITH DEPTH'
      PRINT*, ' '
      PRINT*, '4. VOLUME DISTRIBUTION FUNCTION'
      PRINT*, ' '
      PRINT*, '5. MU-COEFFICIENT'
      PRINT*, ' '
      PRINT*, '6. KAPPA-COEFFICIENT'
      PRINT*, ' '
      PRINT*, '7. NO GRAPHICS i. e. DATA OUTPUT IN A FILE'
      READ(5,580) JJ
      GO TO (100,105,110,130,140,150,200) JJ

C
C      CALL GRAPHICS SUBROUTINES TO DRAW THE COMPUTED OUTPUT
C
C      PLOT THE ACTUAL WAVE SPEED
C
100 UMIN=200.
      UMAX=0.0
      DO J=1,NW
        DO I=1,L
          IF (UREAL(I,J).LE.UMIN) UMIN=UREAL(I,J)
          IF (UREAL(I,J).GE.UMAX) UMAX=UREAL(I,J)
        END DO
      END DO
      WRITE(6,900) UMIN,UMAX
      PRINT*, 'ENTER LOWER & UPPER ORDINATES OF WAVE SPEED'
      READ(5,*) VL,VH
      TITLE='*ACTUAL WAVE SPEED*'

```

```

      XLABEL='$Propagation Depth(in)$'
      YLABEL='$Wave Speed (kin/s)$'
      CALL WAVGRAF(X, 0. 0, X(L), UREAL, VL, VH, L, 1, 3000, 15, LINLABEL,
#XLABEL, YLABEL, TITLE, . TRUE. , . TRUE. )
      GO TO 500

```

C

C

C

```

      PLOT THE AVERAGE WAVE SPEED

105  UMAX=0. 0
      DO J=1, NW
        LINLABEL(J)= ' '
        DO I=1, L
          IF (U(I, J). GE. UMAX) UMAX=U(I, J)
        END DO
      END DO
      WRITE(6, 1000) UMAX
      VL=0. 0
      PRINT*, 'ENTER UPPER ORDINATE OF AVERAGE WAVE SPEED'
      READ(5, *) VH
      J=1
      DO WHILE ( J .NE. 0 )
        PRINT*, 'ENTER THE LINE # TO BE LABELED'
        PRINT*, '(TYPE 0 IF NO LABELS NEEDED )'
        READ(5, *) J
        IF ( J .NE. 0 ) THEN
          PRINT 640, J
          READ(5, 570) LINE
          LINLABEL(J)=LINE
        END IF
      END DO
      TITLE='$AVERAGE WAVE SPEED$'
      XLABEL='$Propagation Depth (in)$'
      YLABEL='$Wave Speed (kin/s)$'
      CALL WAVGRAF(X, 0. 0, X(L), U, VL, VH, L, 1, 3000, 15, LINLABEL,
#XLABEL, YLABEL, TITLE, . TRUE. , . TRUE. )
      GO TO 500

```

C

C

C

```

      PLOT THE AMPLITUDE BEHAVIOR WITH DEPTH

110  TITLE='$AMPLITUDE BEHAVIOR WITH DEPTHS$'
      XLABEL='$Propagation Depth (in)$'
      YLABEL='$Amplitude Ratios$'
      DO J=1, NW
        LINLABEL(J)= ' '
      END DO
      J=1
      DO WHILE ( J .NE. 0 )
        PRINT*, 'ENTER THE LINE # TO BE LABELED'
        PRINT*, '(TYPE 0 IF NO LABELS NEEDED )'
        READ(5, *) J
        IF ( J .NE. 0 ) THEN
          PRINT 640, J
          READ(5, 570) LINE
          LINLABEL(J)=LINE
        END IF
      END DO
      CALL WAVGRAF(X, 0. 0, X(L), AR, 0. , 1. , L, NW, 3000, 15, LINLABEL,
#XLABEL, YLABEL, TITLE, . TRUE. , . TRUE. )
      GO TO 500

```

C

```

C      PLOT PARTICLE DISPLACEMENT TIME PROFILE
C
112  IF (NW.EQ.1) GO TO 117
      DO I = 1,NW
          LINLABEL(I)=' '
      END DO
      J=1
      DO WHILE ( J.NE. 0 )
          PRINT*, 'ENTER THE LINE # TO BE LABELED'
          PRINT*, '(TYPE 0 IF NO LABELS NEEDED )'
          READ(5,*) J
          IF ( J.NE. 0 ) THEN
              PRINT 640, J
              READ(5,570) LINE
              LINLABEL(J)=LINE
          END IF
      END DO
      TITLE='*PARTICLE DISPLACEMENT PROFILE*'
      XLABEL='*Time (secX1.E6)*'
      YLABEL='*Displacement (inX1.E6)*'
      DPLOT(1)=0.0
      TP(1)=T(NV,1)*1.E6
      DO I=2,NW
          TP(I) = T(NV,I)*1.E6
          DPLOT(I)=DISP(NV,I)*1.E6
      END DO
      DISPMAX=0.0
      DO I=1,NW
          IF (DPLOT(I).GE.DISPMAX) DISPMAX=DPLOT(I)
      END DO
      WRITE(6,1050) DISPMAX
      PRINT*, 'ENTER MAX. ORDINATE OF DISPLACEMENT'
      READ(5,*) DHI
      DLO = 0.0
      TMIN=0.0
      TMAX=T(NV,NW)*1.E06
      CALL WAVGRAF(TP, TMIN, TMAX, DPLOT, DLO, DHI, NW, 1, 15, 1, LINLABEL,
      *XLABEL, YLABEL, TITLE, .TRUE., .TRUE.)
      GO TO 500

```

```

C
C      PLOT PARTICLE-VELOCITY TIME PROFILE
C
115  IF (NW.EQ.1) GO TO 117
      DO I=1,NW
          LINLABEL(I)=' '
      END DO
      J=1
      DO WHILE ( J.NE. 0 )
          PRINT*, 'ENTER THE LINE # TO BE LABELED'
          PRINT*, '(TYPE 0 IF NO LABELS NEEDED )'
          READ(5,*) J
          IF ( J.NE. 0 ) THEN
              PRINT 640, J
              READ(5,570) LINE
              LINLABEL(J)=LINE
          END IF
      END DO
      TITLE='*PARTICLE VELOCITY PROFILE*'
      XLABEL='*Time (secX1.E6)*'
      YLABEL='*Velocity (in/s)*'

```

```

VPART(1)=0.0
TP(1)=T(NV,1)*1E6
DO I=2,NW
    TP(I) = T(NV,I)*1.E6
    VPART(I)=V(NV,I)
END DO
VMAX=0.0
DO I=1,NW
    IF (VPART(I).GE.VMAX) VMAX=VPART(I)
END DO
WRITE(6,850) VMAX
PRINT*, 'ENTER THE MAXIMUM ORDINATE OF VELOCITY'
READ(5,*) VHI
VLO=0.0
TMIN=0.0
TMAX=T(NV,NW)*1.E6
CALL WAVGRAF(TP,TMIN,TMAX,VPART,VLO,VHI,NW,1,15,1,LINLABEL,
*XLABEL,YLABEL,TITLE,.TRUE.,.TRUE.)
PRINT*, 'INTERESTED IN ANOTHER PROFILE PLOT, ENTER Y OR N'
READ(5,510) ANS
IF (ANS.EQ. 'Y') GO TO 75
GO TO 500

C
C
C
120 IF (NW.EQ.1) GO TO 117
DO J=1,NW-1
    AB(2*J-1)=A(NV,J)/1000.
    AB(2*J)=A(NV,J)/1000.
    LINLABEL(J)=' '
END DO
J=1
DO WHILE ( J.NE. 0 )
    PRINT*, 'ENTER THE LINE # TO BE LABELED'
    PRINT*, '(TYPE 0 IF NO LABELS NEEDED )'
    READ(5,*) J
    IF ( J.NE. 0 ) THEN
        PRINT 640, J
        READ(5,570) LINE
        LINLABEL(J)=LINE
    END IF
END DO
TPLOT(1)=T(NV,1)*1E6
DO J=1,NW-2
    TPLOT(2*J)=T(NV,J+1)*1.E6
    TPLOT(2*J+1)=T(NV,J+1)*1.E6
END DO
TPLOT(2*NW-1)=(T(NV,NW-1)+DELTR)*1.E6
MNW=NW*2
AMAX=0.0
DO I=1,MNW
    IF (AB(NV,I).GE.AMAX) AMAX=AB(NV,I)/1000.
END DO
WRITE(6,1100) AMAX
PRINT*, 'ENTER THE MAXIMUM ORDINATE OF AMPLITUDE'
READ(5,*) AHI
TITLE='*PARTICLE ACCELERATION PROFILE*'
XLABEL='*Time (secX1.E6)*'
YLABEL='*Acceleration (kin/s/s)*'
TMIN=0.0

```

```

      TMAX=T(NV,NW)*1.E6
      CALL WAVGRAF(TPLOT,TMIN,TMAX,AB,ALO,AHI,MNW,1,40,1,LINLABEL,
#XLABEL,YLABEL,TITLE,.TRUE.,.TRUE.)
      PRINT*, 'INTERESTED IN ANOTHER PROFILE PLOT, ENTER Y OR N'
      READ(5,510) ANS
      IF (ANS.EQ. 'Y') GO TO 75
      GO TO 500
117  WRITE(6,550)
      GO TO 500
C
C      PLOT THE STRESS TIME PROFILE
C
125  IF (NW.EQ.1) GO TO 117
      DO J=1,NW
          LINLABEL(J)= ' '
          PSTRES(J)=STRES(NV,J)
          TP(J)=T(NV,J)*1.E6
      END DO
      STRMAX=0.0
      DO I=1,NW
          IF (STRES(NV,I).GE.STRMAX) STRMAX=STRES(NV,I)
      END DO
      WRITE(6,950) STRMAX
      STRLO=0.0
      PRINT*, 'ENTER THE MAXIMUM ORDINATE OF STRESS'
      READ(5,*) STRHI
      TITLE='*STRESS PROFILE*'
      XLABEL='*Time (secX1.E6)*'
      YLABEL='*Stress (psi)*'
      J=1
      DO WHILE ( J.NE. 0 )
          PRINT*, 'ENTER THE LINE # TO BE LABELED'
          PRINT*, '(TYPE 0 IF NO LABELS NEEDED )'
          READ(5,*) J
          IF ( J.NE. 0 ) THEN
              PRINT 640, J
              READ(5,570) LINE
              LINLABEL(J)=LINE
          END IF
      END DO
      TMIN=0.0
      TMAX=T(NV,NW)*1.E6
      CALL WAVGRAF(TP,TMIN,TMAX,PSTRES,STRLO,STRHI,NW,1,15,1,
#LINLABEL,XLABEL,YLABEL,TITLE,.TRUE.,.TRUE.)
      PRINT*, 'INTERESTED IN ANOTHER PROFILE PLOT, ENTER Y OR N'
      READ(5,510) ANS
      IF (ANS.EQ. 'Y') GO TO 75
      GO TO 500
C
C      PROBABILISTIC CALCULATIONS
C
135  IF (NR.EQ.1) THEN
          PRINT*, 'CANNOT REQUEST PROBABILISTIC CALCULATIONS WITH NR=1'
          GO TO 500
      END IF
190  PRINT*, ' '
      PRINT*, 'ENTER DEPTH PARAMTER < N > FOR THE PROBABILISTIC PLOTS'
      PRINT*, ' '
      READ(5,*) NV
      XCURNT=NV*QL/40.

```

PRINT 680, XCURNT

DO J = 1, NW

TAVG(J) = ((T1(NV, J) + T2(NV, J) + T3(NV, J) + T4(NV, J)) / 4.) * 1. E6

C
C
C

AMPLITUDE CALCULATIONS

EA(J) = (A1(NV, J) + A2(NV, J) + A3(NV, J) + A4(NV, J)) / 4.

EA2 = (A1(NV, J)**2 + A2(NV, J)**2 + A3(NV, J)**2 + A4(NV, J)**2) / 4.

SA = SQRT(EA2 - EA(J)**2)

AP(J) = EA(J) + SA

AM(J) = EA(J) - SA

C
C
C

STRESS CALCULATIONS

ES(J) = (S1(NV, J) + S2(NV, J) + S3(NV, J) + S4(NV, J)) / 4.

SPLOT(J, 1) = ES(J)

ES2 = (S1(NV, J)**2 + S2(NV, J)**2 + S3(NV, J)**2 + S4(NV, J)**2) / 4.

SS = SQRT(ES2 - ES(J)**2)

SP(J) = ES(J) + SS

SPLOT(J, 2) = SP(J)

SM(J) = ES(J) - SS

SPLOT(J, 3) = SM(J)

C
C
C

VELOCITY CALCULATIONS

EV(J) = (V1(NV, J) + V2(NV, J) + V3(NV, J) + V4(NV, J)) / 4.

EV2 = (V1(NV, J)**2 + V2(NV, J)**2 + V3(NV, J)**2 + V4(NV, J)**2) / 4. 0

VV(J, 1) = EV(J)

SV = SQRT(EV2 - EV(J)**2)

VP(J) = EV(J) + SV

VV(J, 2) = VP(J)

VM(J) = EV(J) - SV

VV(J, 3) = VM(J)

C
C
C

DISPLACEMENT CALCULATIONS

ED(J) = (D1(NV, J) + D2(NV, J) + D3(NV, J) + D4(NV, J)) / 4. 0

DD(J, 1) = ED(J) * 1. E6

ED2 = (D1(NV, J)**2 + D2(NV, J)**2 + D3(NV, J)**2 + D4(NV, J)**2) / 4. 0

SD = SQRT(ED2 - ED(J)**2)

DP(J) = ED(J) + SD

DD(J, 2) = DP(J) * 1. E6

DM(J) = ED(J) - SD

DD(J, 3) = DM(J) * 1. E6

END DO

C
C
C

MODIFY AND RE-ASSIGN THE AMPLITUDE AND TIME ARRAYS

DO I = 1, NW-1

APLOT(2*I-1, 1) = EA(I) / 1000.

APLOT(2*I, 1) = EA(I) / 1000.

APLOT(2*I-1, 2) = AP(I) / 1000.

APLOT(2*I, 2) = AP(I) / 1000.

APLOT(2*I-1, 3) = AM(I) / 1000.

APLOT(2*I, 3) = AM(I) / 1000.

LINLABEL(I) = ' '

END DO

TPLLOT(1) = TAVG(1)

DO I = 1, NW-2

TPLLOT(2*I) = TAVG(I+1)


```

        TPLLOT(2*I+1)=TAVG(I+1)
    END DO
    TMIN=0.0
    TMAX=T(NV,NW-1)*1.E06
    TPLLOT(2*NW-1)=TAVG(NW-1)+DELTR*1.E6
    ALO=0.0
    DLO=0.0
    VLO=0.0
    SLO=0.0
    PRINT*, ' '
    PRINT*, 'AVAILABLE PROBABILISTIC OPTIONS ARE'
    PRINT*, ' '
    PRINT*, '1. AMPLITUDE PROFILE PLOT'
    PRINT*, ' '
    PRINT*, '2. VELOCITY PROFILE PLOT'
    PRINT*, ' '
    PRINT*, '3. STRESS PROFILE PLOT'
    PRINT*, ' '
    PRINT*, '4. DISPLACEMENT PROFILE PLOT'
    PRINT*, ' '
    PRINT*, 'ENTER THE OPTION NUMBER'
    READ(5,580) JF
    GO TO (210,220,230,235) JF
210  TITLE='*PROBABILISTIC AMPLITUDE PROFILE*'
    XLABEL='*Time (secX1.E6)*'
    YLABEL='*AMPLITUDE (kin/s/s)*'
    APL=0.0
    NNW=(NW-1)*2
    DO J=1,3
        DO I=1,NNW
            IF (APLOT(I,J).GE.APL) APL=APLOT(I,J)
        END DO
    END DO
    PRINT 1110, APL
    PRINT*, 'ENTER MAXIMUM ORDINATE OF PROBABILISTIC AMPLITUDE'
    READ(5,*) AHI
    J=1
    DO WHILE ( J.NE. 0 )
        PRINT*, 'ENTER THE LINE # TO BE LABELED'
        PRINT*, '(TYPE 0 IF NO LABELS NEEDED )'
        READ(5,*) J
        IF ( J.NE. 0 ) THEN
            PRINT 640, J
            READ(5,570) LINE
            LINLABEL(J)=LINE
        END IF
    END DO
    CALL WAVGRAF(TPLLOT, TMIN, TMAX, APL, ALO, AHI, NNW, 3, 30, 3,
    #LINLABEL, XLABEL, YLABEL, TITLE, .TRUE., .TRUE.)
    GO TO 520
C
220  TITLE='*PROBABILISTIC VELOCITY PROFILE*'
    XLABEL='*Time (secX1.E6)*'
    YLABEL='*Velocity (in/sec)*'
    VPL=0.0
    DO J=1,3
        DO I=1,NW
            IF (VV(I,J).GE.VPL) VPL=VV(I,J)
        END DO
    END DO

```

```

PRINT 1120, VPL
PRINT*, 'ENTER MAXIMUM ORDINATE OF PROBABILISTIC VELOCITY'
READ(5,*) VHI
J=1
DO WHILE ( J .NE. 0 )
  PRINT*, 'ENTER THE LINE # TO BE LABELED'
  PRINT*, '(TYPE 0 IF NO LABELS NEEDED )'
  READ(5,*) J
  IF ( J .NE. 0 ) THEN
    PRINT 640, J
    READ(5,570) LINE
    LINLABEL(J)=LINE
  END IF
END DO
CALL WAVGRAF(TAVG, TMIN, TMAX, VV, VLO, VHI, NW, 3, 15, 3, LINLABEL
#, XLABEL, YLABEL, TITLE, . TRUE. , . TRUE. )
GO TO 520

```

C

```

230  TITLE='*PROBABILISTIC STRESS PROFILE*'
      XLABEL='*Time (secX1.E6)*'
      YLABEL='*Stress (ksi)*'
      SPL=0.0
      DO J=1,3
        DO I=1,NW
          IF (SPLOT(I,J).GE.SPL) SPL=SPLOT(I,J)
        END DO
      END DO
      PRINT 1130, SPL
      PRINT*, 'ENTER THE MAXIMUM ORDINATE OF STRESS'
      READ(5,*) SHI
      J=1
      DO WHILE ( J .NE. 0 )
        PRINT*, 'ENTER THE LINE # TO BE LABELED'
        PRINT*, '(TYPE 0 IF NO LABELS NEEDED )'
        READ(5,*) J
        IF ( J .NE. 0 ) THEN
          PRINT 640, J
          READ(5,570) LINE
          LINLABEL(J)=LINE
        END IF
      END DO
      CALL WAVGRAF(TAVG, TMIN, TMAX, SPLOT, SLO, SHI, NW, 3, 15, 3, LINLABEL
#, XLABEL, YLABEL, TITLE, . TRUE. , . TRUE. )
      GO TO 520
235  TITLE='*PROBABILISTIC DISPLACEMENT PROFILE*'
      XLABEL='*Time (secX1.E6)*'
      YLABEL='*Displacement (inX1.E6)*'
      DPL=0.0
      DO J=1,3
        DO I=1,NW
          IF (DD(I,J).GE.DPL) DPL=DD(I,J)
        END DO
      END DO
      PRINT 1140, DPL
      PRINT*, 'ENTER THE MAXIMUM ORDINATE OF DISPLACEMENT'
      READ(5,*) DHI
      J=1
      DO WHILE ( J .NE. 0 )
        PRINT*, 'ENTER THE LINE # TO BE LABELED'
        PRINT*, '(TYPE 0 IF NO LABELS NEEDED )'

```

```

      READ(5,*) J
      IF ( J .NE. 0 ) THEN
        PRINT 640, J
        READ(5,570) LINE
        LINLABEL(J)=LINE
      END IF
    END DO
    CALL WAVGRAF(TAVG, TMIN, TMAX, DD, DLO, DHI, NW, 3, 15, 3, LINLABEL
*, XLABEL, YLABEL, TITLE, .TRUE., .TRUE.)
    GO TO 520
C
C   PLOT THE VOLUME DISTRIBUTION FUNCTION
C
130  TITLE='$VOLUME DISTRIBUTION FUNCTION$'
      XLABEL='$Depth (in)$'
      YLABEL='$Nu Function$'
      J=1
      DO WHILE ( J .NE. 0 )
        PRINT*, 'ENTER THE LINE # TO BE LABELED'
        PRINT*, '(TYPE 0 IF NO LABELS NEEDED)'
        READ(5,*) J
        IF ( J .NE. 0 ) THEN
          PRINT 640, J
          READ(5,570) LINE
          LINLABEL(J)=LINE
        END IF
      END DO
      CALL WAVGRAF(X, 0.0, X(L), C3, .5, 1.0, L, 1, 3000, 15, LINLABEL,
*XLABEL, YLABEL, TITLE, .TRUE., .TRUE.)
      GO TO 500
C
C   PLOT THE MU COEFFICIENT OF AMPLITUDE
C
140  C1MIN=200.
      C1MAX=-200.
      DO J=1, NW
        DO I=1, L
          IF (C1(I, J) .LE. C1MIN) C1MIN=C1(I, J)
          IF (C1(I, J) .GE. C1MAX) C1MAX=C1(I, J)
        END DO
      END DO
      WRITE(6,700) C1MIN, C1MAX
      PRINT*, 'ENTER LOWER & UPPER Y-COORDINATES OF THE GRAPH'
      READ(5,*) YLO, YHI
      TITLE='$MU-COEFFICIENT OF AMPLITUDE$'
      XLABEL='$Propagation Distance (in)$'
      YLABEL='$Mu-Coefficient (1/in)$'
      CALL WAVGRAF(X, 0.0, X(L), C1, YLO, YHI, L, 1, 3000, 15, LINLABEL,
*XLABEL, YLABEL, TITLE, .TRUE., .TRUE.)
      GO TO 500
C
C   PLOT THE KAPPA COEFFICIENT OF AMPLITUDE
C
150  C2MIN=200.
      C2MAX=-200.
      DO J=1, NW
        DO I=1, L
          IF (C2(I, J) .LE. C2MIN) C2MIN=C2(I, J)
          IF (C2(I, J) .GE. C2MAX) C2MAX=C2(I, J)
        END DO
      END DO

```

```

END DO
WRITE(6,750) C2MIN,C2MAX
PRINT*, 'ENTER LOWER & UPPER Y-COORDINATES OF GRAPH'
READ(5,*) YLO,YHI
  TITLE='*KAPPA-COEFFICIENT OF AMPLITUDE*'
  XLABEL='*Propagation Distance (in)*'
  YLABEL='*K-Coefficient (sec 2/in 2)*'
  CALL WAVGRAF(X,0.0,X(L),C2,YLO,YHI,L,1,3000,15,LINLABEL,
  *XLABEL,YLABEL,TITLE,.TRUE.,.TRUE.)
  GO TO 500
C
C   MAIN ROUTINE COMPUTATION AND GRAPHICS ENDS HERE
C
C   WRITE OUTPUT ON A DATA FILE
C
200  OPEN(UNIT=1,FILE='DATA',STATUS='NEW')
    WRITE(1,240)
240  FORMAT(1X,'N',7X,'X(N)',7X,'UREAL',7X,'U(N)',7X,'A',7X,'AR',
  *7X,'C1(N,J)',7X,'C2(N,J)',7X,'C3(N,J)')
    DO 400 J=1,NW
    DO 300 N=1,L
    WRITE(1,250) N,X(N),UREAL(N,J),U(N,J),A(N,J),AR(N,J),C1(N,J),
  *C2(N,J),C3(N,J)
250  FORMAT(1X,I4,8E13.5/)
300  CONTINUE
400  CONTINUE
    CLOSE(UNIT=1)
500  WRITE(6,*) 'WOULD LIKE TO CONTINUE, ENTER Y OR N'
    READ(5,510) ANS
510  FORMAT(A3)
    IF(ANS.EQ.'Y') GO TO 72
    IF(ANS.EQ.'N') GO TO 630
    IF((ANS.NE.'Y').AND.(ANS.NE.'N')) GOTO 500
520  PRINT*, 'WOULD LIKE ANOTHER PROBABILISTIC PLOT'
    READ(5,540) PANS
    IF(PANS.EQ.'Y') GO TO 190
    IF(PANS.EQ.'N') GO TO 500
    IF((PANS.NE.'Y').AND.(PANS.NE.'N')) GOTO 520
540  FORMAT(A3)
550  FORMAT(1X,'MORE THAN 2 AMPLITUDES NEEDED TO MAKE THIS PLOT')
560  FORMAT(2I5)
570  FORMAT(A20)
580  FORMAT(1I2)
600  FORMAT(1X,'NOTE: MAX. ALLOWABLE N FOR THIS RUN IS = ',I4)
630  STOP
640  FORMAT(1X,'ENTER THE LABEL($--$) OF LINE',I2)
650  FORMAT(1I5)
680  FORMAT(1X,'CURRENT DEPTH IS X =',F8.5,'inch')
700  FORMAT(1X,'MINIMUM MU =',F10.5/
  *1X,'MAXIMUM MU =',F10.5)
750  FORMAT(1X,'MINIMUM KAPA =',F10.5/
  *1X,'MAXIMUM KAPA =',F10.5)
760  FORMAT(1X,'ENTER THE <N> VALUE CORRESPONDING TO DEPTH REQUIRED')
800  FORMAT(1X,'AMPLITUDE(',I2,') =',E13.5)
850  FORMAT(1X,'MAX. PARTICLE VELOCITY =',F10.5)
900  FORMAT(1X,'MINIMUM ACTUAL SPEED =',F10.5/
  *1X,'MAXIMUM ACTUAL SPEED =',F10.5)
950  FORMAT(1X,'MAXIMUM STRESS =',F10.4)
1000 FORMAT(1X,'MAXIMUM AVERAGE SPEED =',F10.5,/)
1050 FORMAT(1X,'MAXIMUM PARTICLE DISPLACEMENT =',F8.4/)

```

```

1100 FORMAT(1X, 'MAXIMUM DETERMINISTIC AMPLITUDE =', F10.5, /)
1110 FORMAT(1X, 'MAXIMUM PROBABILISTIC AMPLITUDE =', F8.4 /)
1120 FORMAT(1X, 'MAXIMUM PROBABILISTIC VELOCITY =', F8.4 /)
1130 FORMAT(1X, 'MAXIMUM PROBABILISTIC STRESS =', F8.4 /)
1140 FORMAT(1X, 'MAXIMUM PROBABILISTIC DISPLACEMENT =', F8.4 /)
      END
      SUBROUTINE GAUSS ( ENUA, JF, KK, NF, ZL, X, UBAR )
C*****
C      GAUSS-LEGENDRE QUADRATURE FOR CALCULATION OF PROPAGATION TIME *
C      AND WAVE VELOCITY USING FOUR-POINT FORMULA FOR INTEGRATION *
C*****
C
      REAL ETA, FKCH, ENUA, ENUB, NUZX, UF, FXCH, ENU, ENUX, X
      DIMENSION ETA(4), NUZX(4), FXCH(4), ENU(4), ENUX(4),
      *UF(4), FKCH(4), PENU(4), PNU(4)
      COMMON /GRAIN/ AFFO, AFFF, BB, DUM, ENUB, FLFFO, FLFFF, GG, GL, GO,
      *TIME
C
C      DEFINE THE CONSTANTS AND THE WEIGHTING COEFFICIENTS
C
      PI=3.141592741012573
      WT1=0.34785485
      WT2=0.65214515
      ETA(1)=-0.86113631
      ETA(2)=-0.33998104
      ETA(4)=-ETA(1)
      ETA(3)=-ETA(2)
C
C      DEFINE THE FUNCTION AND PERFORM THE INTEGRATION
C
      DO 50 I = 1, 4
      FKCH(I)=(ETA(I)*(X-ZL)+(X+ZL))/2.0
      GO TO (20, 30, 40) KK
C
C      PERIODIC VOLUME DISTRIBUTION FUNCTION
C
20    ENU(I)=ENUA+(1.-ENUA)*COS(2.*PI*FKCH(I)/GL)
      NUZX(I)=((ENUA-1.0)/GL)*2.0*PI*SIN(2.*PI*FKCH(I)/GL)
      PP=FLFFO+0.5*AFFO*NUZX(I)**2
      IF(PP.LT.0.0) GO TO 150
      UF(I)=SQRT(PP)
      FXCH(I)=1.0/UF(I)
      GO TO 50
C
C      EXPONENTIAL VOLUME DISTRIBUTION FUNCTION
C
30    PENU(I)=1.0-(1.0-ENUB)*EXP(-BB*GG*FKCH(I))
      ENUX(I)=(1.0-ENUB)*BB*GG*EXP(-BB*GG*FKCH(I))
      TEST=FLFFO+0.5*AFFO*ENUX(I)**2
      IF(TEST.LT.0) GO TO 150
      UF(I)=SQRT(FLFFO+0.5*AFFO*ENUX(I)**2)
      FXCH(I)=1.0/UF(I)
      GO TO 50
C
C      PERIODIC AND EXPONENTIAL COMBINED VOLUME DISTRIBUTION FUNCTION
C
40    ENU(I)=ENUA+(1.-ENUA)*COS(2.*PI*FKCH(I)/GL)
      NUZX(I)=((ENUA-1.0)/GL)*2.0*PI*SIN(2.*PI*FKCH(I)/GL)
      PENU(I)=1.0-(1.0-ENUB)*EXP(-BB*GG*FKCH(I))
      ENUX(I)=(1.0-ENUB)*BB*GG*EXP(-BB*GG*FKCH(I))

```

```

PNU(I)=ENU(I)*ENUX(I)+PENU(I)*NUZX(I)
CHEK=FLFFO+.5*AFFO*PNU(I)**2
IF(CHEK.LT.0) GO TO 150
UF(I) = SQRT(FLFFO+0.5*AFFO*PNU(I)**2)
FXCH(I)=1.0/UF(I)
50  CONTINUE
100  TAUX = WT1*(FXCH(1)+FXCH(4))+WT2*(FXCH(2)+FXCH(3))
    TIME = TAUX*((X-ZL)/2.0)
    TIME = DUM + TIME

C
C  CALCULATE THE AVERAGE WAVE SPEED
C
    UBAR = X/TIME
    GOTO 200
150  WRITE(6,180) NF,JF
180  FORMAT(1X,'INPUT IS INCOMPATIBLE WITH REAL WAVE SPEED IN GAUSS'/
    #1X,      'LOOPING PARAMETER N =',I5,
    #1X,      'WAVE AMPLITUDE NUMBER J =',I3)
    STOP
200  RETURN
    END
    SUBROUTINE RUNKUT(AMP,ENUA,H,K,N,RKAPA,RMU,RVDFUN,RWS,X,YO)
C*****
C  SUBROUTINE RUNGE-KUTTA CALCULATES THE WAVE AMPLITUDE
C  IN THE GRANULAR MEDIA
C*****
C
    REAL AMP,BB,ENU,ENUX,ENUXX,ENUZ,ENUZZ,H,PENU,RKAPA,RMU,RVDFUN,
    #RWS,X,YO
    COMMON /GRAIN/ AFFO,AFFF,BB,DUM,ENUB,FLFFO,FLFFF,GO,QL,GO,TIME
    COMMON /CONTRL/ P,P1,Q,Q1
    DATA PI/3.141592741012573/

C
C  DEFINE THE VOLUME DISTRIBUTION FUNCTIONS AND THEIR DERIVATIVES
C
C  PERIODIC VOLUME DISTRIBUTION FUNCTION
C
    ENU(X)=(ENUA+(1.-ENUA)*COS(2.*PI*X/QL))*P+P1
    ENUZ(X)=(-2.*PI*(1.-ENUA)*SIN(2.*PI*X/QL)/QL)*P
    ENUZZ(X)=(-4.*PI**2.)*(1.-ENUA)*COS(2.*PI*X/QL)/(QL**2))*P

C
C  EXPONENTIAL VOLUME DISTRIBUTION FUNCTION
C
    PENU(X)=(1.0-(1.0-ENUB)*EXP(-BB*GO*X))*Q+Q1
    ENUX(X)=((1.0-ENUB)*BB*GO*EXP(-BB*GO*X))*Q
    ENUXX(X)=(-(1.0-ENUB)*BB**2*GO**2*EXP(-BB*GO*X))*Q

C
C  PERIODIC AND EXPONENTIAL VOLUME DISTRIBUTION FUNCTION COMBINED
C
    PNU(X)=ENU(X)*PENU(X)
    PNUX(X)=ENU(X)*ENUX(X)+PENU(X)*ENUZ(X)
    PNUXX(X)=ENU(X)*ENUXX(X)+PENU(X)*ENUZZ(X)+2.*ENUZ(X)*ENUX(X)

C
C  COMPUTE THE WAVE AMPLITUDE AND THE CONSTANTS MU & KAPA
C
    UFSQ(X)=(FLFFO+0.5*AFFO*PNUX(X)**2)
    FMU(X)=(UFSQ(X)/PNU(X)+AFFO*PNUXX(X)/2.0)*PNUX(X)/(2.*UFSQ(X))
    CKAP(X)=-((FLFFF+AFFF*PNUX(X)**2/2.)/(2.*GO*UFSQ(X)**2))
    FC(X,Z)=CKAP(X)*Z**2-FMU(X)*Z
    AK1=FC(X,YO)

```

```

      AK2=FC(X+H/2.0,YD+H*AK1/2.0)
      AK3=FC(X+H/2.0,YD+H*AK2/2.0)
      AK4=FC(X+H,YD+H*AK3)
      YD = YD+H*(AK1+2.0*AK2+2.0*AK3+AK4)/6.0
      AMP=YD
      RMU=FMU(X)
      RKAPA=CKAP(X)
      RVDFUN=PNU(X)
      IF (UFSQ(X).LT.0) GO TO 10
      RWS=SQRT(UFSQ(X))/1000.
      GO TO 30
10  WRITE(6,20) N,K
20  FORMAT(1X,'INPUT IS INCOMPATIBLE WITH REAL WAVE SPEED IN RUNKUT'/
      #1X,'      'LOOPING PARAMETER N =',I5,
      #1X,'      'WAVE AMPLITUDE NUMBER J =',I3)
      STOP
30  RETURN
      END
C
C *****
C      SUBROUTINE WAVGRAF(X,XMININP,XMAXINP,Y,YMININP,YMAXINP,N,M,
      - NORIG,MORIG,LINLABEL,INDAX,DEPAX,TITLE,INDEVEN,
      - DEPEVEN)
C *****
C
C      To draw a line graph with multiple plots on an 8X11 page,
C      using DI-3000 graphics subroutines
C
C      N: Number of values in each set
C      M: Number of sets of dependent values
C      NORIG Original column dimension of the value arrays
C      MORIG: " " " " " " " "
C      LINLABEL: Character string labels of each set of values
C      INDAX: Character string of independent axis label
C      DEPAX: " " " dependent " "
C      TITLE: " " " title of graph
C      (Note: all character strings should be inclosed in a
C      delimiter mark, such as '$graph$')
C      INDEVEN: Logical variable which is .TRUE. if the independent
C      axis should be extended to terminate at even divisions.
C      DEPEVEN: Logical variable which is .TRUE. if the dependent
C      axis should be extended to terminate at even divisions.
C      VECTOR: Array for graph information storage
C      VSIZE: Size of VECTOR array
C      RATIO: Aspect ratio of the graphics device
C      NSET: Data set counter
C      XDIVMAX: Maximum number of independent axis divisions
C      YDIVMAX: Maximum number of dependent axis divisions
C      SPAN: Range of axes (maximum value minus minimum value)
C      ORDER: order of the axis increments
C      RESOLUTION: Minimum even incremented resolution of the axis
C
C      REAL X( NORIG ), XMININP, XMAXINP, Y( NORIG, MORIG ), YMININP,
      - YMAXINP
      INTEGER N, M, NORIG, MORIG
      CHARACTER LINLABEL(10)*25,INDAX*50,DEPAX*50,TITLE*50
      LOGICAL INDEVEN, DEPEVEN
      REAL ENTER, OUTER, XMIN, XMAX, YMIN, YMAX, RATIO, SPAN, ORDER,
      # RESOLUTION, XINCREMENT, YINCREMENT
      INTEGER VECTOR(15000), VSIZE, NSET, XDIVMAX, YDIVMAX

```

```

DATA VSIZE/15000/, XDIVMAX/5/, YDIVMAX/10/
XMIN=XMININP
XMAX=XMAXINP
YMIN=YMININP
YMAX=YMAXINP

C
C Initialize GRAFMAKER and DI-3000
C
  CALL JCHINI( .TRUE., 1 )
  CALL JCHART( VECTOR, VSIZE )
  CALL JASPEK( 1, RATIO )
  CALL JVSPAC( -1.0, 1.0, -RATIO, RATIO )
  CALL JGRAPH( VECTOR, VSIZE, 1 )

C
C Define title and text characteristics.
C
  CALL JXTEXT( VECTOR, VSIZE, 1, 5, 0.0, 1.0, 0 )
  CALL JTXBOX( VECTOR, VSIZE, 0, 0, 1 )
  CALL JSTNOT( VECTOR, VSIZE, 1, 1, TITLE )
  CALL JPONOT( VECTOR, VSIZE, 1, 1, 500.0, 980.0 )
  CALL JTXHGT( VECTOR, VSIZE, 20.0, 0.0, 0.0 )

C
C If desired, redefine the dependent axis minimum and
C maximum for even axes
C
  SPAN = YMAX - YMIN
  IF (SPAN.LT.1E-6) THEN
    ORDER = LOG10( SPAN*1E12/12.0 ) - LOG10( FLOAT( YDIVMAX ) )
  ELSE
    ORDER = LOG10( SPAN ) - LOG10( FLOAT( YDIVMAX ) )
  END IF
  IF ( ORDER .LT. 0.0 ) ORDER = ORDER - 1.0
  RESOLUTION = 10.0 ** INT( ORDER )
  IF ( SPAN / FLOAT( YDIVMAX ) .LE. RESOLUTION ) THEN
    YINCREMENT = RESOLUTION
  ELSE IF ( SPAN / FLOAT( YDIVMAX ) .LE. 2.0 * RESOLUTION ) THEN
    YINCREMENT = 2.0 * RESOLUTION
  ELSE IF ( SPAN / FLOAT( YDIVMAX ) .LE. 5.0 * RESOLUTION ) THEN
    YINCREMENT = 5.0 * RESOLUTION
  ELSE IF ( SPAN / FLOAT( YDIVMAX ) .LE. 10.0 * RESOLUTION ) THEN
    YINCREMENT = 10.0 * RESOLUTION
  ELSE
    YINCREMENT = 20.0 * RESOLUTION
  END IF
  IF ( INDEVEN ) THEN
    IF ( YMIN .GE. 0 ) THEN
      YMIN = YINCREMENT * FLOAT( INT( YMIN / YINCREMENT + 0.01 ) )
    ELSE
      YMIN = YINCREMENT * FLOAT( INT( YMIN / YINCREMENT - 0.99 ) )
    END IF
    IF ( YMAX .GE. 0 ) THEN
      YMAX = YINCREMENT * FLOAT( INT( YMAX / YINCREMENT + 0.99 ) )
    ELSE
      YMAX = YINCREMENT * FLOAT( INT( YMAX / YINCREMENT - 0.01 ) )
    END IF
  END IF
  CALL JSTVAX (VECTOR, VSIZE, 1, 1, YMIN, YMAX, DEPAX)
  IF ( .NOT. INDEVEN ) THEN
    YMIN = YMIN + YINCREMENT
    IF ( YMIN .GE. 0 ) THEN

```



```

        YMIN = YINCREMENT * FLOAT( INT( YMIN / YINCREMENT + 0.01 ) )
    ELSE
        YMIN = YINCREMENT * FLOAT( INT( YMIN / YINCREMENT - 0.99 ) )
    END IF
    YMAX = YMAX - YINCREMENT
    IF ( YMAX .GE. 0 ) THEN
        YMAX = YINCREMENT * FLOAT( INT( YMAX / YINCREMENT + 0.99 ) )
    ELSE
        YMAX = YINCREMENT * FLOAT( INT( YMAX / YINCREMENT - 0.01 ) )
    END IF
END IF
CALL JTIC (VECTOR, VSIZE, 1, 1, 1, YMIN, YMAX, YINCREMENT)
CALL JTCATR (VECTOR, VSIZE, 1, 1, 1, 0.0, 0.6, 0.0)

```

C
 C If desired, redefine the independent axis minimum and
 C maximum for even divisions
 C

```

    SPAN = XMAX - XMIN
    IF (SPAN.LT. 1E-6) THEN
        ORDER = LOG10( SPAN*1E12/12.0 ) - LOG10( FLOAT( XDIVMAX ) )
    ELSE
        ORDER = LOG10( SPAN ) - LOG10( FLOAT( XDIVMAX ) )
    END IF
    IF ( ORDER .LT. 0.0 ) ORDER = ORDER - 1.0
    RESOLUTION = 10.0 ** INT( ORDER )
    IF ( SPAN / FLOAT( XDIVMAX ) .LE. RESOLUTION ) THEN
        XINCREMENT = RESOLUTION
    ELSE IF ( SPAN / FLOAT( XDIVMAX ) .LE. 2.0 * RESOLUTION ) THEN
        XINCREMENT = 2.0 * RESOLUTION
    ELSE IF ( SPAN / FLOAT( XDIVMAX ) .LE. 5.0 * RESOLUTION ) THEN
        XINCREMENT = 5.0 * RESOLUTION
    ELSE IF ( SPAN / FLOAT( XDIVMAX ) .LE. 10.0 * RESOLUTION ) THEN
        XINCREMENT = 10.0 * RESOLUTION
    ELSE
        XINCREMENT = 20.0 * RESOLUTION
    END IF
    IF ( INDEVEN ) THEN
        IF ( XMIN .GE. 0 ) THEN
            XMIN = XINCREMENT * FLOAT( INT( XMIN / XINCREMENT + 0.01 ) )
        ELSE
            XMIN = XINCREMENT * FLOAT( INT( XMIN / XINCREMENT - 0.99 ) )
        END IF
        IF ( XMAX .GE. 0 ) THEN
            XMAX = XINCREMENT * FLOAT( INT( XMAX / XINCREMENT + 0.99 ) )
        ELSE
            XMAX = XINCREMENT * FLOAT( INT( XMAX / XINCREMENT - 0.01 ) )
        END IF
    END IF
    CALL JSTHAX( VECTOR, VSIZE, 1, 2, XMIN, XMAX, INDAX )
    IF ( .NOT. INDEVEN ) THEN
        XMIN = XMIN + XINCREMENT
        IF ( XMIN .GE. 0 ) THEN
            XMIN = XINCREMENT * FLOAT( INT( XMIN / XINCREMENT + 0.01 ) )
        ELSE
            XMIN = XINCREMENT * FLOAT( INT( XMIN / XINCREMENT - 0.99 ) )
        END IF
        XMAX = XMAX - XINCREMENT
        IF ( XMAX .GE. 0 ) THEN
            XMAX = XINCREMENT * FLOAT( INT( XMAX / XINCREMENT + 0.99 ) )
        ELSE
            XMAX = XINCREMENT * FLOAT( INT( XMAX / XINCREMENT - 0.01 ) )
        END IF
    END IF

```

```

      XMAX = XINCREMENT * FLOAT (INT (XMAX / XINCREMENT - 0.01))
    END IF
  END IF

C
C   DESCRIBE TWO TICK MARK GROUPS TO BE USED ON THE X-AXIS
C
  CALL JTIC (VECTOR, VSIZE, 1, 2, 2, XMIN, XMAX, XINCREMENT)
  CALL JTCATR (VECTOR, VSIZE, 1, 2, 2, 0.0, 15.0, 0)
  ENTER=XMIN+XINCREMENT/2.0
  OUTER=XMAX-XINCREMENT/2.0
  CALL JTIC (VECTOR, VSIZE, 1, 2, 3, ENTER, OUTER, XINCREMENT)
  CALL JTCATR (VECTOR, VSIZE, 1, 2, 3, 0.0, 7.5, 0)
  CALL JTCPAT (VECTOR, VSIZE, 1, 2, 3, 10, 20)

C
C   OPEN UP A LEGEND
C
  CALL JTXBOX (VECTOR, VSIZE, 0, 0, 1)
  CALL JSTLGD (VECTOR, VSIZE, 1, '$$')
  CALL JLGPOS (VECTOR, VSIZE, 1, 500.0, 860.0)
  CALL JTXHGT (VECTOR, VSIZE, 17.0, 0.0, 0.0)

C
C   PASS THE DATA SETS TO GRAFMAKER
C
  CALL JRDATA (VECTOR, VSIZE, 1, X, N)
  CALL JINDEP (VECTOR, VSIZE, 1, 1)
  DO NSET = 1, M
    CALL JRDATA (VECTOR, VSIZE, NSET + 1, Y(1, NSET), N)
    CALL JDEPEND (VECTOR, VSIZE, 1, NSET, NSET + 1)
  C
  C   DEFINE PLOT LINE CHARACTERISTICS
  C
    CALL JXLINE (VECTOR, VSIZE, NSET, NSET, 16383, (NSET-1)*10,
    - 16383)
    CALL JDTATR (VECTOR, VSIZE, 1, NSET, 0, 0, NSET)

C
C   MAKE A LEGEND ENTRY
C
  IF (LINLABEL(NSET)(1:1) .EQ. '$' .AND. LINLABEL(NSET)(2:2)
  -   .NE. '$') CALL JSDLGD (VECTOR, VSIZE, 1, NSET,
  -   LINLABEL(NSET))
  END DO

C
C   SHOW CHART
C
  CALL JCHSHW (VECTOR, VSIZE, -0.70, 0.70, -0.55, 0.55)

C
C   PAUSE FOR VIEWING
C
  CALL JPAUSE (1)

C
C   Terminate GRAFMAKER
C
  CALL JCHTRM (.TRUE.)
  RETURN
  END

```

END

12-86

DTIC